The role of small nucleolar Ribonucleoprotein complexes in lung cancer

Dissertation

for the conferral of the title

Doctor of Doctor rerum naturalium (Dr. rer. nat.)

of the Faculty of Natural Sciences I

at

Martin Luther University,

Halle-Wittenberg

presented by

Chunhong Cui

born on 02.02.1984 in Shandong, China

Experts: Prof. Dr. rer. nat. Mike. Schutkowski

Prof. Dr. med. Carsten Müller-Tidow

Prof. Dr. med. Christoph Schliemann

Prof. Dr. Stefan, Hüttelmaier

Defense time: 16.04.2019

Contents

Abstract

Non-small cells lung cancer (NSCLC) remains a leading cause of cancer death all over the world. New diagnostic and therapeutic targets are urgently needed. Hyperactive ribosomal biogenesis has been reported in cancer. Small nucleolar RNA (snoRNA) pathways play an important role in the post-transcriptional modification of ribosomal RNA. But the detailed role of snoRNA pathways in cancer remains unknown. Recent studies have reported that SNORA42 was overexpressed in lung tumours and could be used as a biomarker in NSCLC. Here, the role of small nucleolar ribonucleic protein complexes (snoRNPs) was investigated in lung cancer. NOP10 was highly expressed in primary lung carcinomas compared to matched lung tissue. Further, expression of NOP10 was tested in tissue microarray (TMA) with immunohistochemistry. We also knocked out the NOP10 protein on the genomic level with the CRISPR/Cas9 system and tested the effects of NOP10 KO on lung cancer cells' growth and metastasis in vitro. High levels of NOP10 protein expression were associated with poor outcome and NOP10 was required for growth and proliferation of lung cancer cells. Unlike the effects of SNORA42 on lung cancer cells in a P53-dependent manner, NOP10 lead to cell cycle arrest due to P53 associated mechanism and P53 independent manner.

The role of single snoRNAs was revealed by snoRNAnome-scale CRISPR-Cas9 knockout screen. The analyses indicated that SNORA65, SNORA7A and SNORA7B affected proliferation of lung cancer cells. Furthermore, TCGA data also showed that SNORA65, SNORA7A and SNORA7B were overexpressed in lung tumours. Expression of SNORA65, SNORA7A and SNORA7B could be inhibited by NOP10 KO in lung cancer cells. As a next step, high levels of H/ACA box snoRNAs was observed in primary lung cancer specimen with associated changes in rRNA pseudouridylation levels. We further knocked out SNORA65, SNORA7A and SNORA7B on the genomic level with the CRISPR/Cas9 system and tested the effects on NSCLC development. We demonstrated that all these three snoRNAs are necessary for growth and proliferation in NSCLC patients.

Taken together, non-small cell lung cancer requires H/ACA box snoRNPs with crucial roles for snoRNP complexes as well as for several specific single snoRNAs.

Keywords: NSCLC, snoRNA, NOP10, Pseudouridylation, P53, SNORA7A, SNORA7B, SNORA65

1 Introduction

Small nucleolar RNAs (snoRNAs) are functional transcripts that mostly accumulate in the nucleolus. They do not code for proteins but play an important role in regulating gene expression and function. The length of snoRNAs is 60 to 300 nucleotides. (Kiss, 2002; Williams and Farzaneh, 2012a). It has been reported that snoRNAs exhibit differential expression patterns in human cancer and have different effects on cell transformation, tumorigenesis and metastasis of lung cancer (Gong et al., 2017; Mannoor et al., 2014; Mei et al., 2012; Siprashvili et al., 2016; Su et al., 2014; Thorenoor and Slaby, 2015). SnoRNA pathways have different functions during cancer development (Mei et al., 2012; Siprashvili et al., 2016; Stepanov et al., 2015; Su et al., 2014; Thorenoor and Slaby, 2015; Williams and Farzaneh, 2012a).

Lung cancer is a malignant lung carcinoma derived from epithelial cells and characterized by uncontrolled cell growth in lung tissues. Lung tumour growth can also spread through the process of metastasis into nearby tissue or other organs of the body. Lung cancer can be divided into two main types: small-cell lung cancer (SCLC) and non-small-cell lung cancer (NSCLC). Almost 80% to 85% of lung cancers are NSCLC; only 10% to 15% are SCLC.

NSCLC is the main cause of cancer death in human beings all over the world (Jemal et al., 2008; Torre et al., 2015). Although novel therapies and technologies have been found for use at its early stage, the median survival of NSCLC patients is about 5 months, and the 5-year survival rate of stage IV NSCLC patients is only 1%. It has been reported that some snoRNAs are highly expressed in lung tumours, and a snoRNA pathway could provide a potential diagnostic test for NSCLC (Mannoor et al., 2014; Mei et al., 2012). But, the exact roles of snoRNAs in the development and progression of lung cancer remain incompletely understood.

1.1 Pathology of NSCLC

Carcinoma is a type of cancer that originate from epithelial cells. Lung carcinomas start in the cells that line the inside of the bronchi, bronchioles and alveoli. Traditionally, the distinction between SCLC and NSCLC played a critical role in clinical treatment decisions. Recently, molecular pathology plays another key role

for the clinical oncology care team in devising the therapy plan and for the molecular laboratory to determine molecular strategies. For example, the epidermal growth factor receptor (EGFR) mutation has been found in 10% to 15% of NSCLC in the United States (Dacic et al., 2010). The pharmaceuticals that target EGFR have shown dramatic efficacy in advanced stage NSCLC (Langer, 2012).

There are mainly three kinds of NSCLC tumours, based on how the cells appear under the microscope, containing adenocarcinoma, squamous cell (epidermoid) carcinoma, large cell (undifferentiated) carcinoma (Fig. 1) and other subtypes such as adenosquamous carcinoma and sarcomatoid carcinoma (Wang et al., 2002). Adenocarcinoma occurs in the cells resembling gland cells, such as the glands that secrete mucus in the lungs. Adenocarcinoma is the most common type of lung cancer, and normally it grows slower than other lung cancers. Squamous cell carcinoma occurs in lung tissue in cells that resemble the flat cells lining the airways; this type of lung cancer accounts for one-quarter of lung cancers. Large cell carcinoma grows and spreads much faster than other lung cancer cells, and it accounts for about 10% of lung cancers.

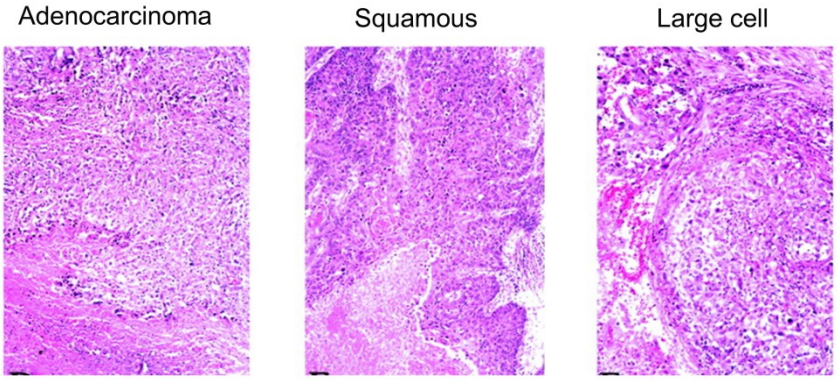

Figure 1: Hematoxylin and eosin stained tissues for three types of NSCLC tumours: adenocarcinoma, squamous cell (epidermoid) carcinoma, large cell (undifferentiated) carcinoma (Wang et al., 2002).

1.2 Small nucleolar RNA

In human beings, after transcription most RNA cannot be translated into protein and these RNAs are called non-coding RNAs (ncRNAs). Beside transfer RNAs (tRNAs) and ribosomal RNAs (rRNAs), which are the most abundant ncRNAs, ncRNAs also

include many other functional small RNAs such as micro RNAs (miRNAs), short interfering RNAs (siRNAs), piwi interacting RNAs (pi-RNAs), small nuclear RNAs (snRNAs), snoRNAs, small Cajal body-specific RNAs (scaRNAs), long non-coding RNAs (lncRNA) and transcribed ultra-conserved regions (T-UCRs). In recent years, many studies have reported that snoRNAs play a role in cancer pathogenesis (Dong et al., 2009; Liao et al., 2010; Mannoor et al., 2014; Mei et al., 2012; Siprashvili et al., 2016). Yet, most ncRNAs are not well studied. In particular, as one large group of ncRNAs, snoRNAs are studied rarely but are associated with physiological and disease processes.

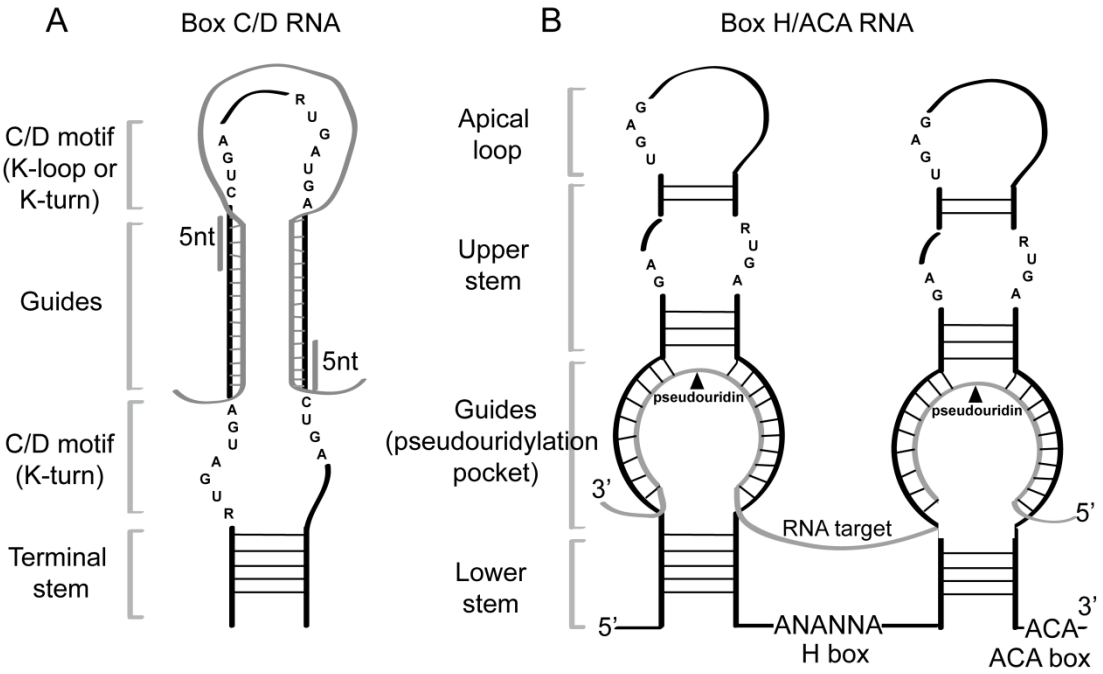

Figure 2: Features of C/D box and H/ACA box snoRNA. (A) Boxes C and D are hallmarks of the C/D box snoRNAs. (B) Boxes H (Hinge region) and ACA are hallmarks of the H/ACA box snoRNAs. In both classes of snoRNAs, short stems bring the conserved boxes close to one another to constitute the structural core motifs of the snoRNAs, which modulate the specific binding of two distinct sets of protein components. These are important for forming the functional snoRNP complexes and for accumulation in the nucleolus (modified from Massenet and Bertrand, 2017) (Massenet et al., 2017).

Small nucleolar RNAs have been found in many organisms, including yeast, plants, vertebrates, and the number is still increasing (Kiss et al., 2006; Matera et al., 2007;

Meier, 2005; Terns and Terns, 2006). SnoRNAs have conserved structure and sequence in different species, which means they play important physiological roles.

Based on sequence and structural features, snoRNAs can be divided into two classes (C/D box and H/ACA box snoRNAs). C/D box snoRNAs contain the conserved C (RUGAUGA, R = A or G) and D (CUGA) box (Fig. 2A). H/ACA box snoRNAs include two single-stranded H (ANANNA, N = A, C, G or U) and ACA box domains (Fig. 2B) (Massenet et al., 2017).

1.2.1 snoRNA processing

Most snoRNA promoters are transcribed by RNA polymerase (pol) II and only a small part of the promoters served through polymerase (pol) III (Dieci et al., 2009). More than 90% of snoRNA gene complements are located in the intron in human beings and other mammals (Dieci et al., 2009; Smith and Steitz, 1998; Tycowski et al., 1996a). Some snoRNAs could also be processed from introns of lncRNA (Smith and Steitz, 1997). Clustering for both independent and intronic snoRNA genes is another characteristic of human snoRNA. For example, locus 15q11q13 of chromosome 15 contains clusters of the snoRNA's HBII-85 and HBII-52, which are present in 24 and 48 in tandem repeats. In addition, this region also includes single copies of other snoRNAs: HBII-13, HBII-436, HBII-437, HBII-438A and HBII-438B. It has been identified that loss of snoRNA copies from this region cause Prader-Willi syndrome (Chamberlain, 2013; Ding et al., 2008; Sahoo et al., 2008)
It has been reported that 98.5% of the genome consists of non-protein-coding DNA sequences, but most of the genome is transcribed into RNA (Boland, 2017). The pre-processed RNA transcripts undergo further processing and generate shorter, metabolically stable RNAs with diverse functions. Previously, experimental evidence identified that most snoRNAs are transcribed by independent RNA polymerase II (less commonly pol III) promoters (Dieci et al., 2009). Because most snoRNAs are located in introns and do not have their own promoter, they are usually co-transcribed with their host genes, which could either be protein- or non-protein-coding transcripts. The snoRNA processing procedure has a tight relationship with the pre-mRNA splicing (Fig. 3).

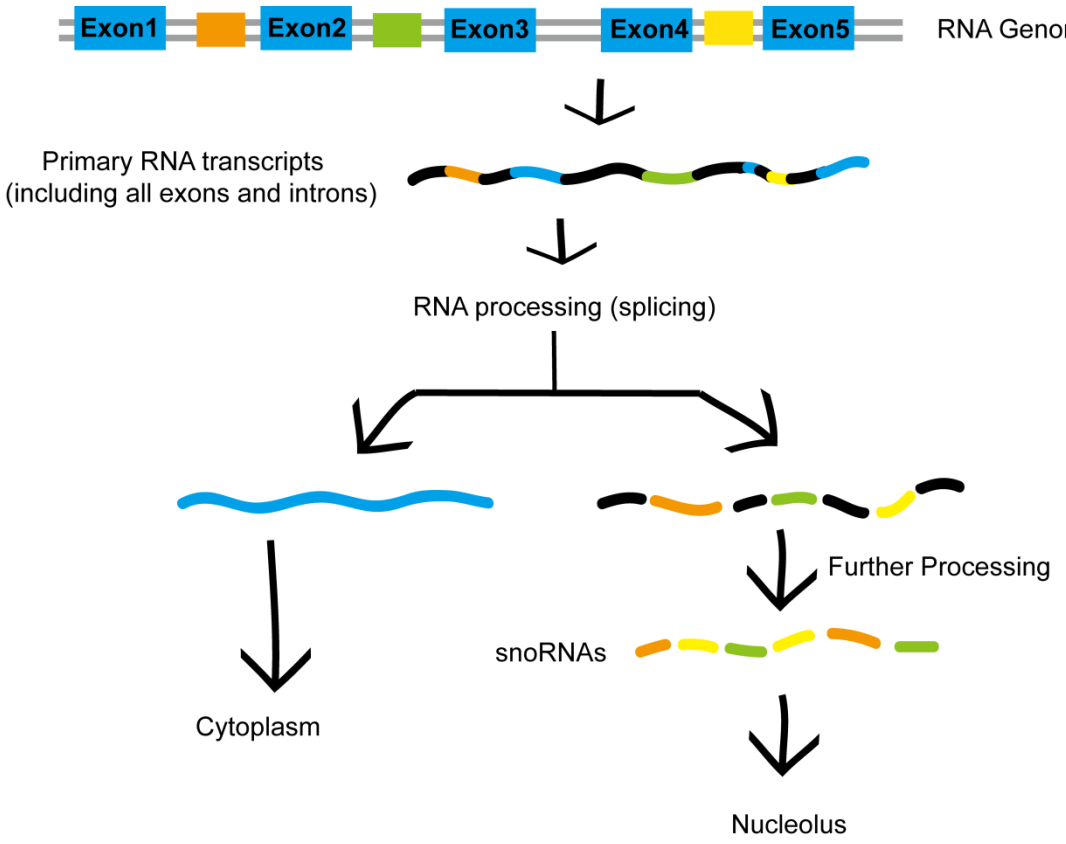

Figure 3: Generation of sno RNAs from primary RNA transcripts. SnoRNAs are located in introns and they are released after several steps of the splicing procedure (modified from Williams and Farzaneh, 2012) (Williams and Farzaneh, 2012b).

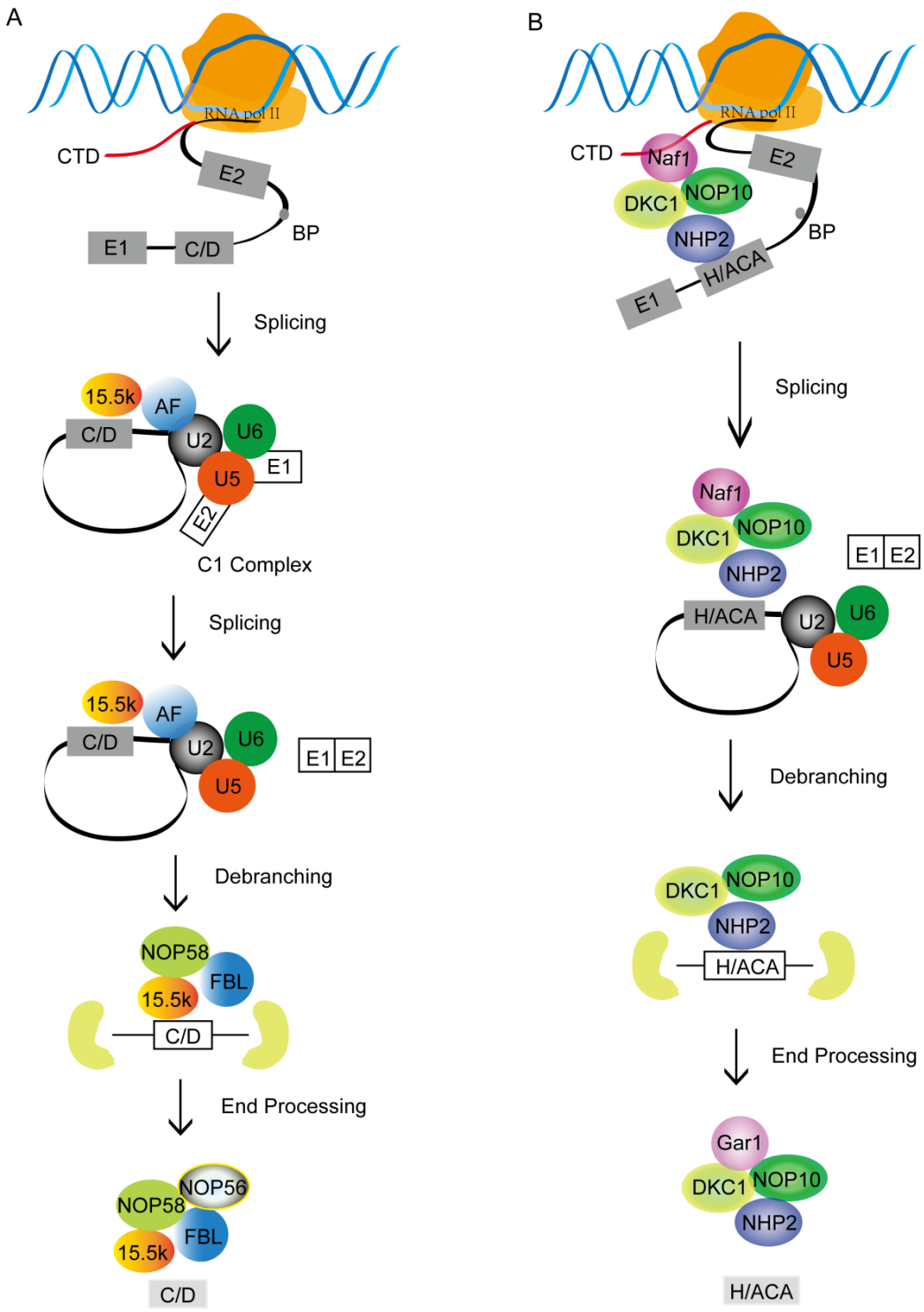

Figure 4: SnoRNA biogenesis model. SnoRNA biogenesis is a complicated procedure correlating with pre-mRNA transcription and splicing and assembly of snoRNP. (A) Biogenesis of C/D box snoRNA. A putative assembly factor (AF) interacts with splicing factors and recruits the 15.5 kDa core protein at the C1-complex stage of mRNA splicing. After the splicing factors interact with the branch point (BP) region, the other three core proteins, fibrillarin (FBL) and the nucleolar proteins Nop56 and Nop58, are also recruited to

the nascent snoRNA. (B) H/ACA box snoRNA biogenesis. During the same time of transcription, nuclear-assembly factor 1 (Naf1) promotes recruitment and binding of the H/ACA core proteins to the nascent snoRNA sequences. Naf1 could interact with the carboxyterminal domain (CTD) of RNA polymerase (pol) II, but in mature H/ACA snoRNPs, Naf1is replaced by Gar1. DKC, dyskerin; NHP2, non-histone chromosome protein 2; Gar1, protein glycine arginine rich 1 (modified from Richard and Kiss, 2006) (Richard and Kiss, 2006).

As described previously, snoRNAs have been divided into two structurally and functionally defined classes (Kiss et al., 2010). C/D box snoRNAs mainly guide ribosome RNA 2'-O-methylation (Kiss-Laszlo et al., 1996; Nicoloso et al., 1996; Tycowski et al., 1996b) whereas H/ACA box snoRNAs direct pseudouridylation of ribosomal RNA (Ganot et al., 1997; Ni et al., 1997). Most of these snoRNAs are intimately associated with some known type of nuclear proteins, called small nucleolar ribonucleoprotein particle (snoRNPs).

During C/D box snoRNA processing, 15.5 kDa C/D box core protein is actively recruited to the intronic C/D box snoRNA site by a putative assembly factor (AF) after primary RNA transcription. Some reports hypothesized that AF can interact with splicing factors related with the branch point (BP) region. It is very important that core proteins Nop58 and fibrillarin combine to the pre-snoRNP to protect snoRNA from degradation after splicing. The newly produced C/D box snoRNAs (pre-snoRNA) are further processed by exonucleases to form mature C/D box snoRNA (Fig. 4A) (Richard and Kiss, 2006).

For H/ACA box snoRNA, it is hypothesized that nuclear-assembly factor 1 (Naf1) promotes recruitment of H/ACA core proteins and interacts with the carboxyterminal domain (CTD) of RNA polymerase (pol) II. The H/ACA core proteins include Nop10, dyskerin and non-histone chromosome protein 2 (Nhp2), which could combine to the nascent snoRNA sequences. The pre-snoRNA are processed through splicing and debranching, then Naf1is replaced by the core protein glycine arginine rich 1 (Gar1) (Fig. 4B) (Darzacq et al., 2006; Dieci et al., 2009; Hoareau-Aveilla et al., 2006; Richard et al., 2006).

1.2.2 Small nucleolar ribonucleic protein complexes (snoRNPs)

SnoRNPs are nucleolus- localized ribonucleoprotein particles, the biogenesis of which is highly complex and involves a dynamic process (Darzacq et al., 2006; Filipowicz and Pogacic, 2002; Hirose et al., 2006). In eukaryotic cells, hundreds of snoRNP particles are involved in modification and processing of pre-rRNA (Tollervey and Kiss, 1997). Most of these snoRNPs can be divided into two kinds: C/D or H/ACA type, because these particles always contain snoRNA components possessing a C/D or H/ACA sequence motif. During snoRNA processing, some snoRNPs are recruited and combine to nascent snoRNA to prevent newly synthesized snoRNA from degrading (Kufel et al., 2000; Samarsky et al., 1998). Some of the snoRNPs also participate in precursor rRNA processing in yeast (Atzorn et al., 2004; Beltrame and Tollervey, 1995; Morrissey and Tollervey, 1993). But the main role of the snoRNPs is RNA 2'-O-methylation guided by C/D box snoRNA and RNA pseudouridylation, guided by H/ACA box snoRNA, which are important to facilitate rRNA folding and stability (King et al., 2003; Ofengand, 2002).

C/D box snoRNAs mainly form functional snoRNPs with four conserved proteins including fibrillarin, the 15.5 kDa protein, and nucleolar proteins Nop56 and Nop58. C/D box snoRNAs guide the snoRNP complex to its target sequence of pre-ribosomal RNA (pre-rRNA), and the methyltransferase activity of fibrillarin catalyses site-specific 2'-O-hydroxyl methylation of ribose in pre-rRNAs (Filipowicz and Pogacic, 2002; Kiss, 2002). The methylated nucleotide is normally in the fifth residue of the D box (Figure 5A) (Brown et al., 2003).

H/ACA box snoRNA, dyskerin, Nop10, non-histone chromosome protein 2 (Nhp2) and Gar1 are mainly parts of snoRNPs. It has been reported that these four snoRNPs are essential for cell growth (Filipowicz and Pogacic, 2002; Kiss, 2002). H/ACA box snoRNAs contain short antisense elements complementary to the target RNA, the short antisense elements called pseudouridylation pockets located in an internal loop of the snoRNA. The pseudouridylation pocket is responsible for binding of rRNA, and then dyskerin catalyses uridine residues to the specific site (Fig. 5B) (Brown et al., 2003).

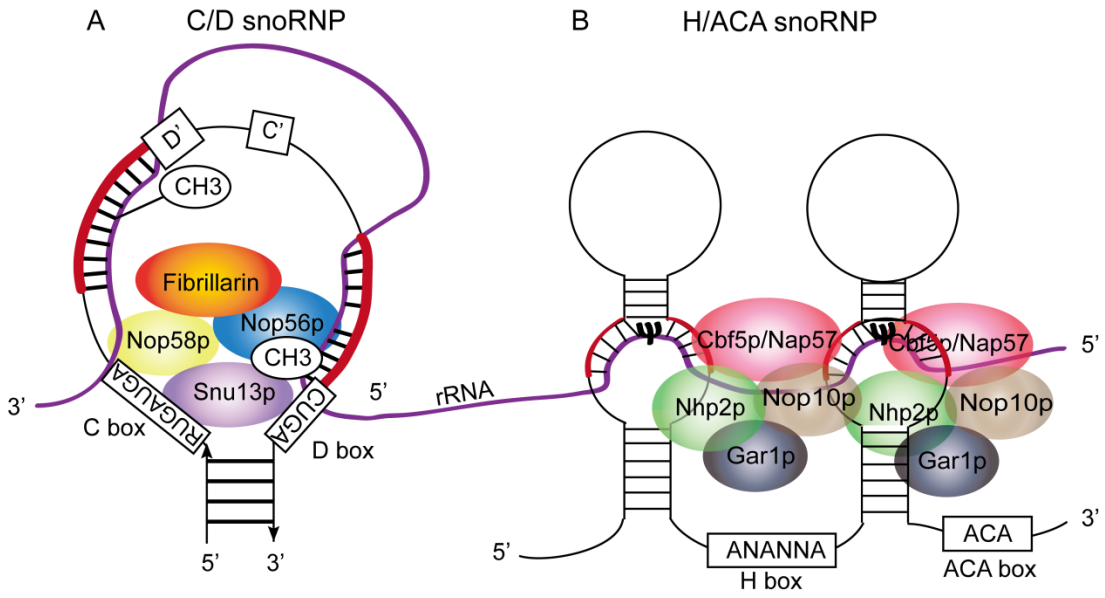

Figure 5: Principal structures of the two classes of snoRNP. The C/D box snoRNAs have two conserved boxes, flanked by short inverted repeats at the 5' and 3' snoRNA ends, respectively (arrows). Next to D box or in internal D' box, there is an rRNA antisense element complementary to a specific region of target rRNA. In yeast, core C/D box snoRNPs are Nop58p, Nop56p, Nop1p and Snu13p, but in humans these four core snoRNPs are NOP58, NOP56, 15.5K and fibrillarin. (b) The H/ACA box snoRNAs include an ACA motif at the 3' end and a Hinge H box linking two stem structures. The C nucleotide is determined by an internal loop in the stems forming short snoRNA–rRNA duplexes flanking the target residue. In yeast H/ACA box core snoRNPs include Nop10p, Nhp2p, Gar1p and Cbf5p , but in humans the four core snoRNPs are NOP10, NHP2, Gar1 and dyskerin *(modified from Brown and Echeverria 2003)* (Brown et al., 2003).

1.2.3 The role of snoRNA in ribosome biogenesis

Ribosome biogenesis plays a key role in many cellular processes. Hyperactive ribosomal biogenesis has been found in cancer (Barna et al., 2008; Kondrashov et al., 2005; Ruggero and Pandolfi, 2003; White, 2005). It has been reported that several tumour suppressors and proto-oncogenes could affect the formation of mature ribosome or regulate the activity of proteins known as translation factors (Boon et al., 2001; Menssen and Hermeking, 2002; Ruggero and Pandolfi, 2003; Seshadri et al.,

1993; Steller, 1995). Some tumour suppressors and proto-oncogenes could regulate malignant progression through altering the ribosome biogenesis. For example, Myc could activate RNA polymerase to promote rDNA transcription (Campbell and White, 2014). Protein biosynthesis is also intimately related with cell cycle and could regulate cell growth. Evidence has shown that changes in rDNA transcription and ribosome biogenesis can contribute to some type of tumorigenesis.

snoRNAs are essential for processing precursor ribosomal RNAs (Lafontaine, 2015; Martin et al., 2014). The majority of snoRNAs are involved in the modification of ribosomal RNAs (rRNA) during their biosynthesis. Our previous results indicated that reduced snoRNA expression and rRNA methylation could impair ribosome biogenesis and protein synthesis (Zhou et al., 2017). Also, the effects of C/D box snoRNA on rRNA methylation contribute to the assembly of functional ribosomes and optimizes translation efficiency.

As showed in Figure. 6, pre-rRNAs are extensively modified by pseudouridylation (ψ) and methylation (M), which are necessary for rRNA right folding, structural stability and interacting potential of rRNA (Kiss et al., 2004; Zemann et al., 2006). snoRNPs take part in this process. Ribosomal proteins are imported into the nucleus and are assembled on the pre-rRNA while it is being transcribed. Then ribosomal proteins assemble the pre-rRNA folds and undergo a series of steps of cleavages to generate the 18S, 5.8S and 28S rRNAs. The 18S rRNA along with 32 ribosomal proteins assembles into the small ribosomal 40S subunit. The 28S, 5.8S and 5S rRNA along with additional 47 ribosomal proteins assembles into the large 60S subunit. Both ribosomal subunits are exported into the cytoplasm in a coordinated manner (Lafontaine, 2015).

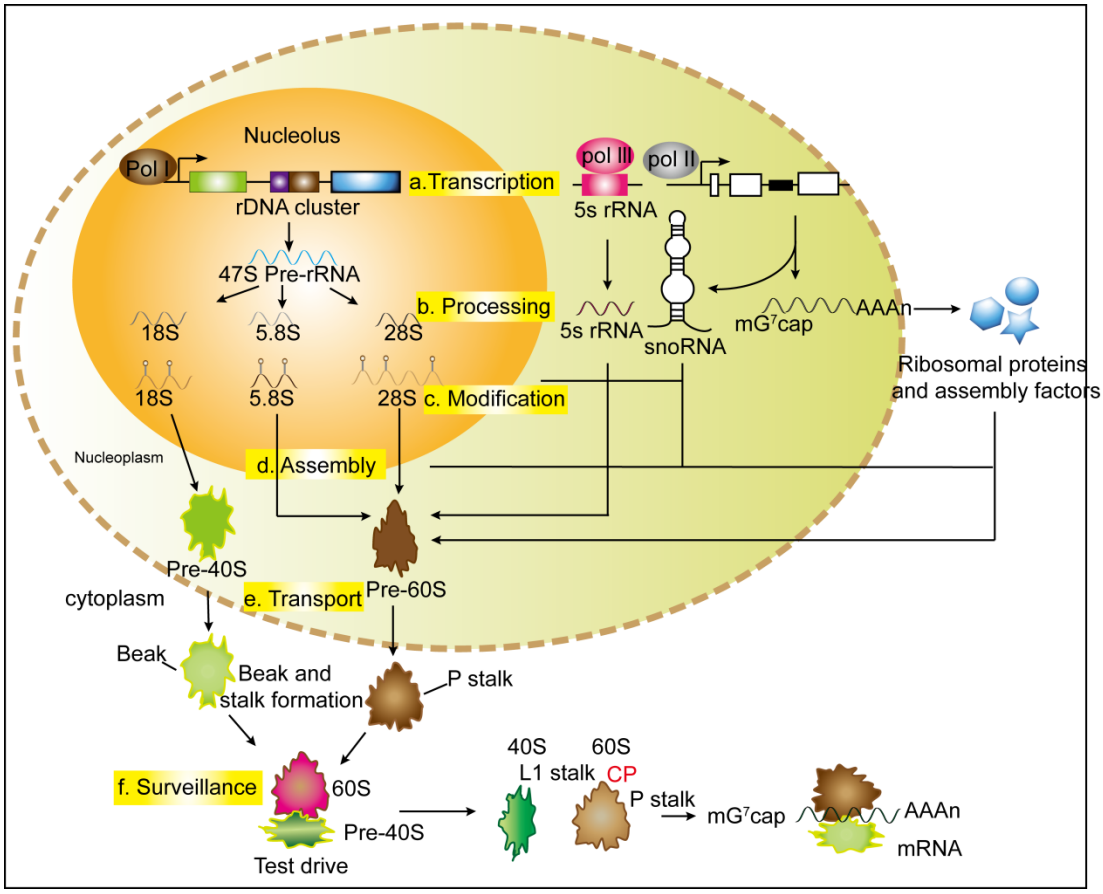

Figure 6: Ribosome biogenesis in eukaryotic cells. (a) transcription of rRNAs, mRNAs encoding ribosomal proteins (RPs) and assembly factors (AFs), and snoRNAs; (b) processing (splicing of pre-rRNAs); (c) modification of pre-RNAs, RPs and AFs; (d) assembly; (e) transport (nuclear import of RPs and AFs; pre-ribosome export to the cytoplasm); and (f) quality control and surveillance. Three rRNAs are transcribed in the nucleolus by Pol I as a long 47S precursor (47S pre-rRNA), which is then processed and modified to yield the 18S, 5.8S and 28S rRNAs that are assembled into the pre-40S (green) and pre-60S (brown) ribosomal subunits. 5S rRNA (pink) is transcribed by Pol III in the nucleoplasm and incorporated into maturing 60S subunits, forming the central protuberance (CP). Eighty RPs, more than 250 AFs and 200 snoRNAs are transcribed by Pol II. These proteins are synthesized in the cytoplasm and imported into the nucleus for assembly. Pre-40S subunits undergo a 'test drive' to prove functionality before final maturation (modified from Denis L. J. Lafontaine, 2015) (Lafontaine, 2015).

1.2.4 The role of pseudouridylation in disease

Post-transcriptional modification of RNA exists in all living organisms. Pseudouridylation is transcriptionally modified by conversion from uridine (U) at a

specific RNA position. Pseudouridylation is the most frequent, ubiquitous and highly conserved modified nucleotide in structured RNAs, containing transfer, ribosomal, and spliceosomal small nuclear RNAs. Although it is known that pseudouridylation can affect the secondary structure and base pairing of RNA, the functional consequences of changes in pseudouridylation have only been clarified in a small number of cases. The functional role of pseudouridylation was first reported in functionally important and evolutionarily conserved regions of tRNA (Grosjean et al., 1995; Hopper and Phizicky, 2003), rRNA (Branlant et al., 1981; Maden, 1990) and snRNA (Karijolich and Yu, 2010; Narlikar et al., 2002). More recently mRNA pseudouridylation was also found in toxoplasma (Nakamoto et al., 2017).

It has been reported that pseudouridylation plays an important role in the function of the ribosome and spliceosome (Karijolich et al., 2010), and mutations in the human pseudouridylation synthase can lead to impaired translation of specific anti-tumour factors and reduced translational fidelity through impairment of the ribosome-ligand interactions (Jack et al., 2011). Also, artificial pseudouridylation could change the genetic code by facilitating non-canonical base pairing in the ribosome decoding centre, dramatically affecting mRNA function (Carlile et al., 2014; Fernandez et al., 2013; Karijolich and Yu, 2011). In toxoplasma gondii, mRNA pseudouridylation could affect RNA metabolism (Nakamoto et al., 2017).

1.2.5 snoRNA in cancer

For many years, snoRNAs have been considered housekeeping genes. But recently, small ncRNAs have been reported to be important in regulating gene expression at many levels, for example, chromatin architecture, transcription, mRNA stability and translation (Karapetyan et al., 2013). . Traditionally, the main focus on the functions of snoRNAs has been ribosome biogenesis or the components of ribonucleoprotein complexes. Recent studies have shown the important role of snoRNA in controlling cell fate and carcinogenesis (Dong et al., 2009; Dong et al., 2008; Liao et al., 2010; Liuksiala et al., 2014; Mei et al., 2012; Su et al., 2014; Valleron et al., 2012). Much evidence also indicates that snoRNAs can promote or suppress tumour development. The first snoRNA found in carcinoma resulted from the study of B cell lymphoma, which identified C/D box snoRNA U50 and its host gene U50HG at the breakpoint of chromosomal translocation (3;6)(q21;q15) (Tanaka et al., 2000). Also, snoRNA

U50 has been found mutation in prostate cancer cells, and U50 mutation and downregulation have also been associated with breast cancer (Dong et al., 2009; Dong et al., 2008).

SNORA42, which is an H/ACA box snoRNA encoded at 1q22, has been reported as frequently over-expressed in NSCLC (Mei et al., 2012; Okugawa et al., 2017). Downregulation of SNORA42 in NSCLC leads to cell line apoptosis and colony formation inhibition. High SNORA42 expression in clinical lung cancer samples has been intimately correlated with patients' poor survival. Furthermore, it has been reported that genomic deletion of either C/D box snoRNA SNORD14D or SNORD35A suppressed clonogenic potential of leukaemia cells in vitro and delayed leukaemogenesis in vivo (Zhou et al., 2017). In addition, it has been reported that snoRNA signatures served as biomarkers in NSCLC (Liao et al., 2010). Liao et al. used three different snoRNAs (snoRD33, snoRD66 and snoRD76) to distinguish NSCLC patients from healthy individuals and chronic obstructive pulmonary disease (COPD) patients with 81.1% and 95.8% specificity (Liao et al., 2010).

In addition to the initial evidence that snoRNAs are involved in cancer development, host genes of snoRNAs might also contribute to the aetiology in cancer. Zfas1, a non-protein-coding snoRNA host gene, has been identified as a tumour-suppressive ncRNA. Downregulation of Zfas1 mRNA in vivo increased proliferation and differentiation without affecting the levels of the snoRNA hosted within its intron. Human ZFAS1 (also known as ZNFX1-AS1), which is predicted to share secondary structural features with mouse Zfas1, is downregulated in breast cancer.

GAS5, another snoRNA host gene, can regulate cell death and survival (Mourtada-Maarabouni et al., 2008; Mourtada-Maarabouni et al., 2009). It has been reported that GAS5 transcripts can regulate both cell death and proliferation. Meanwhile, other investigations found that the snoRNAs encoded in GAS5 have a role in cancer prognosis. SNORD44, which are C/D box snoRNAs that are encoded in GAS5 introns, is significantly associated with prognosis (Appaiah et al., 2011).

Recently, many results have shown the function of different snoRNAs but the molecular mechanism of snoRNA in cancer is still unclear. Increasing evidence

indicates that snoRNAs could be candidates for therapeutic benefits and snoRNA could be used as a biomarker for cancer.

2 Materials and Methods

2.1 Materials

2.1.1 Equipment and Devices

Device	Supplier
CFX96 Touch Real time PCR Detection System	BioRad
Agilent 2100 Bioanalyzer	Agilent Technologies
NanoDrop™ ONE	BioRad
Centrifuge 5427 R	Eppendorf
Centrifuge MiniSpin® plus	Eppendorf
Concentrator plus Gesamtsystem	Eppendorf
Centrifuge 5810	Eppendorf
Centrifuge 5810R	Eppendorf
Rotor A-2-DWP	Eppendorf
Gel Electrophoresis Chamber Sub Cell® GT	BioRad
IKA Vibrax VXR basic	IKA®-Werke
Incubator HeraCell 150	Kendro Laboratory
MACS MultiStand	Miltenyi Biotec GmbH
Magnetic Stirrer IKA RH basic 2	IKA®-Werke
Fluorescence Microscope CKX4	Olympus
Microscope Axiostar Plus Carl	Zeiss
Microscope IMT-2	Olympus
Mini-Protean®3 cell	BioRad
Multipette® plus	Eppendorf
Mr. Frosty™ Freezing Container	Thermo Scientific
NanoDrop Spectrophotometer ND-1000	PEQLAB

Neubauer Counting Chamber 0.0025mm2	Merck
Optimax X-Ray Film Processor	PROTEC
pH-Meter MP225	Mettler-Toledo
Pipetus-Akku	Hirschmann
Powerpack 300	BioRad
Powerpack Biomera	BioRad
CFX Connect™ Real-Time PCR Detection System	BioRad
Precision Scale EG 2200-2NM	Kern & Sohn
Qubit® Fluorometric Quantitation	Life Technologies
QuadroMACS™ Cell Separator	Miltenyi Biote GmbH
TC20 Automated Cell Counter	BioRad
Thermocycler Mastercycler personal	Eppendorf
Thermocycler Mastercycler gradient	Eppendorf
FACS Calibur™	Becton Dickinson
FACS Aria II™	Becton Dickinson
FACS Aria III™	Becton Dickinson
Thermolab 1070 Water Bath	GFL Gesellschaft
Thermomixer comfort	Eppendorf
Thermomixer compact	Eppendorf
Research Pipettes	Eppendorf
Rocker 3D	IKA®-Werke
Scil Vet abc Counter	Scil Animal Care Company
Special Accuracy Scale Mettler AM100	Mettler-Toledo
Vortex Genie2	Bender & Hobein
X-Cell SureLock Electrophoresis Cell	Invitrogen

2.1.2 Consumables

Consumable	Supplier
Cell Strainer, 70 µm Nylon	BD Biosciences
Discardit II syringes	BD Biosciences
Falcon tubes, 15 and 50 ml	BD Biosciences
Microlance Injection Needles	BD Biosciences
Polypropylene Round Bottom-Tubes, 14ml	BD Biosciences
Polystyrene Tubes w/ Cell Strainer Cap, 5ml	BD Biosciences
Combitips	Eppendorf
DNA LoBind Tubes	Eppendorf
Cell Culture Flasks	Greiner Bio-One
CellStar dish	Greiner Bio-One
Multi-well plate	Greiner Bio-One
Hyperfilm™ ECL	GE Healthcare
PVDF Membrane Hybond-P	GE Healthcare
Cell Scraper	Sarstedt
Cryo Pure Tubes	Sarstedt
Flow Cytometry tubes	Sarstedt
Filtropur Filters, S 0.45 and S 0.2	Sarstedt
Biosphere® Filter Tips	Sarstedt
Heparin Capillaries	Sarstedt
Petri dish, 92x16 mm	Sarstedt
Pipette Tips	Sarstedt
Tissue Culture Dish with grid	Sarstedt
Flat 8 Cap PCR Strips	Thermo Fischer Scientific
ThermoFast 96 PCR Detection Plate	Thermo Fischer Scientific

MicroAmp® Fast Optical 96 well reaction plate Applied	Biosystems
MicroAmp™ Optical Adhesive Film Applied	Biosystems
PCR Soft Tubes	Biozym
Reaction Tubes	Biozym
Gel Blotting Paper	Schleicher & Schuell
Glass slides	Engelbrecht Labortechnik
Omnifix® -F single-use syringe, 1 ml	Braun
Supra single-use needles, 2.00x80 mm	Vivomed
Stripettes	Corning
Tube AFA Fiber & Cap 12x12mm	Covaris

2.1.3 Chemicals and reagents

Chemical	Supplier
Ethanol p.a.	Carl Roth
Methanol p.a.	Carl Roth
Milk Powder Blotting Grade	Carl Roth
Sodium dodecyl sulfate (SDS)	Carl Roth
Tris base	Carl Roth
Ethidium bromide (1%)	Carl Roth
4-Thiouridine	Sigma-Aldrich
4-hydroxytamoxifen	Sigma-Aldrich
Etoposide	Sigma-Aldrich
Propidium iodide	Sigma-Aldrich
Glycerol	Sigma-Aldrich
Isopropanol p.a.	Merck
Tween®20	Merck

GeneRuler 50 bp DNA Ladder	Fermentas
GeneRuler™ DNA Ladder Mix	Fermentas
Agar	BD Biosciences
Luria Broth base (LB)	Invitrogen
Nuclease free water	Invitrogen
Novex® Bis-Tris Gel, 4-12%, 10%	Invitrogen
NuPAGE® MOPS SDS Running Buffer	Invitrogen
SeeBlue® Protein Marker	Invitrogen
Trizol reagent	Invitrogen
Phenol/Chloroform/Isoamylalcohol (25:24:1)	Invitrogen
RNase OUT™	Invitrogen
Alexa Fluor® 647 Azide	Invitrogen
TurboFect Transfection Reagent	Thermo SCIENTIFIC
Agarose LE	Biozym
PBS Dulbecco w/o Ca2+, w/o Mg2+	Sigma-Aldrich
Glycogen	Roche
Proteinase Inhibitor Complete	Roche
Random Hexamers Applied	Biosystems
dNTPs	NatuTec
Sephadex G-50 fine DNA Grade	GE Healthcare
ECL-plus Reagent	GE Healthcare
β-Mercaptoethanol	Gibco
Dithiothreitol (DTT)	Promega
Ethylendiaminetetraacetate (EDTA)	Serva
Formaldehyde	Baker
Recombinant RNasin® Ribonuclease Inhibitor	Promega

Agencourt AMPure XP	BECKMEAN COULTER
RNAlater® Solutions	Ambion
O-propargyl-puromycin	Jena Bioscience
SsoAdvanced SYBR® Green Supermix	BioRad

2.1.4 Buffer

Buffer/Solution	Composition
LB-Medium	10 g Bacto-tryptone, 5g yeast extract. 10 g NaCl in 1L H2O, Autoclaved
LB-Agar	15 g/L Agar in LB-Medium, Autoclaved
SOC-Medium	20 g Bacto-tryptone, 5 g Yeast Extract, 2 ml of 5M NaCl, 2.5ml of 1M KCl, 10 ml of 1 M MgCl2, 10 ml of 1M MgSO4, 20 ml of 1 M glucose in 1 LH2O
SOB-Medium	20 g Bacto-tryptone, 5 g Yeast Extract, 2 ml of 5 M NaCl, 2.5 ml of 1 M KCl, 10 ml of 1 M MgCl2, 10 ml of 1 M MgSO4 in 1 L H2O
RIPA Buffer	150 mM NaCl, 1% NP40, 0.5% Deoxycholic acid, 0.1% SDS 50 mM Tris, pH 8.0
Western Blot Transfer Buffer (10×)	144 g Glycin, 30.2 g Tris-base in 1 L ddH2O
Add	20% Methanol before use
Tris-acetate-EDTA Buffer (TAE)	242 g Tris base, 57.1 ml Glacial acetic acid, 100 ml
	0.5M EDTA, pH 8.0 in 20 L ddH2O
FACS buffer	2% FCS in PBS

2.1.5 Cell culture media, reagent and cytokines

Reagent	Supplier
Dulbecco's Modified Eagle Medium (DMEM)	Sigma-Aldrich

Iscove's Modified Dulbecco's Medium (IMDM)	Sigma-Aldrich
RPMI1640	Sigma-Aldrich
Dulbecco's Phosphate Buffered Saline	Sigma-Aldrich
Fetal Calf Serum (FCS)	Biochrom AG
Methocult™ M3434 Methylcellulose	Stem Cell Technologies
Methocult™ M3234 Methylcellulose	Stem Cell Technologies
murine interleukine-3 (IL-3)	Peprotech
human interleukine-6 (IL-6)	Peprotech
murine stem cell factor (SCF)	Peprotech
L-Glutamine	PAA Laboratories
Puromycin	Sigma-Aldrich
Streptomycin	PAA Laboratories
Trypsin	Sigma-Aldrich

2.1.6 Enzymes

Enzyme	**Supplier**
Biotherm™ DNA-Polymerase	Natutec
Pfu Turbo Cx hotstart DNA polymerase	Agilent Technologies
M-MLV Reverse Transcriptase	Promega
Restriction Endonucleases	New England Biolabs
RNase-free DNase I	New England Biolabs
T4 DNA Ligase	New England Biolabs
RNase-free DNase I	New England Biolabs
Proteinase K	Merck
RNase A	Sigma-Aldrich

2.1.7 Kit

Kit	Supplier
5 Prime FastPlasmid Mini Kit	Prime
Z-Competent E. coli Transformation Buffer Set	Zymo Research
Qiagen Rneasy, Micro and Mini	Qiagen
Endo-free Plasmid Midi, Maxi Kit	Qiagen
QIAquick Gel Extraction Kit	Qiagen
QIAquick PCR Purification Kit	Qiagen
BCA™ Protein Assay	Thermo Fischer Scientific
BigDye Terminator Sequencing Kit 3.1 Applied	Biosystems,
Gateway Cloning	Invitrogen
MACS Lineage Cell Depeletion Kit	Miltenyi Biotech
mirVana™ miRNA Isolation Kit	Life Technologies
ChIP-IT ® Express Chromatin Immunoprecipitation Kits	Active Motif
IPure kit	Diagenode
TruSeq ChIP Sample Prep Kit	Illumina
Qubit® dsDNA HS Assay Kit	Life Technologies
PEG-it™ Virus Precipitation Solution System	Biosciences (SBI)
Click-iT® Cell Reaction Buffer Kit	Life Technologies
TruSeq Stranded Total RNA Sample Prep Kit	Illumina

2.1.8 Antibodies

2.1.8.1 Antibodies for Protein Detection by Western Blot

Antibody Cat No.	Dilution	Supplier
Anti-NOP10 antibody ab133726	1:1000	abcam
Anti-NOP58 antibody ab155969	1:2000	abcam

Nop56 Antibody (Q-24) sc-133839	1:2000	abcam
Fibrillarin (C13C3) mAb 2639 S	1:1000	abcam
anti-β-actin monoclonal (8C-15)	1:5000	Sigma-Aldrich
mouse IgG polyclonal	1:5000	Dianova
rabbit IgG polyclonal	1:5000	Dianova

2.1.8.2 Antibodies for Flow Cytometry

Antibody Clone	Conjugate	Supplier
Anti-BrdU 552598	APC	BD Biosciences
Anti-IL7Rα A7R 34	PE-Cy™7	BioLegend

2.1.9 Primers

Gene / Oligo name Application Sequence (5'→3')

Name	Application	Sequence (5'-3')
NOP10-KO-1-S	Clone	CACCGccagtattacctcaacgagc
NOP10-KO-1-AS	Clone	AAACgctcgttgaggtaatactggC
NOP10-KO-2-S	Clone	CACCGagatcgagtctatacgctga
NOP10-KO-2-AS	Clone	AAACtcagcgtatagactcgatctC
NOP10-KO-3-S	Clone	CACCGGAGCAGAAATTTGACCCGA
NOP10-KO-3-AS	Clone	AAACTCGGGTCAAATTTCTGCTCC
NOP10-KO-4-S	Clone	CACCGcctgctcagcccatcctgct
NOP10-KO-4-AS	Clone	AAACagcaggatgggctgagcaggC
NOP10-KO-5-S	Clone	CACCGcaaccgcgccctgtcctctg
NOP10-KO-5-AS	Clone	AAACcagaggacagggcgcggttgC
NOP10-KO-6-S	Clone	CACCGAGGACAGGGCGCGGTTGCT
NOP10-KO-6-AS	Clone	AAACAGCAACCGCGCCCTGTCCTC
NOP10-KO-7-S	Clone	CACCgTCATCTGGGGAGAACCGAGC
NOP10-KO-7-AS	Clone	AAACGCTCGGTTCTCCCCAGATGAc
NOP10-KO-8-S	Clone	CACCGACCCTCAGAGGACAGGGCG
NOP10-KO-8-AS	Clone	AAACCGCCCTGTCCTCTGAGGGTC
SNORA 76-KO-1-S	Clone	CACCgCGGTTAAAAAGGCCGCCCGC

SNORA 76-KO-1-AS	Clone	AAACGCGGGCGGCCTTTTTAACCGc
SNORA 76-KO-2-S	Clone	CACCgCTTGTCGCTCGCGGTTAAAA
SNORA 76-KO-2-AS	Clone	AAACTTTTAACCGCGAGCGACAAGc
SNORA 76-KO-3-S	Clone	CACCGAGCTTCCTCGTGGCGCCGG
SNORA 76-KO-3-AS	Clone	AAACCCGGCGCCACGAGGAAGCTC
SNORA 31-KO-1-S	Clone	CACCgTGTGGCGGCCCAGATTGAAT
SNORA 31-KO-1-AS	Clone	AAACATTCAATCTGGGCCGCCACAc
SNORA 31-KO-2-S	Clone	CACCgAATTGTTCAAGGTCTATCAG
SNORA 31-KO-2-AS	Clone	AAACCTGATAGACCTTGAACAATTc
SNORA 31-KO-3-S	Clone	CACCgCAAAGACAGACAGAAAGCGC
SNORA 31-KO-3-AS	Clone	AAACGCGCTTTCTGTCTGTCTTTGc
SNORA 63-KO-1-S	Clone	CACCgTGTATGAGACCAAGCGTCCC
SNORA 63-KO-1-AS	Clone	AAACGGGACGCTTGGTCTCATACAc
SNORA 63-KO-2-S	Clone	CACCgCAAGCGTCCCTGGCTGCTAC
SNORA 63-KO-2-AS	Clone	AAACGTAGCAGCCAGGGACGCTTGc
SNORA 63-KO-3-S	Clone	CACCgACAACTTTATTTTAAGCAGG
SNORA 63-KO-3-AS	Clone	AAACCCTGCTTAAAATAAAGTTGTc
SNORA 68-KO-1-S	Clone	CACCgCAAGCGGATCTTGTCGCCTT
SNORA 68-KO-1-AS	Clone	AAACAAGGCGACAAGATCCGCTTGc
SNORA 68-KO-2-S	Clone	CACCgCGTGCCCCTCAAAGTGAATT
SNORA 68-KO-2-AS	Clone	AAACAATTCACTTTGAGGGGCACGc
SNORA 68-KO-3-S	Clone	CACCgCGGATCTTGTCGCCTTTGGG
SNORA 68-KO-3-AS	Clone	AAACCCCAAAGGCGACAAGATCCGc
SNORA 26-KO-1-S	Clone	CACCGTGTTAGCCTCTTAAAGCAC
SNORA 26-KO-1-AS	Clone	AAACGTGCTTTAAGAGGCTAACAC
SNORA 26-KO-2-S	Clone	CACCGCTCCTCTTTGGATCCTGTC
SNORA 26-KO-2-AS	Clone	AAACGACAGGATCCAAAGAGGAGC
SNORA 26-KO-3-S	Clone	CACCgTGTTAGCCTCTTAAAGCACT
SNORA 26-KO-3-AS	Clone	AAACAGTGCTTTAAGAGGCTAACAc
SNORD76-KO-1-S	Clone	CACCGGGTGCCTCAGTTAAGATAA
SNORD76-KO-1-AS	Clone	AAACTTATCTTAACTGAGGCACCC
SNORD76-KO-2-S	Clone	CACCgAACCACCATTATCTTAACTG
SNORD76-KO-2-AS	Clone	AAACCAGTTAAGATAATGGTGGTTc
SNORD76-KO-3-S	Clone	CACCgTCTTGAGTGCTAGAATGATG
SNORD76-KO-3-AS	Clone	AAACCATCATTCTAGCACTCAAGAc
SNORD14D-KO-1-S	Clone	CACCgTGACTGACTCGCTATGATGA
SNORD14D-KO-1-AS	Clone	AAACTCATCATAGCGAGTCAGTCAc

SNORD14D-KO-2-S	Clone	CACCgTTTCTGGTGGAAACTACGAA
SNORD14D-KO-2-AS	Clone	AAACTTCGTAGTTTCCACCAGAAAc
SNORD14D-KO-3-S	Clone	CACCgAATGGTCGCTCAAACATCCA
SNORD14D-KO-3-AS	Clone	AAACTGGATGTTTGAGCGACCATTc
SCR-1-S	Clone	CACCGATATCCGGAATTCGCGCGAT
SCR-1-AS	Clone	AAACATCGCGCGAATTCCGGATATC
SCR-2-S	Clone	CACCGTCGATCGTCAAGCAGATCG
SCR-2-AS	Clone	AAACCGATCTGCTTGACGATCGAC
Scrambel-ko-3-S	Clone	CACCGCACTACCAGAGCTAACTCA
Scrambel-ko-3-AS	Clone	AAACTGAGTTAGCTCTGGTAGTGC
Scrambel-ko-4-S	Clone	CACCgCGCTGAGTACTTCGAAATGT
Scrambel-ko-4-AS	Clone	AAACACATTTCGAAGTACTCAGCGc
LV-NOP10-GFP-S	Clone	CTCCCCAGGGGGATCCAtgtttctccagta ttacctcaacgagcag
LV-NOP10-GFP-AS	Clone	TGGCGACCGGTgcgaggacagggcgcggttg ctg
SNORA65-OV-S	Clone	caccggcgccggatccATTGAGGTGGTGCC TTCTGCCTC
SNORA65-OV-AS	Clone	tgctcaccatctcgagCAGAGAGTTCTCTGG CTAAGGAT
SNORA7A/B-KO-S-1	Clone	CACCgTCTGCCAGCTTCGGAAAGGG
SNORA7A/B-KO-AS-1	Clone	AAACCCCTTTCCGAAGCTGGCAGAc
SNORA7A/B-KO-S-2	Clone	CACCgTgacctcctgggatcgcatc
SNORA7A/B-KO-AS-2	Clone	AAACgatgcgatcccaggaggtcAc
SNORA7A/B-KO-S-3	Clone	CACCgTATTCTGCCAGCTTCGGAAA
SNORA7A/B-KO-AS-3	Clone	AAACTTTCCGAAGCTGGCAGAATAc
SNORA7A/B-KO-S-4	Clone	CACCgtctccagatgcgatcccagg
SNORA7A/B-KO-AS-4	Clone	AAACcctgggatcgcatctggagac
NOP10(MUS)-KO-S-1	Clone	CACCgCCAATATTACCTCAACGAGC
NOP10(MUS)-KO-AS-1	Clone	AAACGCTCGTTGAGGTAATATTGGc
NOP10(MUS)-KO-S-2	Clone	CACCgCGATCGCGTTTATACGCTGA
NOP10(MUS)-KO-AS-2	Clone	AAACTCAGCGTATAAACGCGATCGc

Name	Application	Sequence (5'-3')
SNORA3	Real-Time PCR	GAGGCTAGAGTCACGCTTGG
SNORA80B-RT-S	Real-Time PCR	GATTATGACAGGCCCATCCCC
SNORA6-RT-S	Real-Time PCR	CTGAGTGTCGGAAGTGTGCTA

SNORA67-RT-S	Real-Time PCR	CTCTCCAAGGGGACATCAGT
SNORA64-RT-S	Real-Time PCR	TTCACCCGTGTGACTTTCGT
SNROA52-RT-S	Real-Time PCR	CTAATCCCTGCCGGTCCATC
NOP10 (hum)-RT-S	Real-Time PCR	TACCTCAACGAGCAGGGAGA
NOP10 (hum)-RT-AS	Real-Time PCR	CTGGGTCATGAGCACCTTGA
DKC1 (hum)-RT-S	Real-Time PCR	CGGTCATCTCTACCTGCGAC
DKC1 (hum)-RT-AS	Real-Time PCR	TGGCAGACTCACTGTAGTCAA
ACTIN (hum)-RT-S	Real-Time PCR	AGGCACCAGGGCGTGAT
ACTIN (hum)-RT-AS	Real-Time PCR	GCCCACATAGGAATCCTTCTGAC
SNORA9	Real-Time PCR	TGCTTGGGTCTGCAGTGAC
SNORA7A/7B-RT-S	Real-Time PCR	gtattctgccagcttcggaaagg

2.2 Methods

2.2.1 Molecular Biology

2.2.1.1 Polymerase Chain Reaction (PCR)

DNA template	5 ng
Primer For (10 µM)	1 µl
Primer Rev (10 µM)	1 µl
dNTPs (10 mM)	1 µl
10× PCR Reaction Buffer	5 µl
DNA polymerase*	1 µl
Nuclease-Free Water	Fill up to 50 µl
Total Volume	50 µl

*For cloning PCR, HerculaseII DNA fusion polymerase was used,

PCR for other purpose Taq DNA-Polymerase was used

Thermal Cycling program:

	Temperature	Time	Number of Cycle
Initial denaturation	95 °C	3 minutes	1
Denaturation	95 °C	30 seconds	30-34
Annealing	55-60 °C *	30 seconds	
Extension	72 °C	1 kb/min	
Final extension	72 °C	10 minutes	1
Hold on	4 °C		

* depends on melting temperature of primer

PCR product was loaded on agarose gel, and then purified with Zymoclean™ Gel DNA Recovery Kit.

2.2.1.2 Restrict digestion, DNA ligation

FastDigest Restriction enzymes were used according to the manufacturer's instructions concerning FastDigest buffer, addition of DTT. PCR fragment with restriction sites or less than 1µg plasmid DNA were digested in 30µl reaction volume for subcloning. Normally 1µg plasmid DNA was used for analytical digestion. Then the digested DNA was loaded on agarose gel for separation and analysis.

Digested DNA fragment with blunt or stick end and vector were ligated with T4 DNA ligase from ThermoFisher (5U/ul). The molecular ratio of PCR fragment and vector was 1:1 to 5:1. Ligation reaction was performed in thermal cycler at 22°C for more than 2 hours.

2.2.1.3 Agarose gel electrophoresis, visualization, extraction

According to different size of PCR fragment or vector, agarose gel electrophoresis has been performed with gels containing 1-2.5% agarose and 0.5 mg/ml ethidium bromide at constant voltage of 100 V for 60-120 minutes. 1×TAE buffer has been used for the running buffer. Appropriate DNA standard marker and DNA samples

were mixed with 6 × loading dye. VILBER imaging system has been used to visualize the gel under UV light.

Gel extraction was performed with Zymoclean™ Gel DNA Recovery Kit following user's manual guide.

2.2.1.4 RNA isolation

Total RNA was isolated from NSCLC patients samples, cultured cells or FACS-sorted cells using mirVana™ miRNA Isolation Kit according to manufacturer's instructions. Briefly, patients tissue or up to 5×10^5 freshly processed cells or cells stored in RNAlater® Solutions were properly pelleted by centrifuge. Cell pellet was resuspended in 600 µl lysis/binding buffer and was pipetted vigorously to completely lyse the cells to obtain a homogenous lysate. 60 µl MiRNA Homogenate Additive was added to the cell lysate and mixed by vortexing 30 seconds; kept the mixture on ice for 10 minutes. Acid-Phenol: 60 µl Chloroform was added and vortex for 1 minute to mix completely. Phase separation was achieved by centrifugation at 10,000 × g for 5 minutes at room temperature. Carefully removed the upper colorless phase, which contains total RNA, transferred it to a new tube. 750 µl 100% ethanol was added to the upper phase, the lysate/ethanol mixture was applied to the filter cartridge. RNA was isolated by centrifugation at 10,000 × g for 15 seconds at room temperature. Finally total RNA was eluted in 100 µl RNase-free water after two times washing with wash solution. Isolated RNA was stored at -80 °C or immediately used for cDNA synthesis.

2.2.1.5 cDNA synthesis

0.5-1 µg RNA was used for reverse transcription (cDNA synthesis). Before reverse transcription, RNA was treated with DNase I at 37 °C for 30 minutes to remove the residual DNA in the RNA preparations:

RNA	0.5-1 µg
DNaseI (1U/ µl)	1 µl
10 × DNase I Buffer	1 µl
RNase out	1 µl

RNase-free water	
Total Volume	10 µl

After incubation, 1 µL 50 mM EDTA was added and incubated at 65 °C for 10 min to inactive DNase I. Then 1 µl random primer (300 nM) was added to the RNA and incubated at 70°C for 5 minutes to melt secondary structure of RNA template. After a quick chill on ice, reverse transcription was performed as:

RNA template/primer	12 µl
dNTPs (10 mM)	1 µl
5× M-MLV Reaction Buffer	5 µl
RNase out	1 µl
M-MLV RT (H–) Point Mutant	1 µl
Nuclease-Free Water	5 µl
Total Volume	25 µl

The cDNA was diluted into 100 µl by adding 75 µl Nuclease-Free water and stored at -20 °C after measurement by NanoDrop Spectrophotometer ND-1000.

2.2.1.6 Real-time PCR

All primers for quantitative real time PCR were designed by the Primer-BLAST tool from National Center for Biotechnology Information (NCBI, http://www.ncbi.nlm. nih .gov/tools/primer-blast/). Specificity of all primers was checked by blast search to specified database. And all the primers were synthesized by the company Biolegio. Real-time RT-PCR was performed using a SYBR green supermix as following:

SYBR Green LowROX Mix (2×)	6.25 µl
Forward Primer (1 µM)	1 µl
Reverse Primer (1 µM)	1 µl
cDNA template (about 200 ng/ µl)	1 µl
Nuclease-Free Water	3.25 µl

Total volume	12.5 µl

Reaction was run on CFX96^{TM} Real-Time System with Thermal Cycling program:

	Temperature	Time	Number of Cycle
Enzyme Activation	95 °C	15 minutes	1
Denaturation	95 °C	15 seconds	40
Annealing	55-60 °C *	30 seconds	
Extension	72 °C	1 minute	
Dissociation	95 °C	15 seconds	1
	60 °C	1 minute	
	95 °C	15 seconds	

*depends on melting temperature of each pair of primer

For each pair of primer, one no template control (NTC) was always included to ensure that all solutions used for real-time PCR have not been contaminated by template DNA. Meanwhile *GAPDH* or *beta-actin* was used as loading control for the normalization of mRNA, *U6* or *5.8s rRNA* was used to normalize small nucleolar RNA (snoRNA). Relative quantification of gene expression was performed using the comparative threshold method.

2.2.1.7 Vector construction

pLKO.1 vectors expressing shRNA targeting NOP10 have been described previously ((Steffen et al., 2011; Yan et al., 2006). To clone pLKO.1 vectors expressing shRNA against human NOP10, annealed oligoes were inserted into the AgeI and EcoRI double digested vector. pL-CRISPR.EFS.GFP vectors expressing SpCas9 and sgRNA has been described in addgene. To clone pL-CRISPR.EFS.GFP vectors expressing sgRNA against human or mouse NOP10, DKC1 and snoRNAs, annealed oligoes were inserted into the Esp3I digested vector. All vectors were confirmed by sequencing before use.

2.2.1.8 Isolation of genomic DNA

For isolation of genomic DNA from cultured cells, DNase Blood and Tissue kit from QIAGEN was used according to manufacturer's instruction. Briefly, 100 cells up to 5 x 10^6 cells were pelleted by centrifuge and washed with PBS for one time. Cell pellet was suspended in 200 µl PBS. Then 20 µl proteinase K and 200 µl Buffer ALwas added. Mixed thoroughly by vortexing, and incubated at 56°C for 10 min. Added 200 µl ethanol (96–100%) to the sample, and mixed thoroughly by vortexing. Pipetted this mixture into the DNeasy Mini spin column placed in a 2 ml collection. Centrifuged at 6000 x g for 1 minute. Washed the column with the buffer provided by the kit. Finally genomic DNA was eluted in 200 µl elution buffer and stored at -80 °C.

2.2.1.9 Western blot analysis

30 µg to 40 µg total cell lysates were resolved by NuPAGE™ 4-12% SDS-PAGE (ThermoFisher), and proteins were transferred to nitrocellulose membranes (GE Healthcare). Membranes were blocked with 5% milk in PBST at 4 °C overnight, and then incubated with PBST (0.05% Tween 20) diluted primary antibodies for 2 hours at room temperature. Membranes were washed six times with PBST and incubated in 5% milk diluted HRP-conjugated secondary antibodies for 90 minutes at room temperature. Membranes were then washed six times with PBST and were incubated with ECL reagent for 1 minute and took image with Amersham Imager 600. Primary and secondary antibodies used for detection are listed in Table with indicated dilution. Beta-actin was used as loading control for normalization of protein level.

2.2.2 Cell culture, lentivirus infection, protein extraction

2.2.2.1 Cell culture

The 293T cells were cultured in Dulbecco's modified Eagle's medium (DMEM) supplemented with 10%FBS and 1% P/S. Human A549, Pc-9, H1650, H661, H358, H1975 cells were cultured in RPMI1640 medium supplement with 10% FBS and 1% P/S. Human leukemic Kasumi-1 cells were cultured in RPMI1640 medium with 20% FBS and 1% P/S. All cells were maintained in incubator at 37°C and 5% CO2. To digest adherent cells, firstly the culture media was completely removed from the

flask or dish, and wash the cells with 1×PBS for one time, then add 0.05 % trypsin-EDTA to the flask or dish and incubate at 37 °C for 5 minutes to make cells detach from the bottom of flask. Add appropriate prewarmed media to the detached cells and collected cell pellet by centrifugation at 1200 rpm for 5 minutes at room temperature. The cell pellet was resuspended in appropriate volume of prewarmed culture medium and desired number of cells was transferred to new culture flasks or dishes. Suspension cells were passaged once two or three days.

For freezing cells, each cell pellet were resuspended in 1ml of ice-cold freezing FBS with 10% DMSO and transferred into cryotubes. Then, cryotubes were placed in Mr. Frosty™ Freezing Container, stored at -80 °C overnight and transferred into liquid nitrogen for long-term storage.

2.2.2.2 Lentivirus production and cell infection

Lentivirus was made by the third generation system. Change the media one hour before transfection. pL-CRISPR.EFS.GFP vector expressing SpCas9 and sgRNA (transfer vector) together with packaging vectors (VSVG, pLP1 and pLP2) were transfected into 293T cell using Turbofect as following:

For 150 cm dish:

VSVG	4 μg
pLP1	7.2 μg
pLP2	2.4 μg
pL-CRISPR.EFS.GFP	10.4 μg
Total DNA	24 μg
Turbofect	48 μl

Incubated the mixture at room temperature for 20 minutes, and added the mixture to each plate at a droplet manner. Changed the media 5 hours after transfection. 72 hours post transfection, the media containing lentivirus particles was collected and filtered through 0.45μm filter unit to get rid of cell debris, then concentrated the virus at 29000rpm, 2 hours with extra centrifuge. Concentrated lentivirus was aliquoted immediately and sorted at -80 °C. The whole process should be performed on ice.

To infect human NSCLC cell line A549, Pc-9, H1650, H661, H358, H1975, 50 μl concentrated virus and polybrene (final concentration should be 8 μg/ml) was added into one well of 6-well plate which containing 5×10^5 cells in 2ml media and cultured for 48 hours. To infect human Kasummi-1 100 μl concentrated virus and polybrene (final concentration should be 8 μg/ml) was added into one well of 12-well plate which containing 1×10^6 cells in 1ml medium and centrifuge at 600g for 40 minutes, then cultured cells for 48 hours. Infected cells were checked through expression of GFP under fluorescent microscope. After 48 hours, cells were sorted by FACS. Then sorted cells were used for western blot, colony-forming assay, differentiation, cell apoptosis and cell cycle analysis.

2.2.2.3 Colony formation of human cancer cells

Sterile 2% soft agar in PBS was prepared before starting colony formation assay. GFP positive human NSCLC cell lines A549, Pc-9, H1650, H661, H358 and H1975 were sorted and put into RPMI1640 media supplement with 10% FBS and 1% P/S, incubated at 37 °C overnight to allow cells recover from potential damage from FACS sorting. The next day melt 2% soft agar with microwave, and diluted it to 0.5% soft agar with prewarmed RPMI1640. Added 2 ml 0.5% soft agar to each well of 6-well plate, and incubated at room temperature for 20 minutes. Prewarmed 8.5 ml RPMI1640 media supplement with 10% FBS and 1% P/S for each kind of cells. Then digested the cells and resuspended the cells in RPMI1640 medium supplement with 10% FBS and 1% P/S. Counted the cells, added 3.3×10^4cells for each tube including prewarmed meida. Added 1 ml 2% soft agar to each tube and mixed immediately, aliquoted 1 ml mixture to each well containing 2 ml base agar. Incubated at room temperature for 20 minutes, added 1 ml RPMI1640 media supplement with 10% FBS and 1% P/S on the top agar. The plate was incubated at 37°C and 5% CO2 for two weeks.

For human leukemia cell line Kasumi-1, cells were put back into RPMI1640 media supplement with 20% FBS and 1% P/S after sorting. The next day prepared methylcellulose at the density of 300 cells per ml methylcellulose each well of 6-well plate, incubate the plate at 37°C and 5% CO2 for one week.

Only colonies contained more than 50 cells were counted. Three independent experiments were performed for each kind of cells, and the number of colonies was compared using paired *t* test.

2.2.2.4 Protein extraction

To get total cells lysates, 2×10^6 cells were pelleted by centrifuge at 1400 rpm at room temperature for 5 minutes, and wash the cells with cold PBS for two times. Then cell pellet was suspended in 200µl ice-cold RIPA buffer supplement with complete proteinase inhibitor. Cell lysate was incubated on ice for 10 minutes. Centrifuge the cell lysate at 13,000 rpm (4 °C) for 10 minutes and removed the insoluble material. The supernatant was transferred to new 1.5ml eppendorf tube and protein concentration was measured with BCA™ Protein Assay kit on Nanodrop ONE. Added 4×loading buffer to the protein lysate and incubate at 70 °C for 10 minutes. Protein lysate can be used directly for western blot or frozen at -80 °C for long term storage.

2.2.2.5 Protein synthesis measurement

Up to 1×10^5 sorted cells expressing scramble or gene specific sgRNA were plated in 2ml RPMI1640 media with 10% FBS and 1% P/S in 12-well plate. After 24 hours, O-propargyl-Puromycin was added to the culture media to a final concentration of 50µM, and incubated it at 37°C, 5% CO2 for 1 hour, and then cells were digested and collected from wells by centrifugation, then washed the cells with Ca^{2+} and Mg^{2+} free phosphate buffered saline (PBS) for two times. Cells were fixed in 500 µl of 1% paraformaldehyde on ice for 15 minutes. Cells were washed with 2ml PBS for two times, and then permeabilized with 200 µl 0.1% saponin containing 3% fetal bovine serum at room temperature for 5 minutes. The azide-alkyne cycloaddition was performed using the Click-iT Cell Reaction Buffer Kit and azide conjugated to Alexa Fluor 647 at 2.5 µM final concentration. After incubation at room temperature for 30 minutes, the cells were washed with 2 ml PBS for two times and then resuspended in 400 µl staining buffer for analysis by flow cytometry. The FACS data was collected and analyzed on FlowJo software.

2.2.2.6 Transwell

Prepare cell suspensions in serum free culture medium containing 5000 cells/ml for 24 well invasion chambers. Add 0.2 ml of cell suspension (1000 cells) to each 24 well invasion chamber. Add 0.75 ml chemoattractant (10% FBS culture medium) to the bottom wells of 24 well plates; be sure that no air bubbles are trapped beneath the permeable support membranes. Incubate cell invasion chambers overnight in a humidified tissue culture incubator at 37 ^{o}C, 5% CO2 atmosphere. The bottom medium was changed every day. After three days, cleaned the cells on top of the membrane with cotton and stained cells on the lower level of the membrane.

2.2.3 BrdU staining

Cells were plated in 6-well plate after sorting. The next day adherent cell cultures was pulsed by adding 60 ml of the diluted BrdU (1mM) to each well and incubating for 2 hours at 37°C. The medium from the wells was removed, digested cells with Tripson, washed the cells with PBS for one time. The cells were fixed by adding 100 µl of BD Cytofix/Cytoperm Buffer per tube, incubated the cells for 30 minutes at room temperature. Cells were washed with 1 mL 1X BD Perm/Wash Buffer. Centrifuged for 5 minutes at 1500rpm, and discarded the supernatant. Cells were resuspended in 1 ml staining buffer and put in 4 degree freezer overnight. Centrifuged for 5 minutes at 1500rpm, and discarded the supernatant at the second day. Cells were resuspended in 100 µl of BD Cytoperm Permeabilization Buffer Plus per tube. Then the cells were incubated for 10 minutes at RT. Washed the cells in 1 mL 1× BD Perm/Wash Buffer. Cells were resuspended in 100 µl of BD Cytofix/Cytoperm Buffer per tube and incubated the cells for 5 minutes at room temperature. Cells were washed with 1 ml 1× BD Perm/Wash Buffer. Centrifuged for 5 minutes at 1500rpm, and discarded the supernatant. Resuspended the cells in 100 µl of diluted DNase (diluted to 300 µg/mL in DPBS) per tube. Cells were incubated for 1 hour at 37°C and washed the cells in 1 mL of 1X BD Perm/Wash Buffer. Centrifugd for 5 minutes at 1500rpm, and discarded the supernatant. Cells were resuspended in 50 µL of BD Perm/Wash Buffer containing diluted fluorescent anti-BrdU, and incubated the cells for 20 minutes at room temperature, washed the cells in 1 mL 1X BD Perm/Wash Buffer. Centrifuged for 5 minutes at 1500rpm, and discarded the supernatant. Then cells were resuspended in 20 µl of the 7-AAD

solution. 300 ml staining buffer was added. Stained cells were acquired on a flow cytometer. The FACS data was collected and analyzed on FlowJo software.

2.2.4 BrdU pulse chase

2×10^5 sorted cells expressing scramble or gene specific sgRNA were plated in 2ml RPMI1640 media with 10% FBS and 1% P/S in 6-well plate. Pulse the adherent cell cultures by adding 60 ml of the diluted BrdU (1mM) to each well and incubated for 1 hour at 37°C, 5% CO2. Removed the medium from the wells, added new fresh medium and incubated continually at 37°C, 5% CO2. Cells were collected with Tripson at different time point (0 hour, 2.5 hours, 5 hours, and 7.5 hours after incubation). Cells were washed with PBS for one time and fixed cells by adding 100 µl of BD Cytofix/Cytoperm Buffer per tube, incubated cells for 30 minutes at room temperature. Cells were washed with 1 mL 1X BD Perm/Wash Buffer and centrifuged cells for 5 minutes at 1500rpm, and discarded the supernatant. Resuspended the cells in 1 ml staining buffer and put in 4 degree freezer overnight. Centrifuged for 5 minutes at 1500rpm, and discarded the supernatant at the second day. Cells were resuspended in 100 µl of BD Cytoperm Permeabilization Buffer Plus per tube and incubated cells for 10 minutes at room temperature. Then cells were washed in 1 ml of 1X BD Perm/Wash Buffer and centrifuged for 5 minutes at 1500rpm, and discarded the supernatant. Cells were resuspended in 100 µl BD Cytofix/Cytoperm Buffer per tube and incubate the cells for 5 minutes at room temperature. Washed cells in 1 ml 1X BD Perm/Wash Buffer. Centrifuged for 5 minutes at 1500rpm, and discarded the supernatant. Resuspended the cells in 100 µl of diluted DNase (diluted to 300 µg/mL in DPBS) per tube. Cells were incubated cells at 37°C for 1 hour and washed the cells in 1 ml of 1X BD Perm/Wash Buffer. Then cells were resuspended in 50 µl of BD Perm/Wash Buffer containing diluted fluorescent anti-BrdU and incubated the cells for 30 minutes at room temperature. Cells were then washed with 1 ml of 1X BD Perm/Wash Buffer. Centrifuged for 5 minutes at 1500rpm, and discarded the supernatant. To stain the nuclear, cells were resuspended in 20 µl of the 7-AAD solution. Finally 300 µl staining buffer was added to the tube and acquired stained cells on a flow cytometer. The FACS data was collected and analyzed on FlowJo software.

2.2.5 Cell divisions assay

Cells were prepared in 6-well plate. Cells were washed two times to remove any serum. Cells were digested with trypsin, and resuspended cells in 5 μM solution of Cell Proliferation Dye eFluor™ 670. Cells were incubated for 10 minutes at 37°C in the dark and stopped labeling by adding 4-5 volumes of cold complete media (containing ≥10% serum) and incubated on ice for 5 minutes. Cells were washed 3 times with complete media and incubated with complete media at 37°C, 5% CO2. The FACS data were collected after 24 hours and analyzed on FlowJo software.

2.2.6 Senescence β-Galactosidase Staining

2×10^5 sorted cells expressing scramble or gene specific sgRNA were plated in 2ml RPMI1640 media with 10% FBS and 1% P/S in 6-well plate. The next day growth media was removed from the cells and rinsed the plate one time with 1X PBS. Added 1 ml of 1× Fixative Solution to each well and allowed cells to fix for 10-15 min at room temperature. Then the plate was rinsed two times with 1X PBS. 1 ml of the β-Galactosidase Staining Solution was added to well and the plate was incubated at 37°C at least overnight in a dry incubator (no CO_2). While the β-galactosidase was still on the plate, check the cells under a microscope (200 × total magnifications) for the development of blue color. Finally removed the β-Galactosidase staining solution and overlay the cells with 70% glycerol. The plate was stored at 4°C fridge.

2.2.7 Statistical analysis

All numerical data were expressed as Mean ± SD or Mean ± SEM. Data were analyzed using the student's t test or one-way ANOVA analysis. $P<0.05$ was considered statistically significant (*, $P<0.05$; **, $P<0.01$; ***, $P<0.005$).

3. Results

3.1 H/ACA box snoRNPs expression in NSCLC

3.1.1 NOP10 is upregulated in lung cancer tissue

To identify expression of conserved H/ACA box snoRNPs in NSCLC, western blot was performed for several matched normal-tumour NSCLC specimens. These western blot results showed that NOP10 protein was highly expressed in tumour samples compared to non-afflicted lung tissue (Fig. 7). In addition, DKC1 and Gar1 proteins were also highly expressed in tumour samples. However, NHP2 protein was lower expressed in tumour samples compared to normal tissue (Fig. 7).

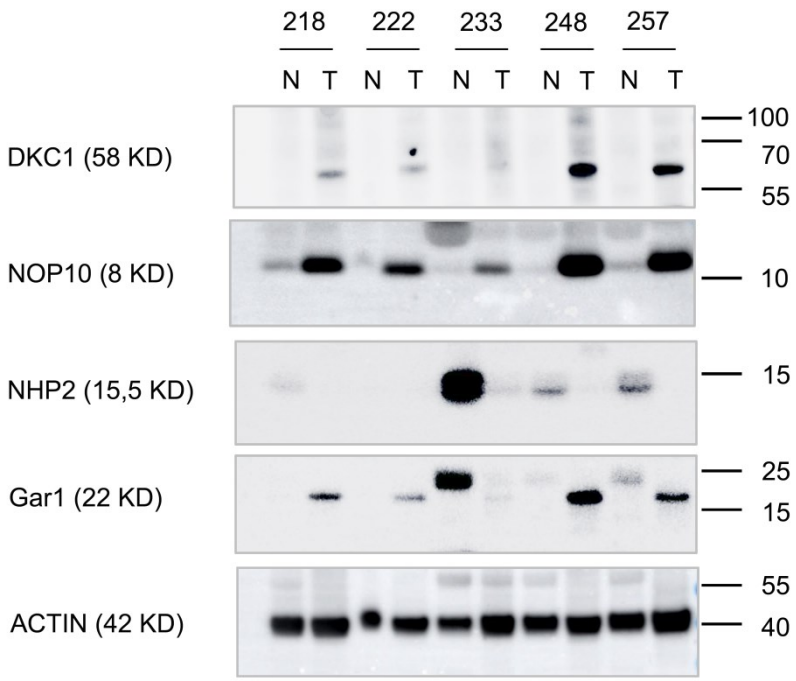

Figure 7: SnoRNPs have different expression patterns in tumour samples compared with normal samples. The expression of snoRNPs was analyzed by western blot. *β*-actin was used as loading control.

To further identify NOP10 expression level in lung cancer samples, statistical analysis of western blot was performed in 10 paired normal-tumour NSCLC

specimens. The results still showed that NOP10 expression was upregulated in lung cancer patients (Fig. 8). Taken together, these results indicate that NOP10 plays an important role in NSCLC development.

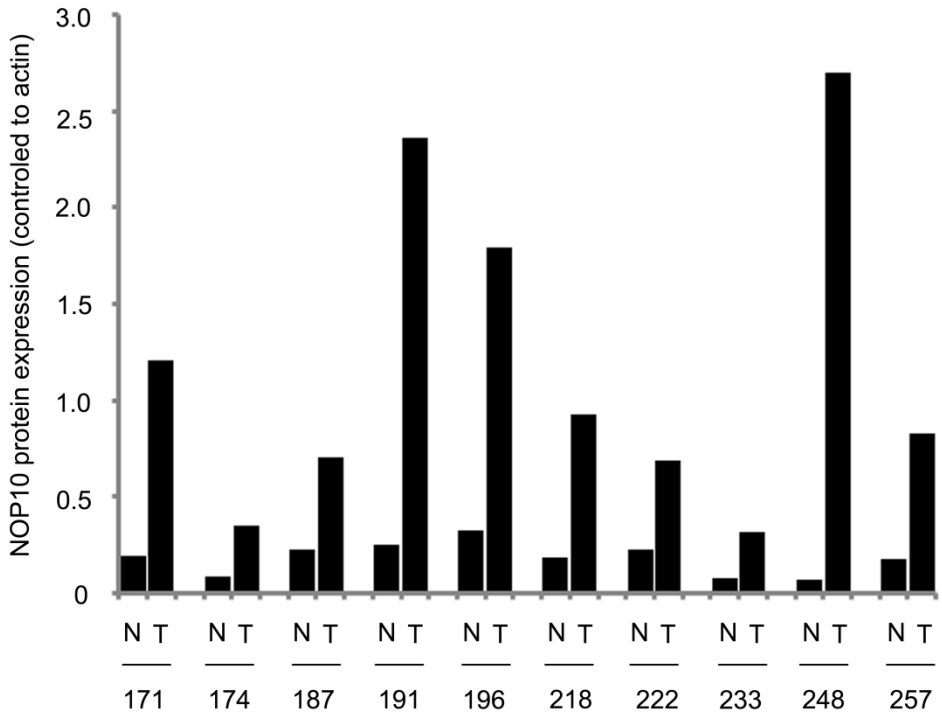

Figure 8: NOP10 is highly expressed in lung cancer samples. The relative gray value of western blot from 10 paired NSCLC samples showed that NOP10 is highly expressed in tumour tissue than paired normal tissue.

3.1.2 High expression of NOP10 correlates with poor prognosis in NSCLC patients

To evaluate the prognostic impact of NOP10 expression in NSCLC patients, we analysed NOP10 protein expression levels in tumours from 172 NSCLC patients using tissue microarrays (TMAs). The information of patients is shown in Table 1. As revealed by immunohistochemistry staining, NOP10 expression correlated significantly with poor overall survival of NSCLC patients (Fig. 9). Age, smoking, and tumour stage had no influence on overall survival of the patients, while sex did affect (female survive longer) (data not shown).

Table 1: Baseline demographics and clinical characteristics

	Patients (n=172)
Sex	
Men	142 (83%)
Women	30 (17%)
Age, years	
<70	114 (66%)
≥70	58 (34%)
Smoke	
None smokers	39 (22.7%)
Smokers	132 (76.7%)
No information	1 (0.06%)
Disease State	
Invasion	
No	20 (12%)
Yes	152 (88%)
Grade	
Low degree of malignancy	3 (1.7%)
Mean degree of malignancy	50 (29.1%)
High degree of malignancy	94 (54.7%)
Very high degree of malignancy	25 (14.5%)
Survival	
Live	111 (65%)
Dead	61 (35%)

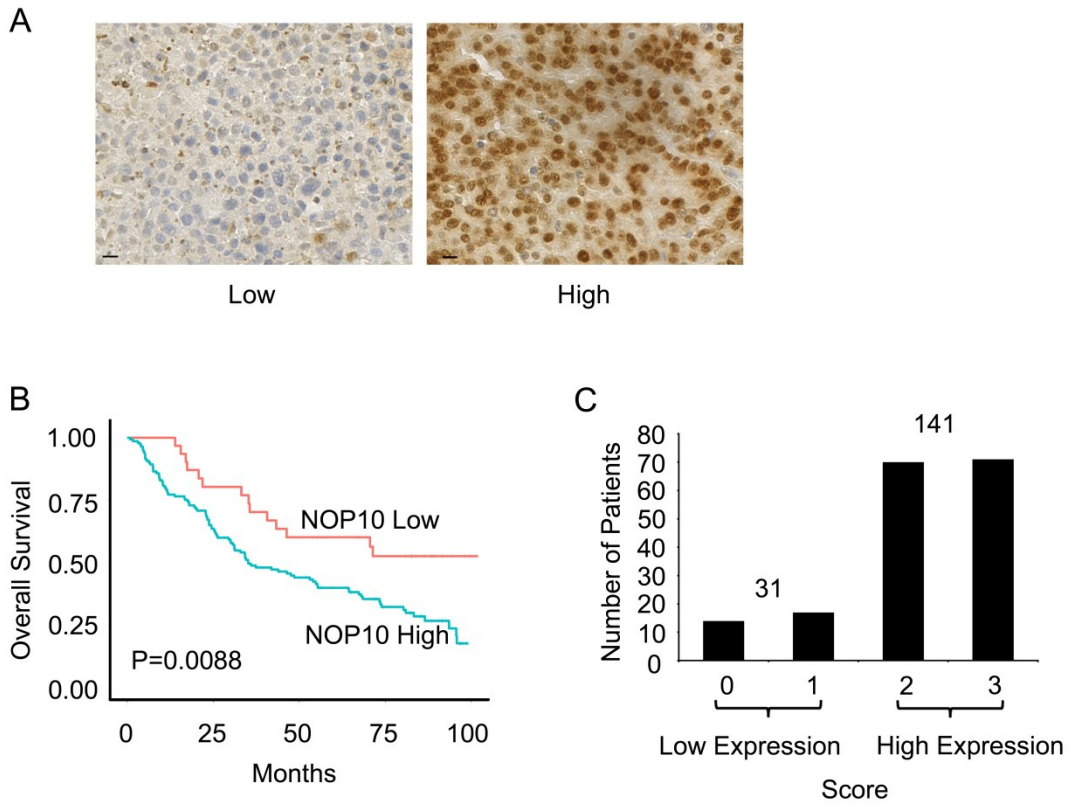

Figure 9: High expression of NOP10 relates with poor overall survival in NSCLC patients. (A) Immunohistochemistry staining of NSCLC samples from 183 patients. Representative high-level and low-level staining are shown. Scale bars, 10 μm. (B) Kaplan-Meyer plots for overall survival of NSCLC patients with high and low NOP10 expression are shown ($P < 0.05$). (C) Bar graphs shows the number of patients with high and low NOP10 expression. Nuclear staining of NSCLC TMA was assessed with Qupath software.

3.1.3 H/ACA box snoRNPs mRNA expression levels and outcome in NSCLC patients

Previous studies have reported that the snoRNA pathway played important roles in cancer development (Okugawa et al., 2017; Su et al., 2014; Thorenoor and Slaby, 2015; Zhou et al., 2017). Kaplan-Meier Plotter analysis showed us correlation between H/ACA box snoRNPs mRNA level and NSCLC patients' overall survival l (Gyorffy et al., 2013). This result was consistent with survival curve described in Fig. 9. In general, there was no correlation between DKC1, Gar1, NHP2 mRNA expression level and NSCLC patients' overall survival (Fig. 10B-D). Interestingly, a

high NOP10 mRNA expression level correlated with patients' poor overall survival (Fig. 10A).

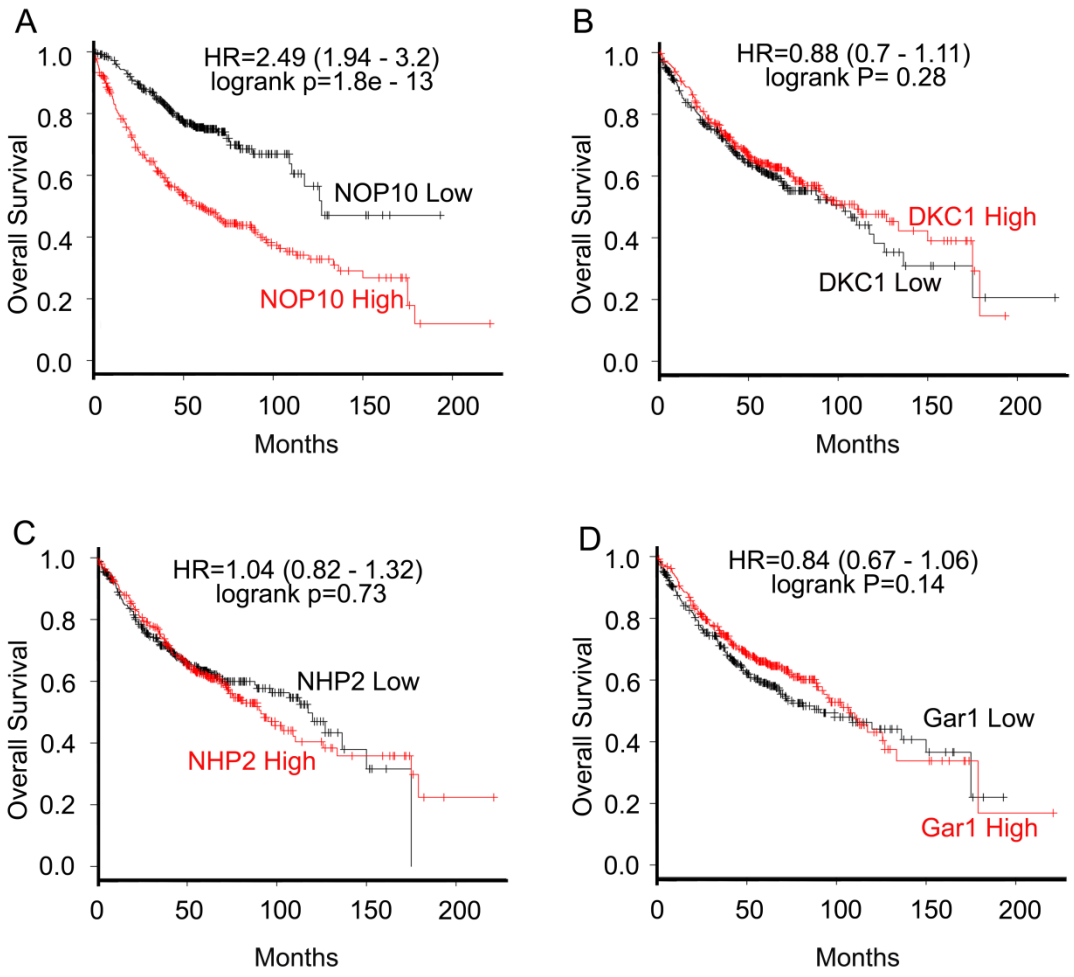

Figure 10: Expression of H/ACA box snoRNA proteins correlate differently with NSCLC patients' overall survival. (A) High NOP10 mRNA expression level leads to poor overall survival in NSCLC patients (P = 1.8e-13); (B-D) High levels of DKC1 (B), NHP2 (C), and Gar1 (D) mRNA expression have no relationship with patients' overall survival.

3.2 NOP10 protein is required for NSCLC development

3.2.1 NOP10 is downregulated in vitro

CRISPR/Cas9 is a useful tool for editing gene expression at the genome level (Garneau et al., 2010; Gasiunas et al., 2012; Jinek et al., 2012; Ran et al., 2013).

Upon cleavage by Cas9, the target locus typically undergoes DNA damage repair and product insertion/deletion mutations under non-homologous end joining (NHEJ) (Fig. 11A). In the next step, we designed eight guide RNAs targeting the NOP10 genome with the CRISPR/Cas9 system. We found an obvious mutation peak from the Sanger sequence results in A549 cells and Pc-9 cells (Fig. 11B). Also, as showed in the western blot results, the NOP10 knockouts (KO) in bulk cells induced significant loss of NOP10 expression (Fig. 11C-D).

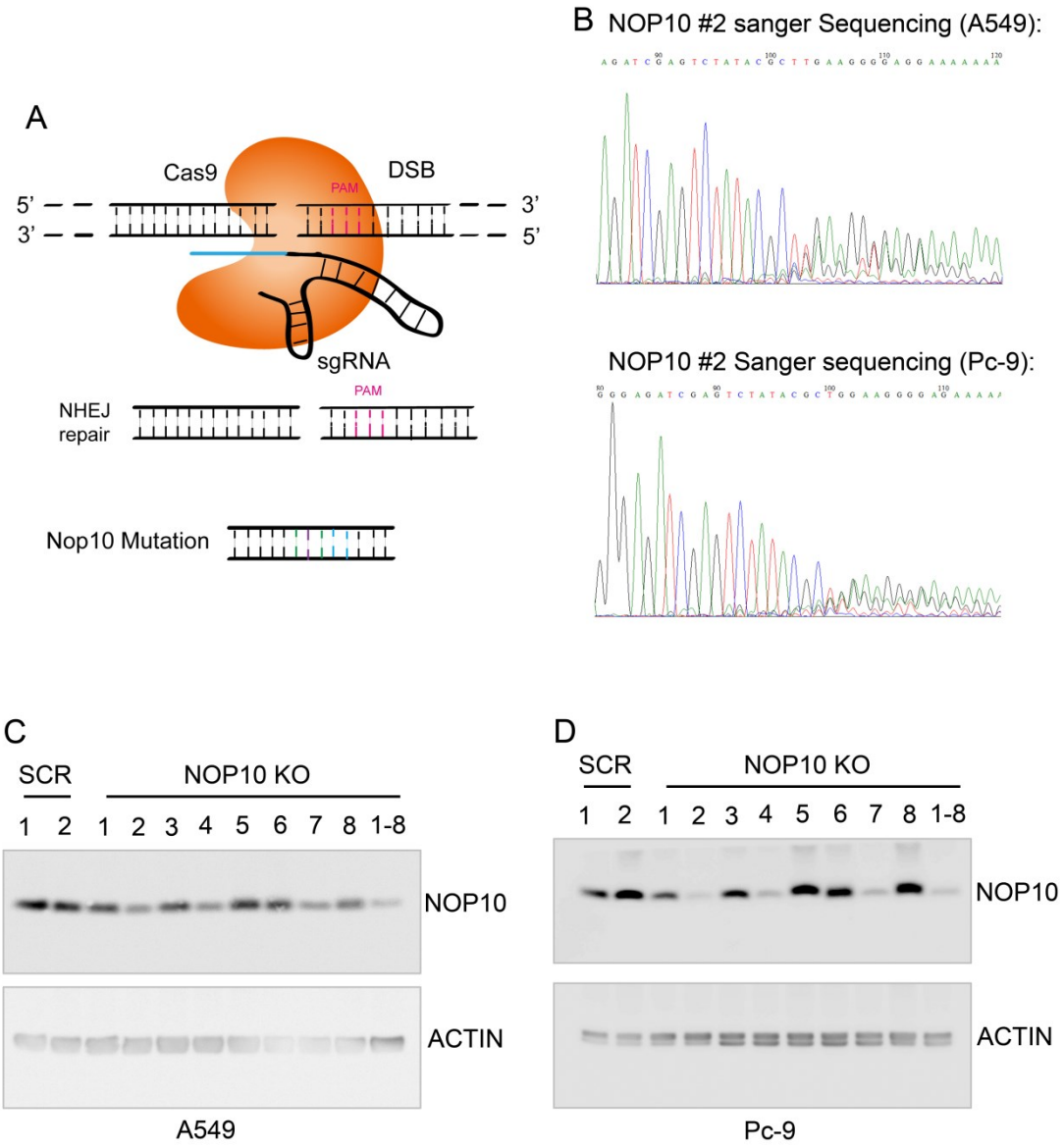

Figure 11: NOP10 protein expression is inhibited in NSCLC cell lines with CRISPR/Cas9 system. (A) Schematic of the RNA-guided Cas9 nuclease. The Cas9

nuclease is targeted to genomic DNA by a single guide RNA (sgRNA) consisting of a 20-nt guide sequence and a scaffold. The guide sequence pairs with the DNA target, directly upstream of a requisite 5′-NGG adjacent motif (PAM; pink). Cas9 mediates a DSB ~3 bp upstream of the PAM. (B) Sanger sequence showed the mutation region in NOP10 genomic DNA 3 days after transduction in A549 and Pc-9 cells. (C) Western blot analysis of NOP10 KO in A549 cells is shown. *β*-actin was used as loading control. (D) Western blot analysis of NOP10 KO in Pc-9 cells is shown. *β*-actin was used as loading control.

3.2.2 NOP10 KO inhibits proliferation in different lung cancer cells

We analysed whether H/ACA box snoRNPs have a different effect on lung cancer development. A proliferation assay was performed in A549 cells and Pc-9 cells. As shown in the results, NOP10 KO inhibited cell proliferation (Fig. 12A-B).

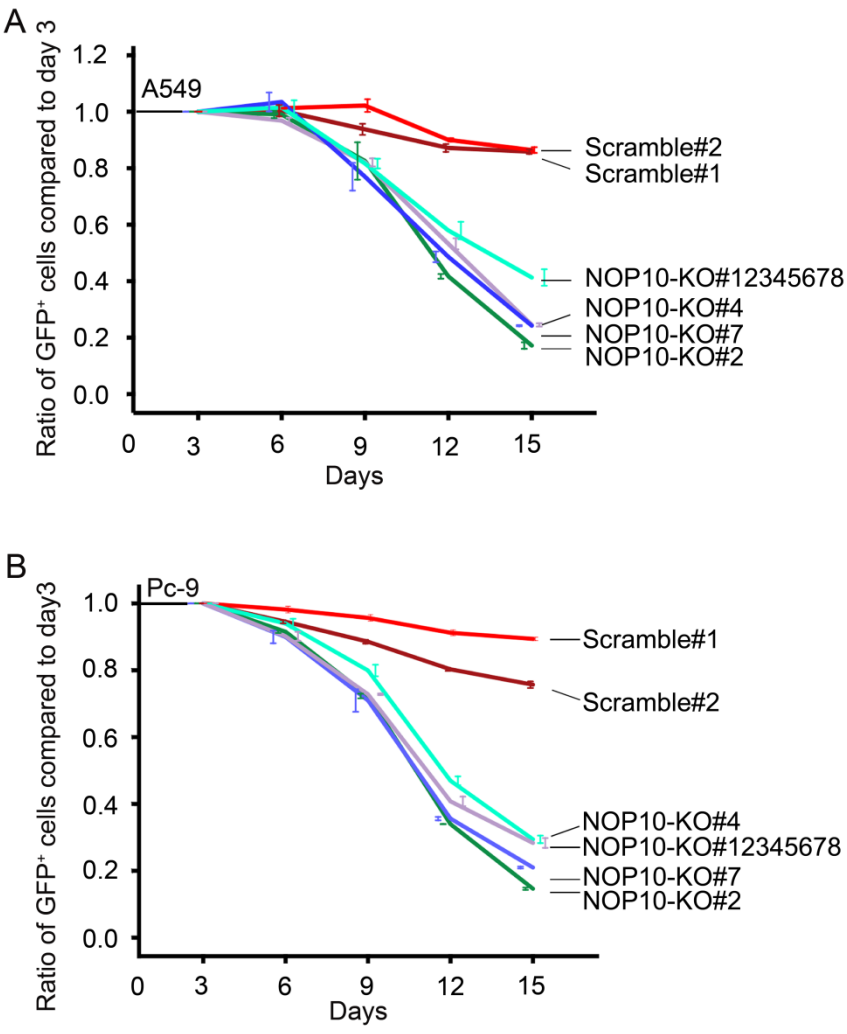

Figure 12: NOP10 KO inhibites lung cancer cell proliferation. (A-B) Proliferation performed in (A) A549 cells and (B) Pc-9 cells. Ratio of GFP positive cells was tested every 2 days with a flow cytometer. Scramble sgRNA was used as a control.

To confirm these findings, we knocked out NOP10 expression in other several lung cancer and leukaemia cell lines. As shown in the western blot results, NOP10 KO CRIPR/Cas9 system could effectively inhibit NOP10 expression in H1975, H358 and Kasumi-1 cells (Fig. 13).

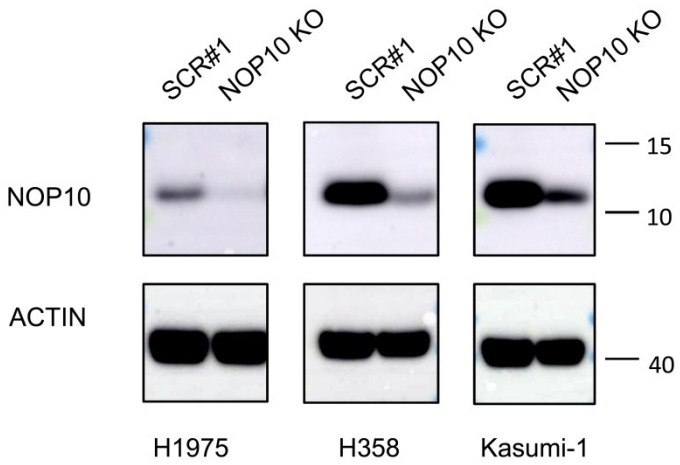

Figure 13: NOP10 expression is suppressed in several NSCLC cell lines and an AML cell line. Western blot was performed in H1975, H358 and Kasumi-1 cell lines after NOP10 KO. *β*-actin was used as loading control.

In order to further identify the effect of NOP10 on lung cancer development, as a next step we performed a proliferation assay in four different lung cancer cell lines. As shown in Fig. 14, NOP10 KO could significantly inhibit proliferation in H1975, H1650, H661 and H358 lung cancer cells (Fig. 14A-D).

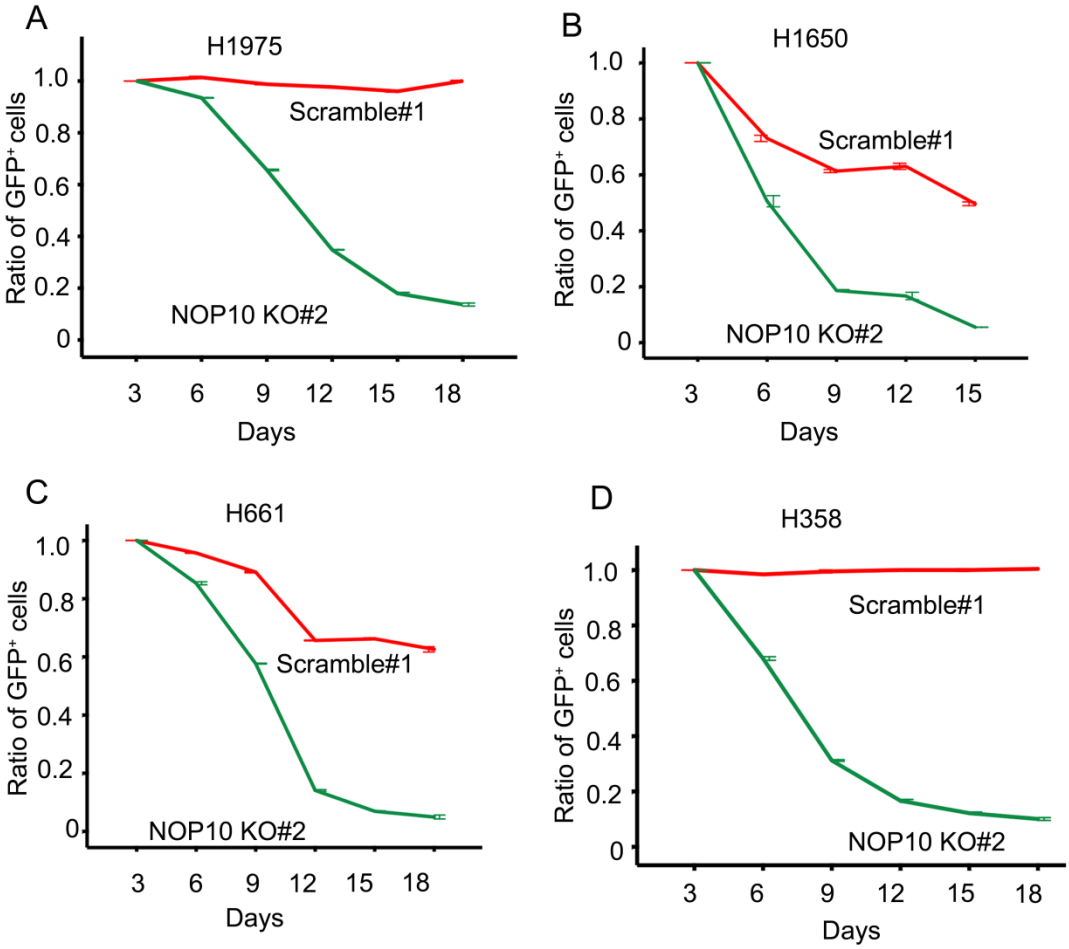

Figure 14: NOP10 KO inhibits lung cancer cell proliferation. (A.B.C.D) A proliferation assay was performed in H1975, H1650, H661 and H358 cell lines after NOP10 KO. Ratio of GFP positive cells was tested every 3 days with a flow cytometer. Scramble sgRNA was used as a control.

It has been reported that loss of NOP10 did not affect colony formation of Kasumi-1 or other leukaemia cells (Zhou et al., 2017). We wanted to further identify if NOP10 KO has an effect on leukaemia cells. A proliferation assay was performed in MV4-11 and U937 cells. The results showed that NOP10 KO could significantly inhibit proliferation of AML cells (Fig. 15).

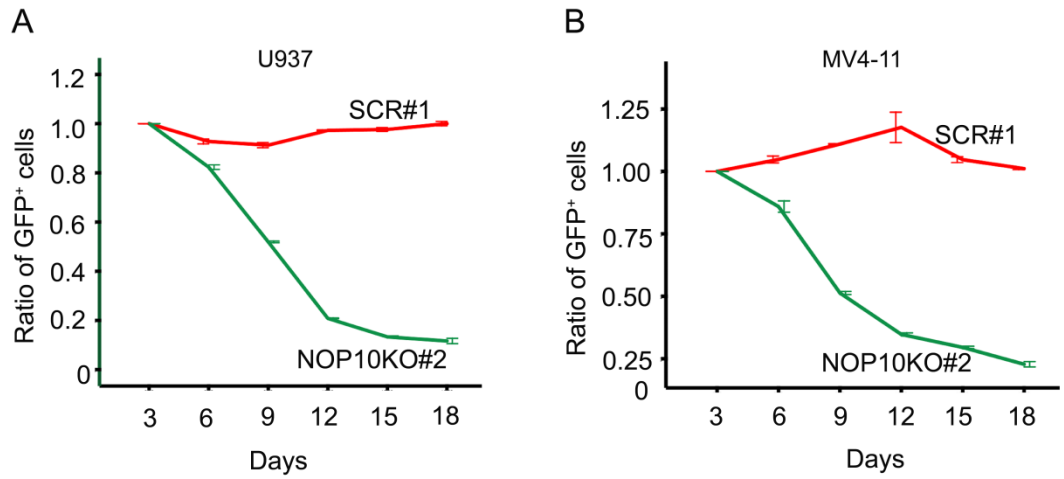

Figure15: NOP10 KO inhibits proliferation of AML cell line. (A-B) A proliferation assay was performed in in MV4-11 and U937 cells. The ratio of GFP positive cells was tested every 3 days with a flow cytometer. Scramble sgRNA was used as a control.

3.2.3 NOP10 KO inhibits colony formation in different lung cancer cell lines

The soft agar colony formation assay is a technique widely used to evaluate cellular transformation *in vitro* and is considered to be one of the most stringent tests for malignant transformation in cells (Borowicz et al., 2014). Our previous results identified that NOP10 KO could specifically inhibit proliferation of lung cancer cells. Here, in order to know if NOP10 KO has an effect on tumorgenesis of lung cancer cells in vitro, we performed a colony formation assay with soft agar. As shown in the colony image and statistical results, NOP10 KO significantly inhibited colony formation in Pc-9 cells (Fig. 16 A and C). We obtained similar results in A549 lung cancer cells (Fig. 16 B and D).

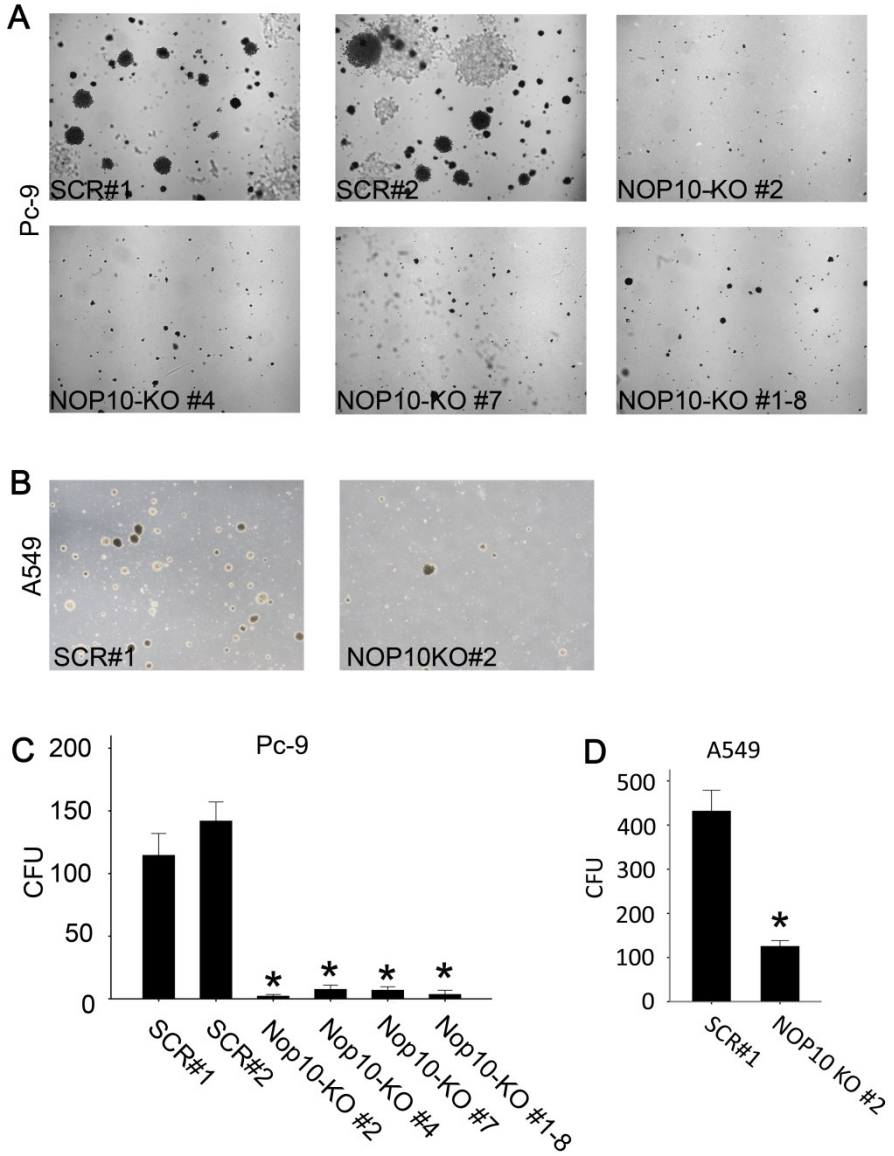

Figure 16: NOP10 KO inhibits colony formation in lung cancer cell line. (A) Representative images of colony formation assay derived from Pc-9 cells with NOP10 KO. (B) The number of colonies derived from Pc-9 cells was calculated and is shown in the graph bar. (C) Representative images of colony formation assay derived from A549 cells with NOP10 KO. (D) The number of colonies derived from A549 cells was calculated and is shown in the graph bar.

3.2.4 NOP10 KO inhibits cell migration in vitro

Cancer cell migration and invasion are initial steps in metastasis (van Zijl et al., 2011). During metastasis, primary tumour cells migrate and invade neighbouring

tissues to establish new tumour sites. As such, we wanted to know if NOP10 could regulate lung cancer cell migration and invasion. Cell migration and invasion assays measure cell motility and invasiveness (Justus et al., 2014). We performed trans-well assays. After 48 hours, we found that after NOP10 KO, A549 cells and Pc-9 cells inhibited cell migration (Fig. 17A). The statistical analyses confirmed these observatons (Fig. 17B-C). These results suggest that NOP10 could regulate lung cancer cell migration and invasion.

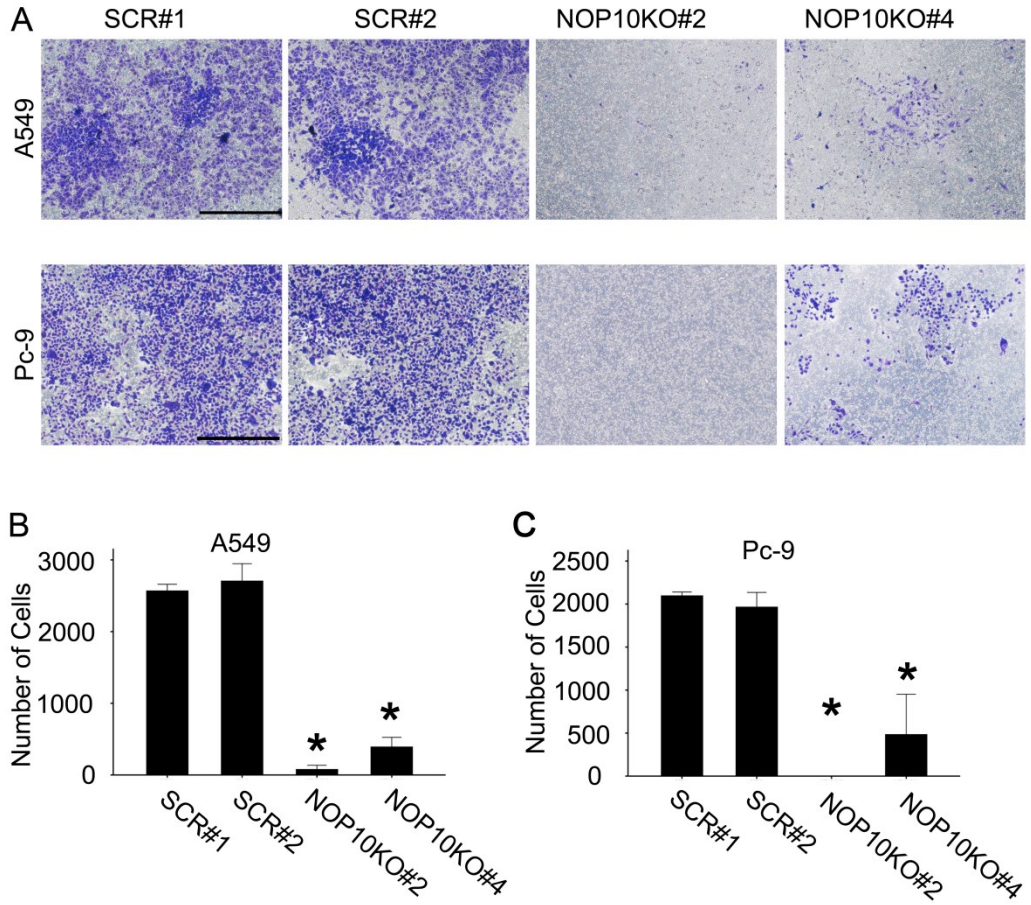

Figure 17: NOP10 KO inhibits migration in different lung cancer cells. (A) Representative images of migrated cells after NOP10 KO in A549 cells and Pc-9 cells were shown. The migrated lung cancer cells were stained by crystal violet. Scale bar, 0.5 mm. (B-C) Quantitative result of cells' number in (A) are shown. The results are expressed as Mean ± SD (*$p < 0.05$).

3.3 SnoRNAs are decreased by NOP10 suppression in lung cancer cells

These data indicated that NOP10 could regulate lung cancer cells. NOP10 protein is one of the conserved snoRNPs that plays an important role during ribosome RNA pseudouridylation, guided by H/ACA box snoRNA. First, we tried to identify whether inhibition of NOP10 could affect expression of snoRNA. Consistent with previous reports, small RNA sequencing results showed that NOP10 KO significantly inhibited expression of H/ACA box snoRNA (Fig. 18A) but did not affect C/D box snoRNA (Fig. 18B).

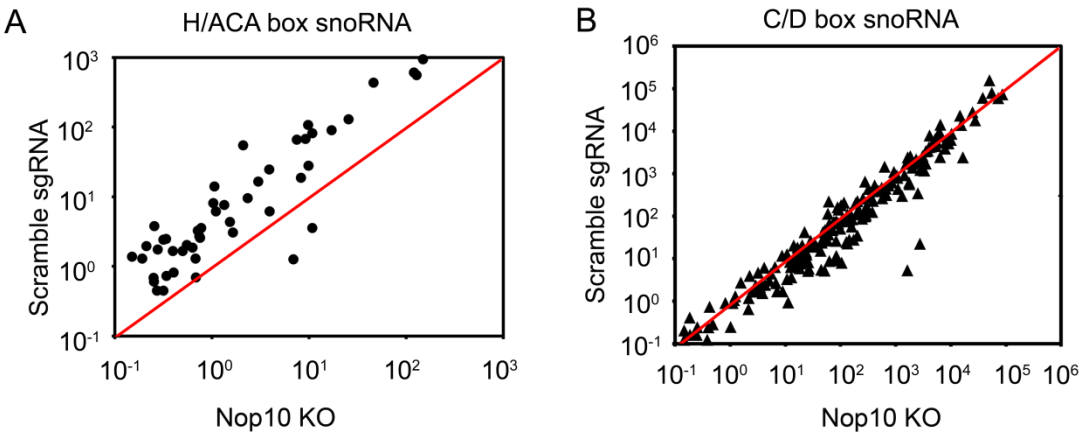

Figure 18: NOP10 KO inhibits H/ACA box snoRNA expression. (A) Scatterplot presents H/ACA box snoRNAs expression ratios in control (scramble sgRNA) and NOP10 KO A549 cells. (B) Scatterplot presents C/D box snoRNAs expression ratios in control (scramble sgRNA) and NOP10 KO A549 cells.

3.4 SnoRNA expression in primary lung cancer specimens.

As a next step we examined the global expression of snoRNAs in seven paired normal and tumour samples. Notably, human lung cancer cells expressed overall lower levels of H/ACA box snoRNAs compared to C/D box snoRNAs (44% mapped reads for 242 box C/D snoRNAs and 0.3% mapped reads for 67 box H/ACA snoRNAs) (Fig. 19A). Interestingly, more H/ACA box snoRNA were higher expressed in tumour tissue compared to paired normal tissue (Fig. 19B). The

snoRNAs which were overexpressed in tumour samples include SNORD14DA, SNORD42A, SNORD42B and SNORA42 (Fig. 19C).

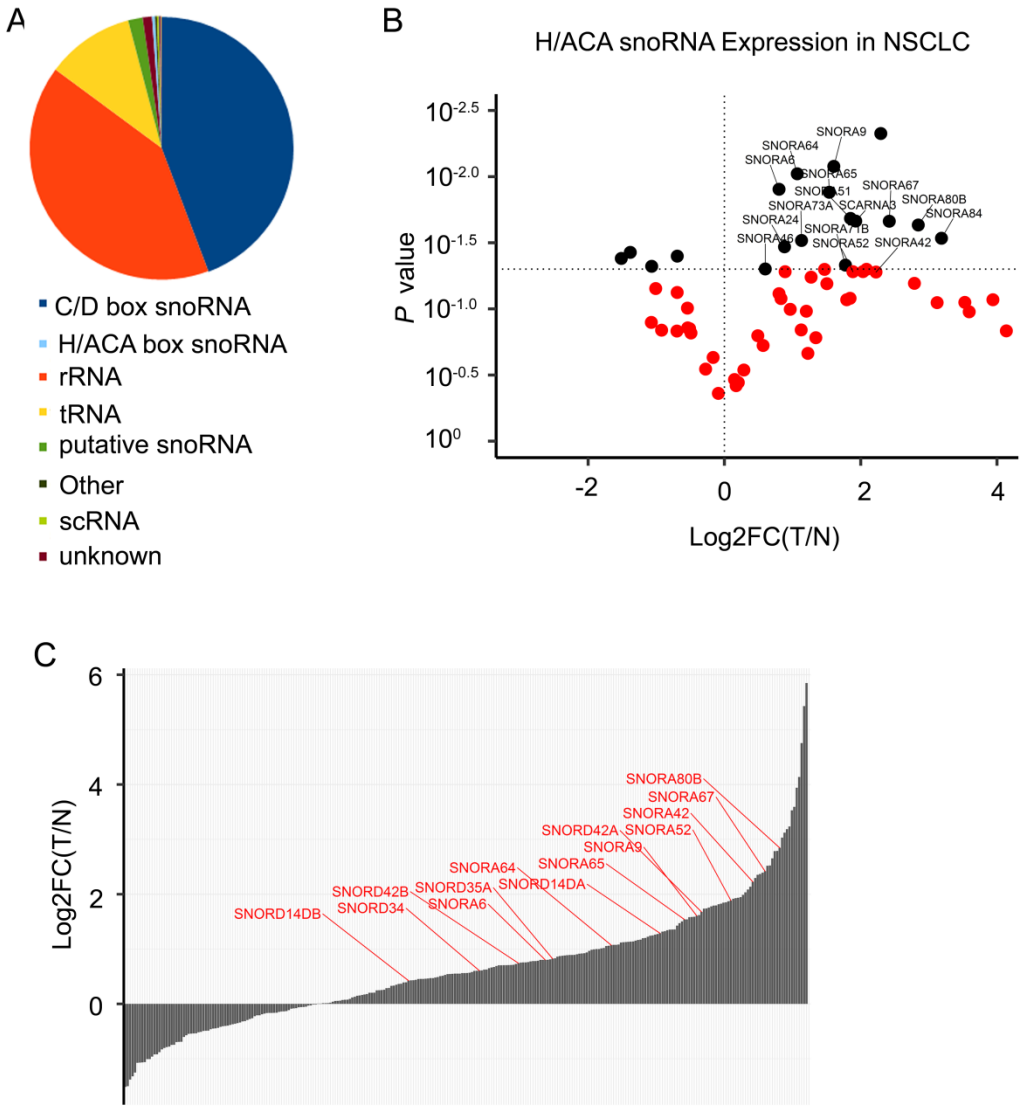

Figure 19: Expression pattern of snoRNAs across NSCLC patients. (A) Distribution of snoRNA sequence reads of different RNA species with percentages of the total mapped reads. (B) The volcano plot indicates the log-fold change in H/ACA box snoRNA expression (horizontal axis) and P values (t-test; vertical axis) in NSCLC patients with normal versus tumour tissue (n = 7). (C) Waterfall chart presents C/D box snoRNAs and H/ACA box snoRNAs expression patterns in lung cancer tissue compared with paired normal tissue.

3.5 18S and 28S ribosomal RNA exhibit altered patterns of pseudouridylation in lung cancer specimens

Studies have reported that H/ACA box snoRNPs are responsible for RNA pseudouridylation modification based on H/ACA box snoRNA's 10-12nt stretch of complementarity to the target sequence (Stepanov et al., 2015). Pseudouridylation of rRNA was analysed in 5 paired normal and tumour NSCLC samples (Fig. 20).

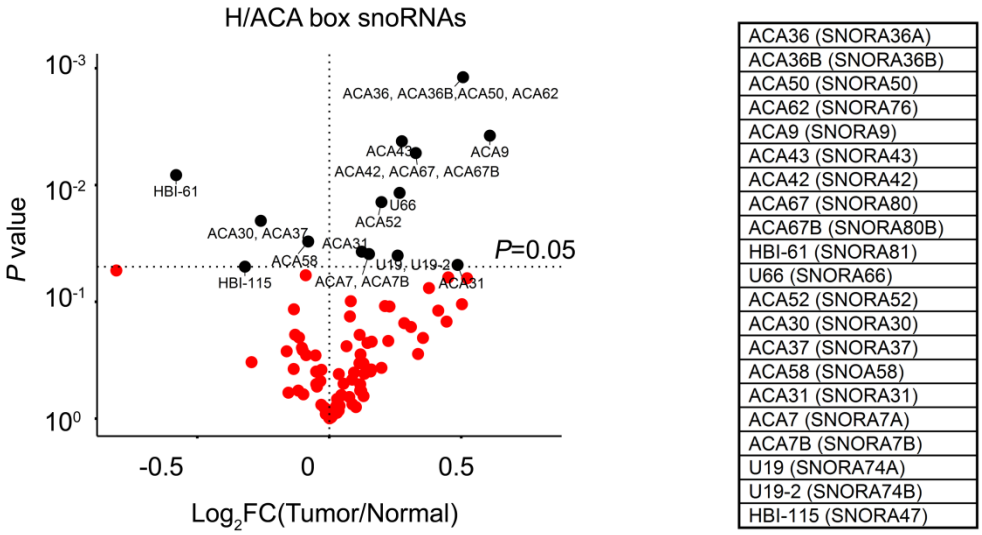

Figure 20: Ribosomal RNAs show different pseudouridylation pattern in NSCLC patients. The volcano plot indicates the log-fold change in pseudouridylation level (horizontal axis) and P values (t-test; vertical axis) in NSCLC patients with normal versus tumour tissue (n = 5).

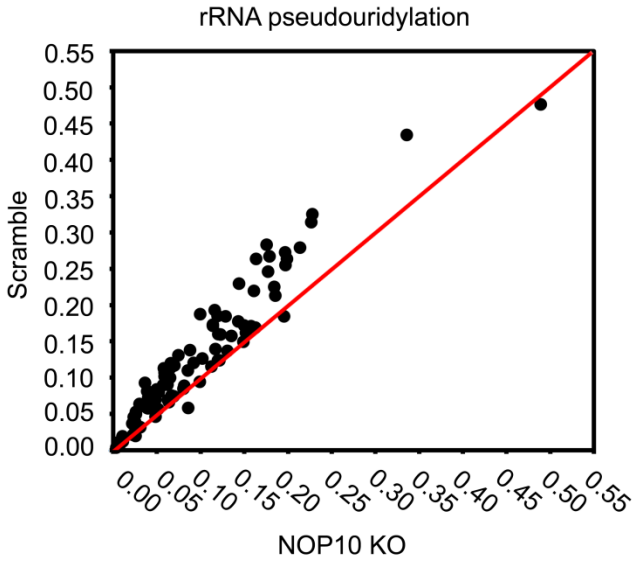

Figure 21: NOP10 KO inhibits rRNA pseudouridylation in lung cancer cells. Scatter plot presents pseudouridylation ratios of 18S and 28S ribosome RNA in control (scramble sgRNA) and NOP10 KO A549 cells.

We also performed pseudouridylation analysis in A549 cells after NOP10 KO. The results showed that pseudouridylation levels on most snoRNA target ribosome RNA sites were inhibited after NOP10 KO compared with the control group (Fig. 21).

Furthermore, we performed immuno-northern blotting (INB) for the detection of the modified nucleosides with antibodies against pseudouridine (Mishima et al., 2015). NOP10 KO could inhibit all kinds of RNA peudouridylation levels, including ribosomal RNA, transfer RNA and small nuclear RNAs (Fig. 22).

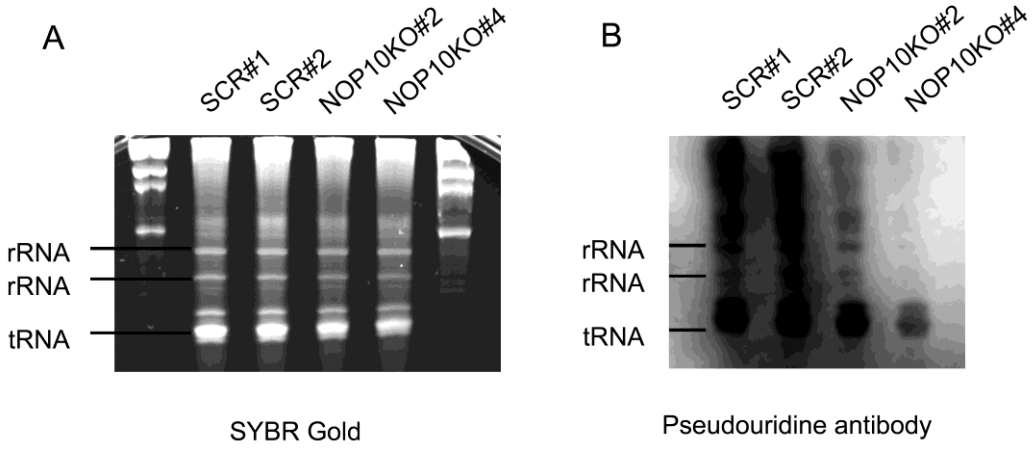

Figure 22: NOP10 KO decreases rRNA pseudouridyaltion in vitro. Total RNA isolated from control (scramble sgRNA) and NOP10 KO Pc-9 cells was separated in 6% polyacrylamide urea denaturing gel and analysed by SYBR staining (A) and immuno-northern blotting (INB) using anti-Ψ antibodies (B).

3.6 SnoRNAs are essential for lung cancer proliferation

In order to identify snoRNAs that promote proliferation of lung cancer cells, snoRNAnome-scale CRISPR-Cas9 KO screen with a pooled LentiCRISPR library was used (Shalem et al., 2014). We designed a library of sgRNAs targeting 1,500 snoRNAs in the human genome with an average of 5-6 sgRNAs per snoRNA gene, and each target site was selected to minimize off-target modification. We used a

LentiCRISPR vector that simultaneously delivers Cas9 and sgRNA. We transduced the human lung cancer cell line A549 with the GeCKO library at a MOI of 0.3. Then we collected the cells at different time points, day 0, day 4, day 9. After extracting the genomic DNA from these cells, two steps of PCR were performed. Then the PCR product from the second step was sent for sequence (Fig. 23).

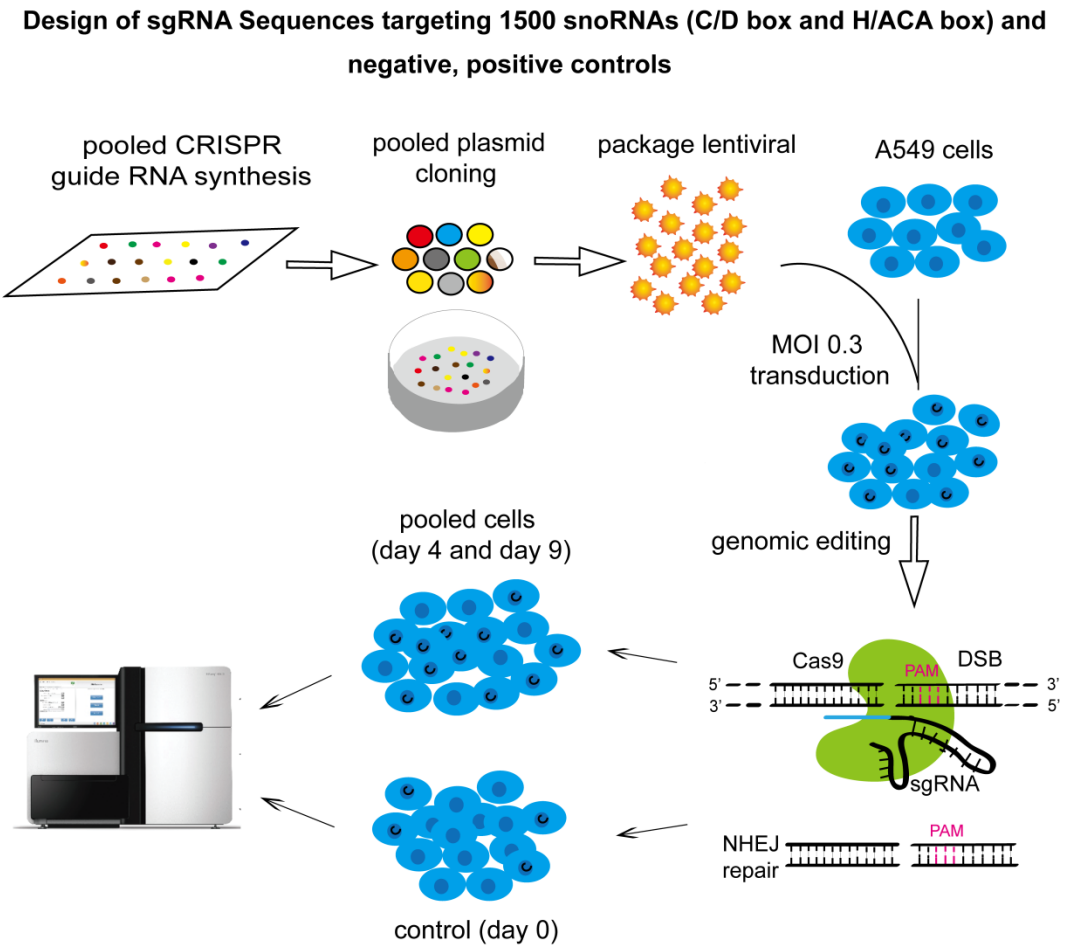

Figure 23: Schematic diagram of GeCKO library design and application for snoRNA screening. Design sgRNA snoRNAs in human cells with lentiviral vector, and transduced A549 cells with low MOI. Pick up cells at different time points, day 0, day 4, day 9 and extract genomic DNA. Then prepare the PCR samples and send for sequencing (modified from High Throughput Genome Engineering (HTGE)).

From the deep sequencing results we did not find significant changes in the diversity of sgRNAs in the surviving A549 cells (Fig. 24) (Wilcoxon rank sum test). We obtained informative results through analysing the positive rank control (TP53) and negative rank control (Myc). Also, this library screening showed that NOP10 KO

negatively promoted proliferation phenotype of A549 cells, which is consistent with our previous results. Combined with the RNA sequence and pseudouridylation sequence results, we found three interesting snoRNAs, SNORA65, SNORA7A, and SNORA7B, which could negatively affect cell proliferation in the screening library (Fig. 25).

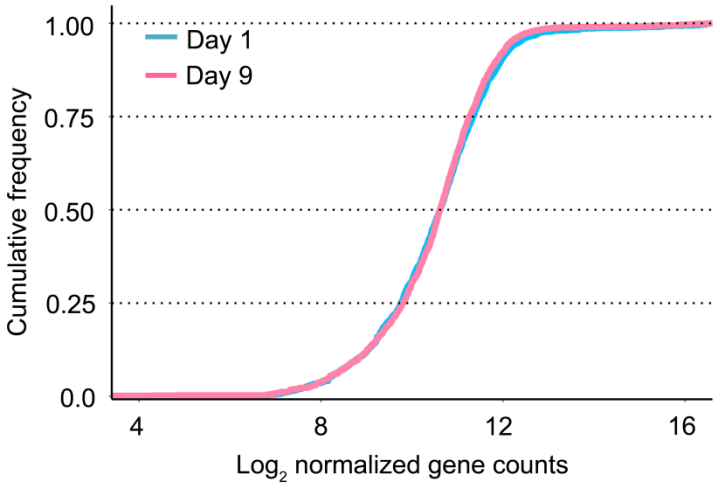

Figure 24: Control and experimental snoRNA screen sequencing data. Cumulative frequency of sgRNAs 0 and 9 days after transduction in A549 lung cancer cells, respectively. There is no obvious shift in the 9-day curve compared with 0-day curve.

Figure 25: Positively and negatively selected snoRNAs from snoRNA screen. Negative and positive proliferation sgRNA cells are labelled in the waterfall chart.

3.7 SNORA65 in lung cancer

3.7.1 SNORA65 is highly expressed in lung cancer.

To complement the functional data we performed small RNA sequencing in paired Tumor/Normal samples from NSCLC patients. SNORA65 was highly expressed in tumour samples compared with paired normal samples (Fig. 26A). This result is also consistent with TCGA data, which showed that SNORA65 was highly expressed in lung adenocarcinoma tissue compared to normal tissue (Fig. 26B).

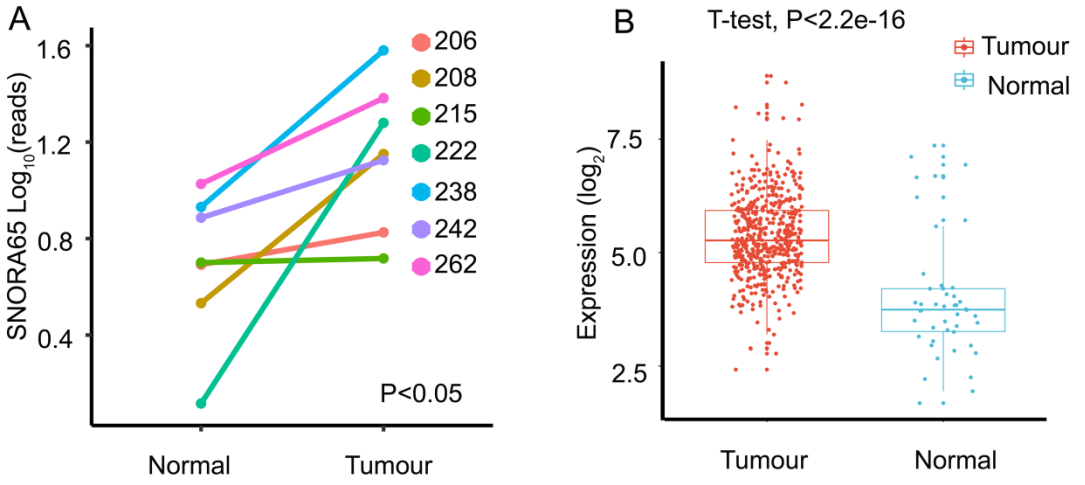

Figure 26: SNORA65 has higher expression in lung cancer tissue compared to normal tissue. (A) The diagram shows that SNORA65 is highly expressed in tumour tissue compared to paired normal tissue in NSCLC patients ($P < 0.05$). (B) SNORN65 expression phenotype in TCGA lung cancer data ($P < 0.05$).

3.7.2 NOP10 KO inhibits SNORA65 expression

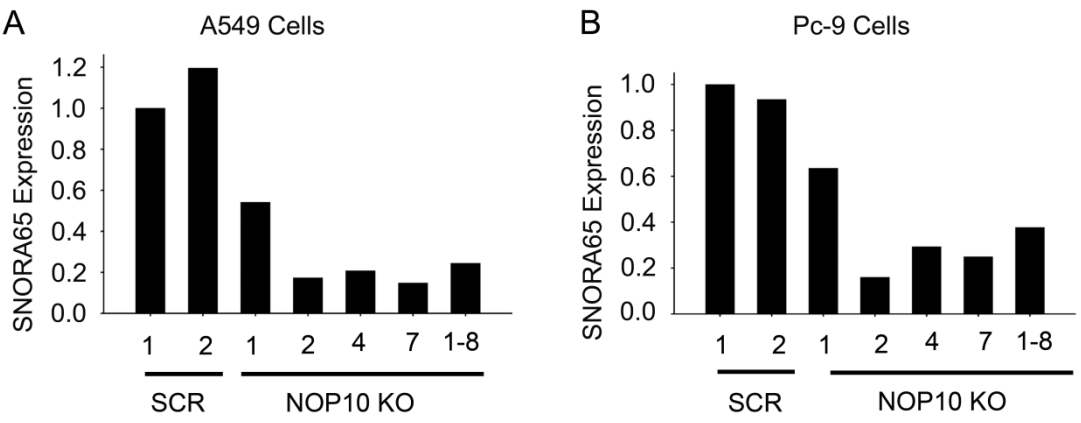

Figure 27: NOP10 KO decreases SNORA65 expression levels. (A) RT-PCR analysis showed SNORA65 expression in control (scramble sgRNA) and NOP10 KO A549 cells. (B) RT-PCR analysis showed SNORA65 expression in control (scramble sgRNA) and NOP10 KO Pc-9 cells.

Inhibition of NOP10 expression decreased expression of SNORA65 in A549 cells and Pc-9 cells (Fig. 27).

3.7.3 SNORA65 deletion with the CRISPR/Cas9 system affects cellular functions

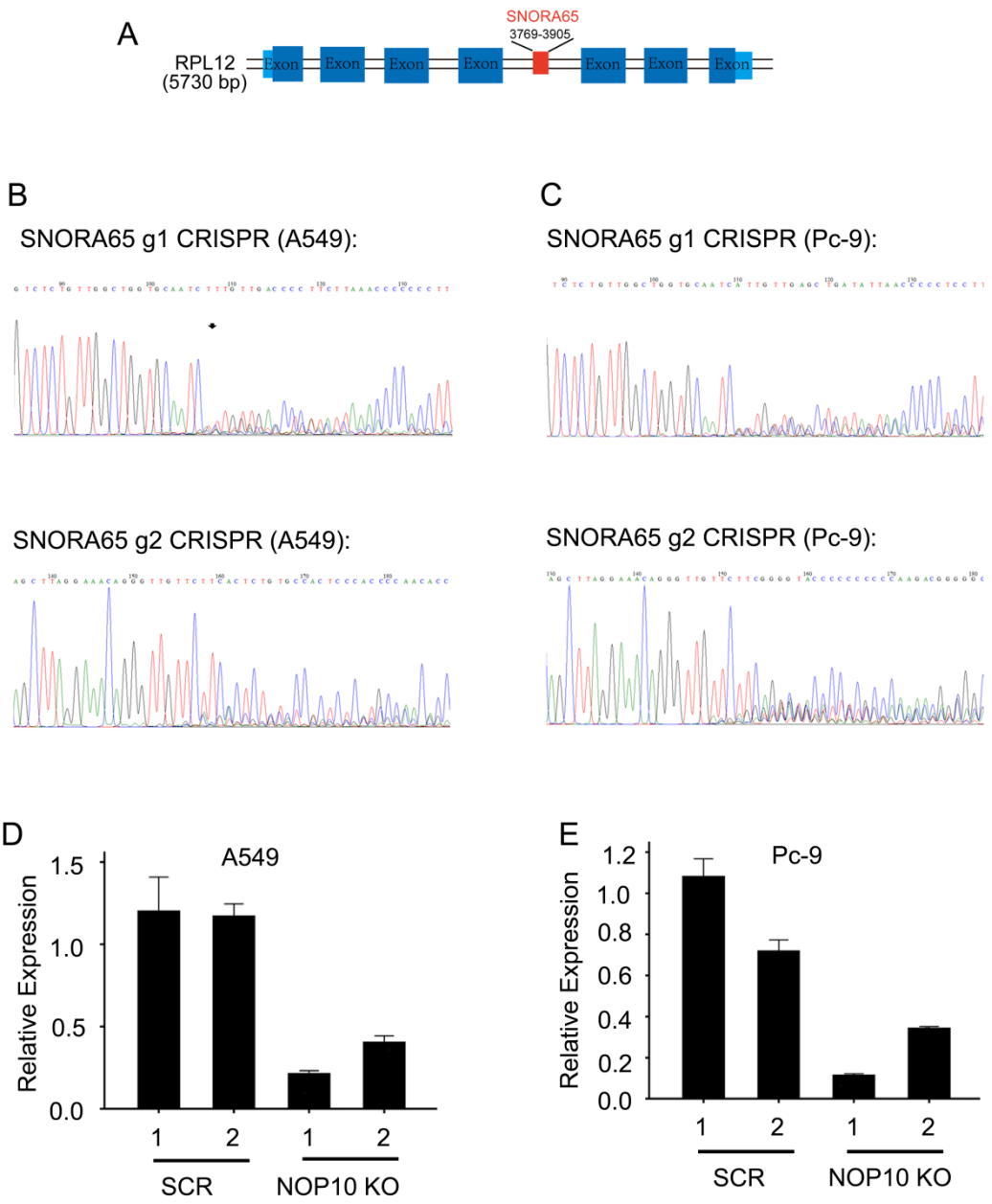

Figure 28: SNORA65 KO in lung cancer cell line. (A) The location of SNORA65 in genomic DNA. (B-C) Sanger sequence showed the mutation region in SNORA65 genomic DNA 3 days after transduction of SNORA65 CRISPR/Cas9 in A549 cells and Pc-9 cells. (D-E) RT-PCR results indicated that SNORA65 expression was significantly inhibited after SNORA65 mutation in A549 cells and Pc-9 cells.

In humans, most snoRNAs are co-expressed from introns of their host genes (Dieci et al., 2009; Smith and Steitz, 1998; Tycowski et al., 1996a). The host gene of SNORA65 is ribosomal protein L12 (RPL12) (Fig. 28A). In order to know if SNORA65 could affect lung cancer cell functions, we designed and used guide RNAs targeting the SNORA65 genome with the CRIPR/Cas9 system (Fig. 28B-C). In addition, real-time PCR was performed. Both guide RNAs could effectively inhibit expression of SNORA65 at the mRNA level (Fig. 28D-E).

3.7.4 SNORA 65 KO inhibits colony formation in vitro

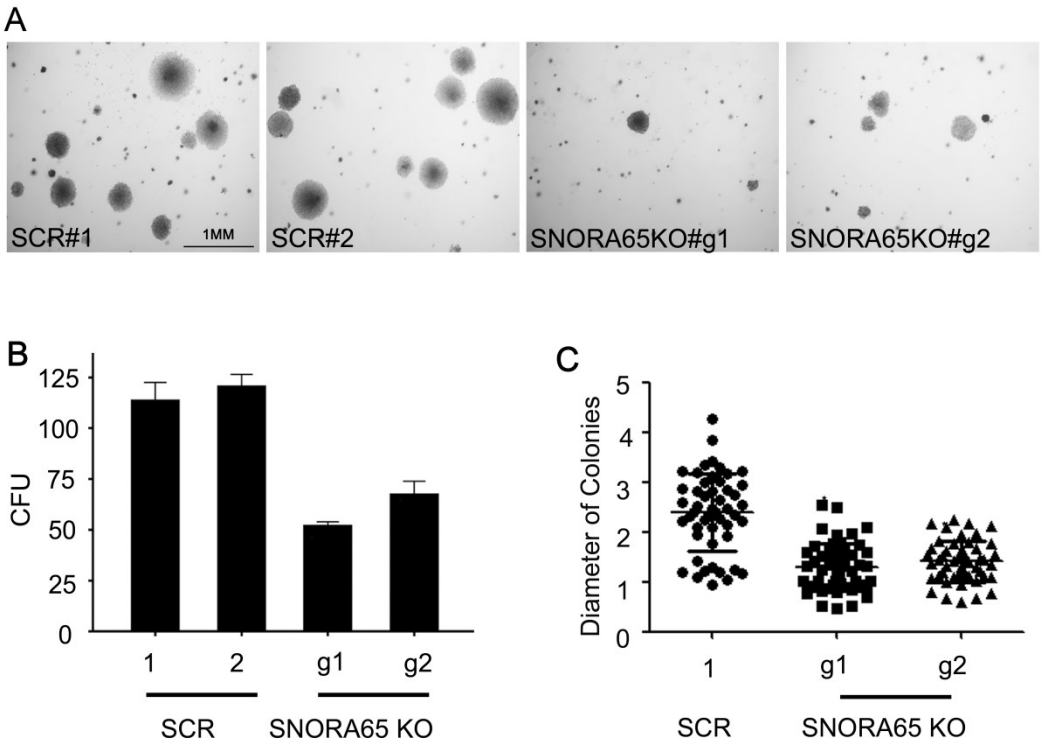

Figure 29: SNORA65 expression inhibition decreases colony forming capacity in Pc-9 cells. (A) Representative images of colony formed by scramble or SNORA65 KO Pc-9 cells.

Scale bar, 1mm. (B) Quantitative result of colony numbers in (A) was shown (*p < 0.05). (B) Quantitative result of size of colony in (A) is shown (*p < 0.05).

To explore if SNORA65 KO could repress tumorigenicity of NSCLC in lung cancer cells, the capacity of colony formation in soft agar was evaluated in Pc-9 cells. As shown in the results, inhibition of SNORA65 decreased the number of colonies in Pc-9 cells (Fig. 29 A-B). Interestingly, SNORA65 KO displayed much smaller size colonies compared with scrambled guide RNA control (Fig. 29 A and C).

Also, we obtained the same result in the A549 cell line; SNORA65 KO inhibited colony formation significantly in vitro (Fig. 30).

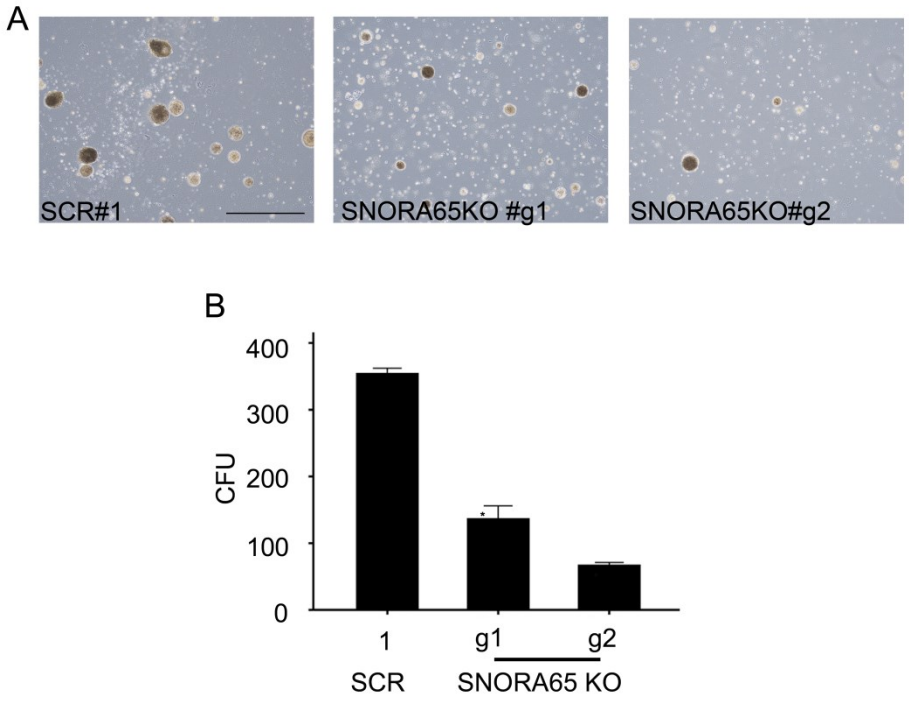

Figure 30: SNORA65 expression inhibition decreases colony forming capacity in A549 cells. (A) Representative images of colonies formed by scramble or SNORA65 KO A549 cells. Scale bar, 1mm. (B) Quantitative result of colony numbers in (A) is shown (*p < 0.05).

These results imply that suppression of SNORA65 diminishes the tumorigenicity of NSCLC cells in vitro.

3.8 SNORA7A/7B regulates NSCLC development

3.8.1 Pseudouridylation level is upregulated in lung canncer

The snoRNA library screen revealed SNORA7A and SNORA7B as another two interesting H/ACA box snoRNAs. It has been reported that pseudouridylation plays an important role in nuclear gene expression (Zhao et al., 2018). In the pseudouridylation sequence results we found that the ribosomal RNA 28S 1771 site, which is pseudouridylated by SNORA7A/7B, was highly pseudouridylated in tumour samples compared to matched normal samples (Fig. 31A). All the pseudouridylation sites have been showed in Figure 32. Location of SNORA7A/7B target site which is around the peptidyl transferase center was shown (Fig. 32). Of note, TCGA data showed that SNORA7A and SNORA7B were higher expressed in tumour samples compared to normal samples (Fig. 31 B-C).

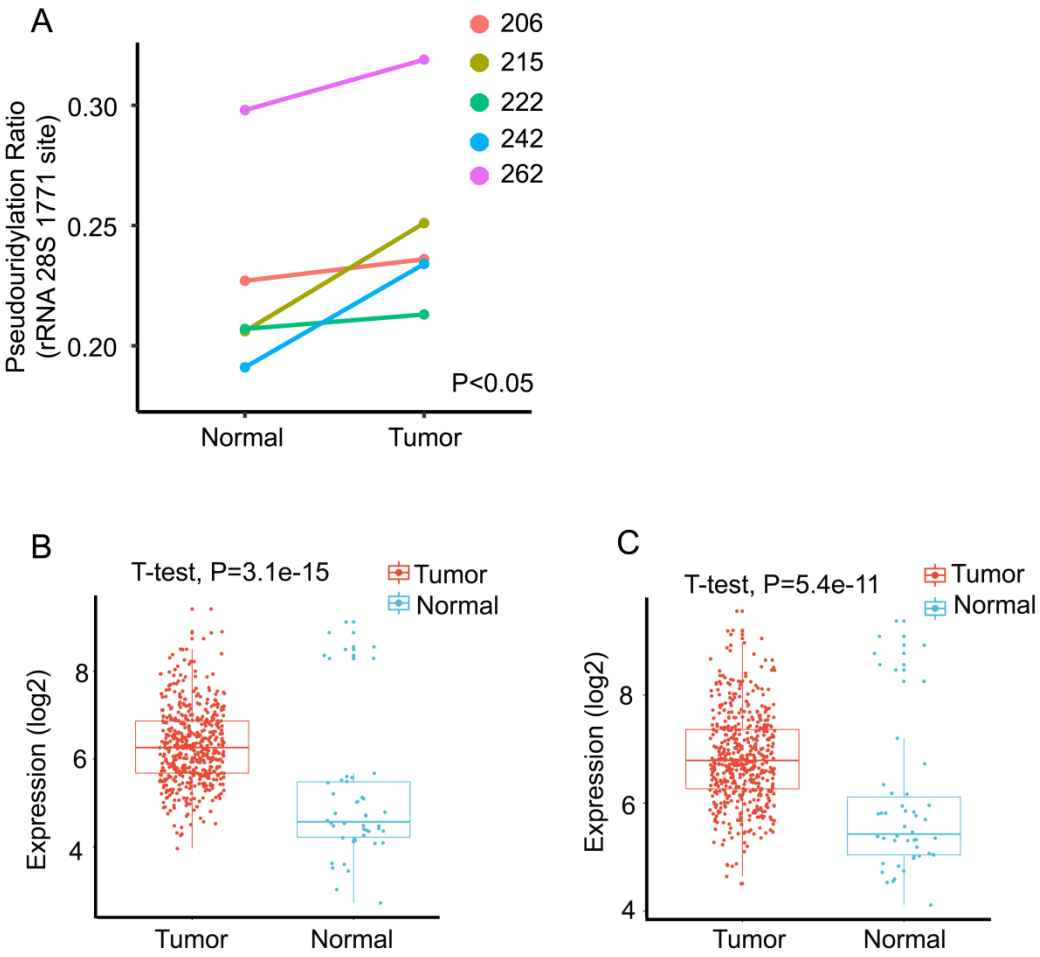

Figure 31: SNORA7A and SNORA7B is highly expressed in lung cancer. (A) The diagram shows that in NSCLC patients, the 28S ribosome RNA 1771 site targeted by SNORA7A/7B has a higher pseudouridylation level in tumour tissue than in paired normal tissue ($P < 0.05$). (B-C) The expression pattern of SNORA7A and SNORA7B in NSCLC patient is shown. The data are from TCGA ($P < 0.05$).

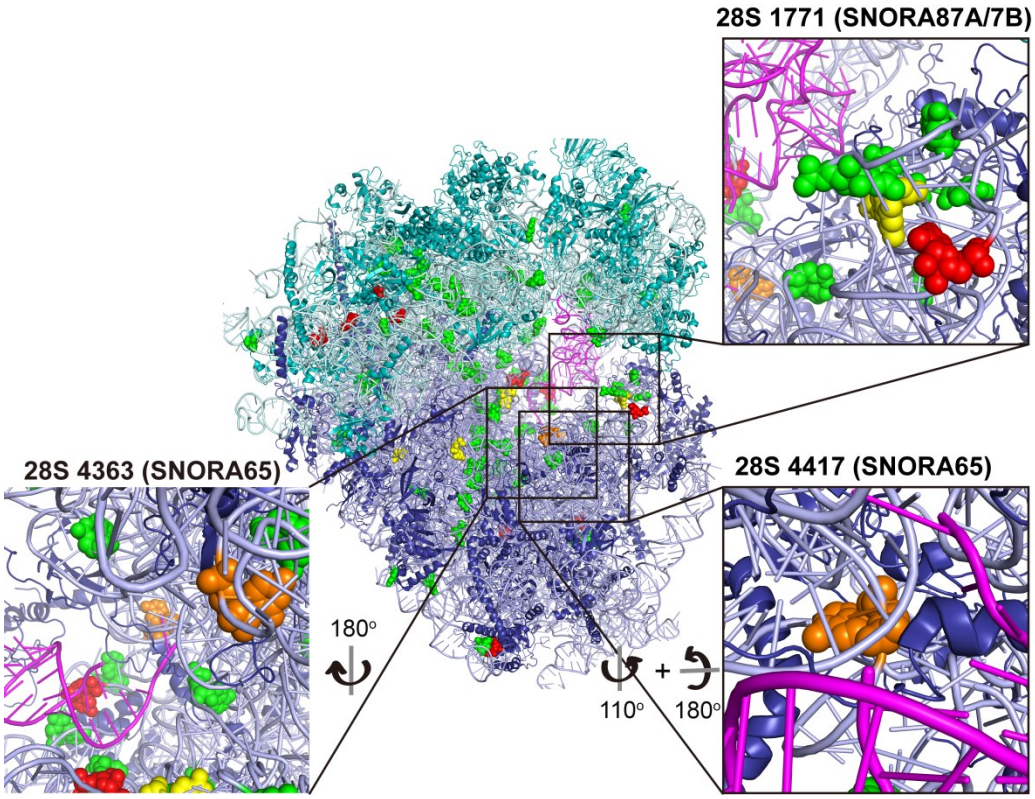

Figure 32: Pseudouridylation sites of eukaryotic ribosome. Green: non-significant changes; red: higher pseudouridylation in tumour; yellow: lower pseudouridylation in tumour; orange: prediction pseudouridylation site (SNORA65)

3.8.2 SNORA7A/7B KO could inhibit colony formation and proliferation in vitro

SNORA7A resides in intron 2 of ribosomal protein 32 (PRL32); SNORA7B resides in intron 2 of ribosomal protein P3 (RPLP3) (Fig. 33A). To investigate the effect of SNORA7A and SNORA7B on NSCLC development, we designed two guide RNAs with the CRISPR/Cas9 system. Because SNORA7A and SNORA7B are highly homologous, we designed guide RNAs that could simultaneously knock out

SNORA7A and SNORA7B. The real-time PCR results showed that these two guide RNAs could inhibit expression of SNORA7A and SNORA7B at the same time (Fig. 33B).

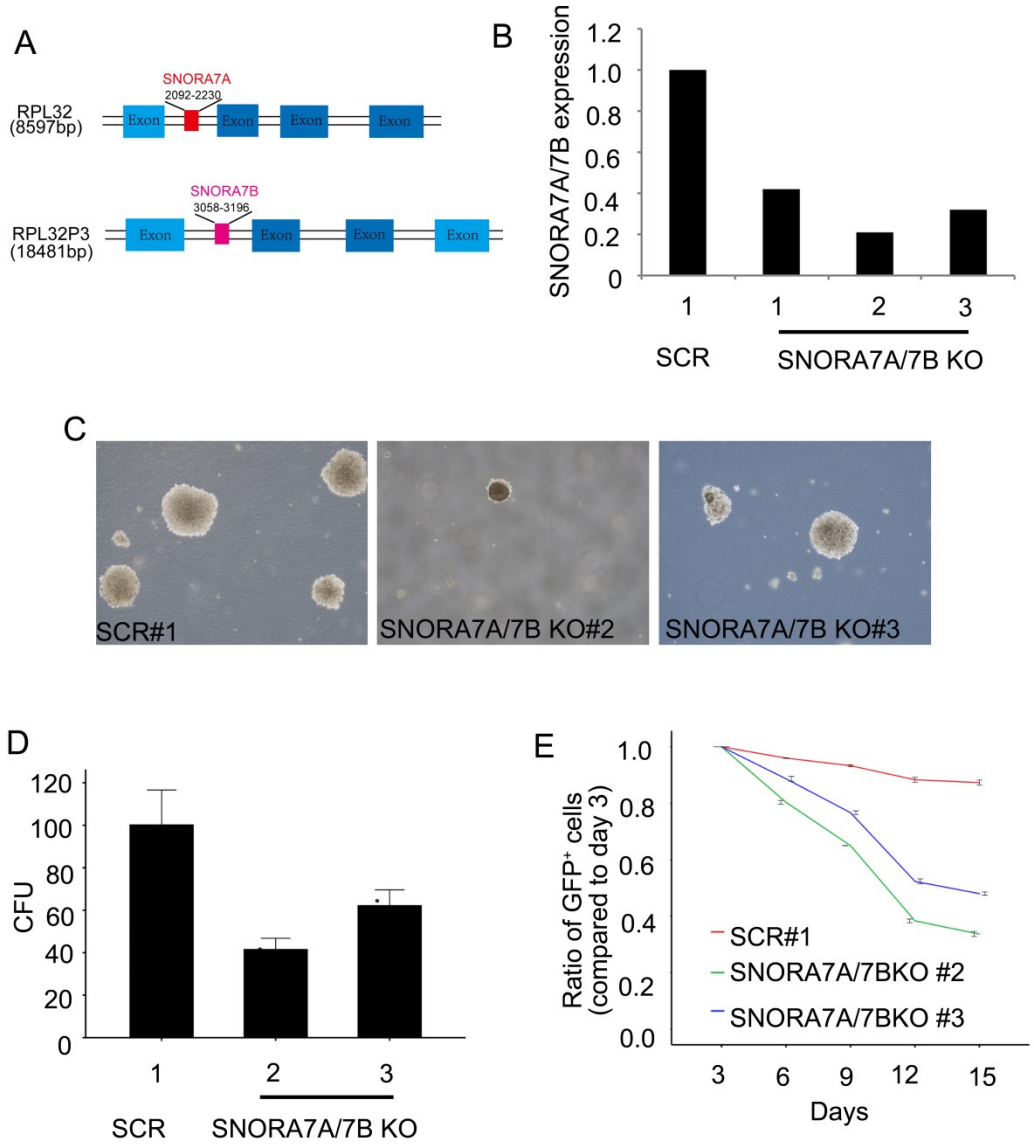

Figure 33: SNORA7A/7B KO inhibits proliferation and colony formation in Pc-9 cells. (A) The location of SNORA65 in genomic DNA. (B) RT-PCR analysis of SNORA7A/7B expression level in Pc-9 cells is shown. Values are normalized to that of scramble cells. U6 expression is used as a control. Results are expressed as Mean ± SD. (C) Representative images of colonies formed by scramble or SNORA7A/7B KO Pc-9 cells are shown. Scale bar, 1mm. (D) Quantitative result of colonies numbers in (C) is shown. (E) Proliferation curve derived from scramble or SNORA7A/7B KO Pc-9 cells is shown.

To explore if SNORA7A/7B KO could inhibit tumorigenicity of NSCLC in lung cancer cells, a colony formation assay in soft agar was performed in Pc-9 cells. As shown in the results, inhibition of SNORA7A/7B could decrease the number of colonies in Pc-9 cells compared with scrambled guide RNA control (Fig. 33 C-D). In addition, SNORA7A/7B KO could also inhibit proliferation of Pc-9 cells (Fig. 33E). These results further confirmed that SNORA7A/7B KO could inhibit lung cancer cell in vitro.

To confirm this result, similar experiments were repeated in A549 cells. As shown in Figure 34, SNORA7A/7B KO decreased the number of colonies in A549 cells. Also, inhibition of SNORA7A/7B expression led to lower proliferation capacity in A549 cells compared with the scrambled control (Fig. 34 C).

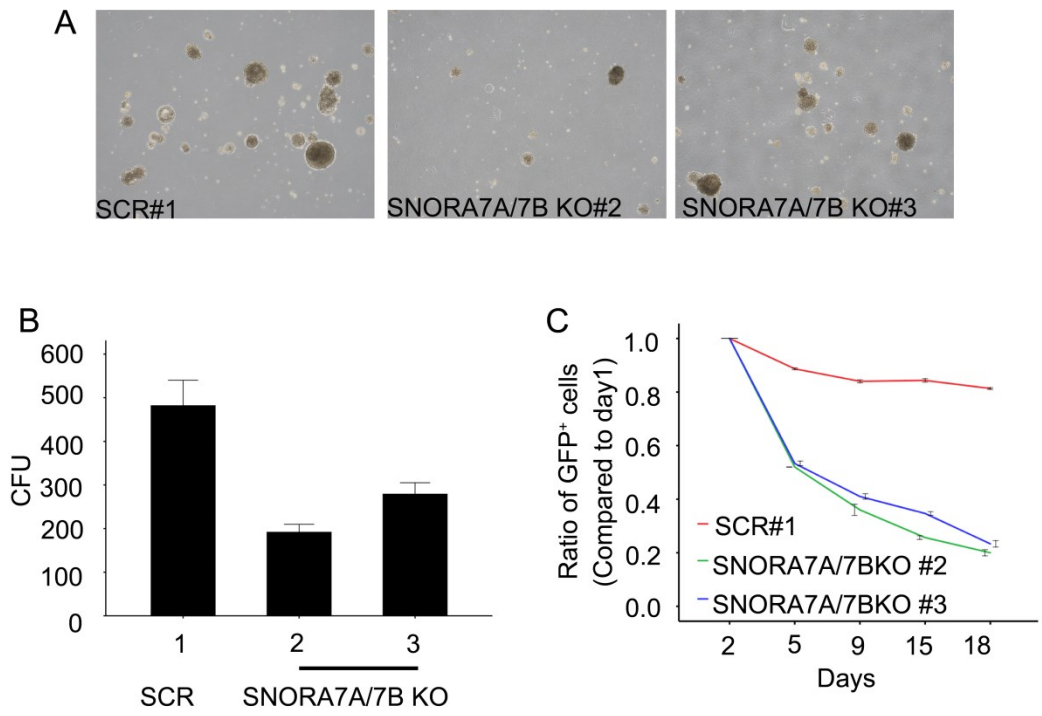

Figure 34: SNORA7A/7B KO inhibits proliferation and colony formation in A549 cells. (A) Representative images of colonies formed by scramble or SNORA7A/7B KO A549 cells are shown. (B) Quantitative results of colony numbers in (A) are shown. (C) Proliferation curve derived from scramble or SNORA7A/7B KO A549 cells is shown.

3.9 The effect of NOP10 KO on ribosomal RNA

From previous results we can get to the hypothesis that NOP10 could affect NSCLC development via snoRNA. NOP10 KO could inhibit rRNA pseudouridylation in vitro. But how does it work? First, we wanted to check if NOP10 knockout has an effect on the phenotype of ribosomal RNA. We tested the quality of total RNA in NOP10 KO pooled A549 cells and Pc-9 cells with a bioanalyzer. We could not find obvious effects on total RNA after NOP10 KO in both cell lines (Fig. 35 A - C).

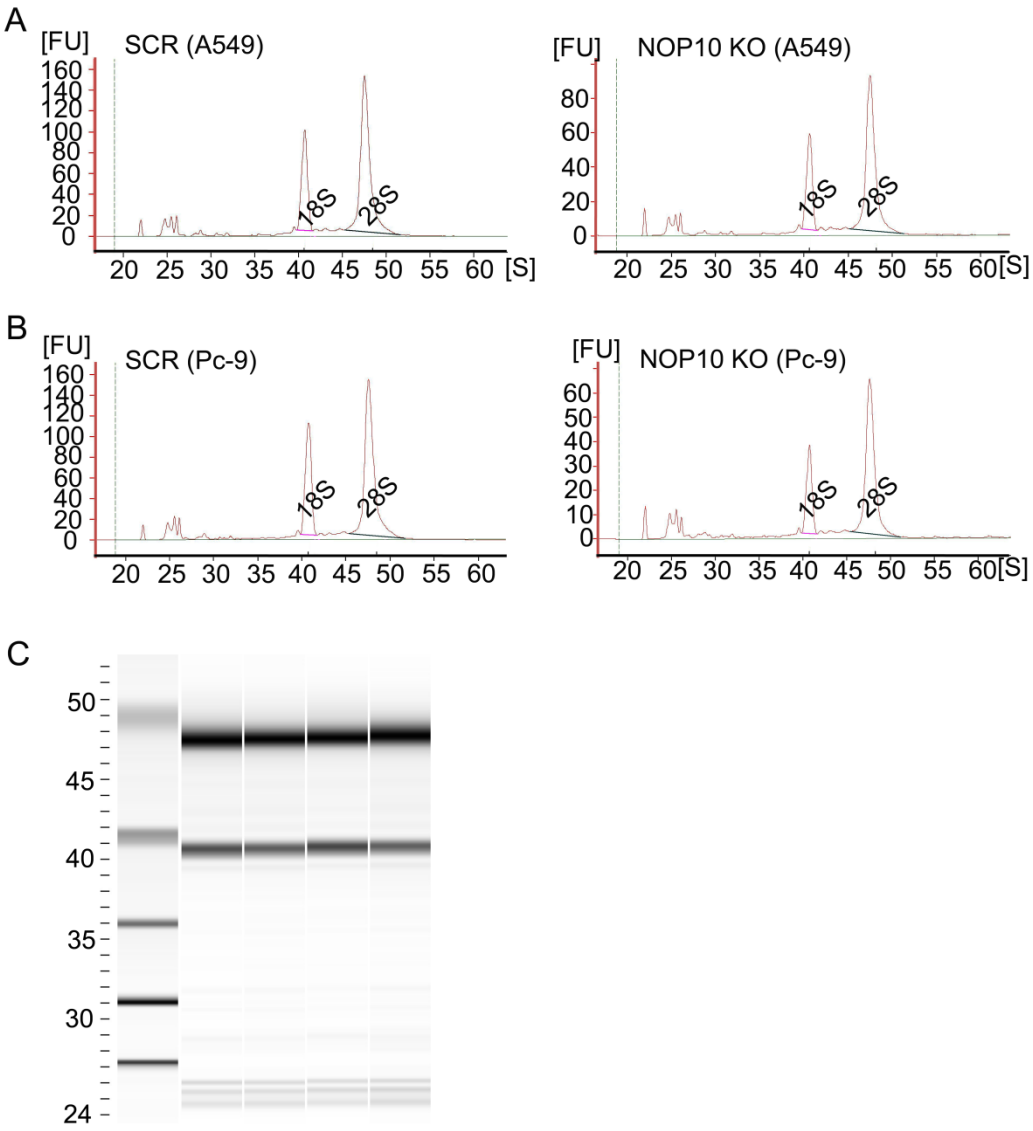

Figure 34: NOP10 KO has no obvious effect on ribosomal RNA expression. (A-B) Total RNA extracted from A549 cells (A) and Pc-9 cells (B) were analysed through a bioanalyzer. (C) The image showed a total RNA gel like-image produced by bioanalyzer.

3.10 NOP10 KO affects the cell cycle in lung cancer

3.10.1 NOP10 KO effects differ among lung cancer cell lines and Kasumi-1 leukaemia cells

We performed kinetic measurements of DNA synthesis in vitro by measuring BrdU incorporation into NOP10 KO A549 and Pc-9 cells. The amount of BrdU-incorporated cells decreased significantly in NOP10 KO A549 cells compared with scramble control cells (Fig. 36). Interestingly, NOP10 KO could increase the BrdU incorporated into Pc-9 cells (Fig. 36).

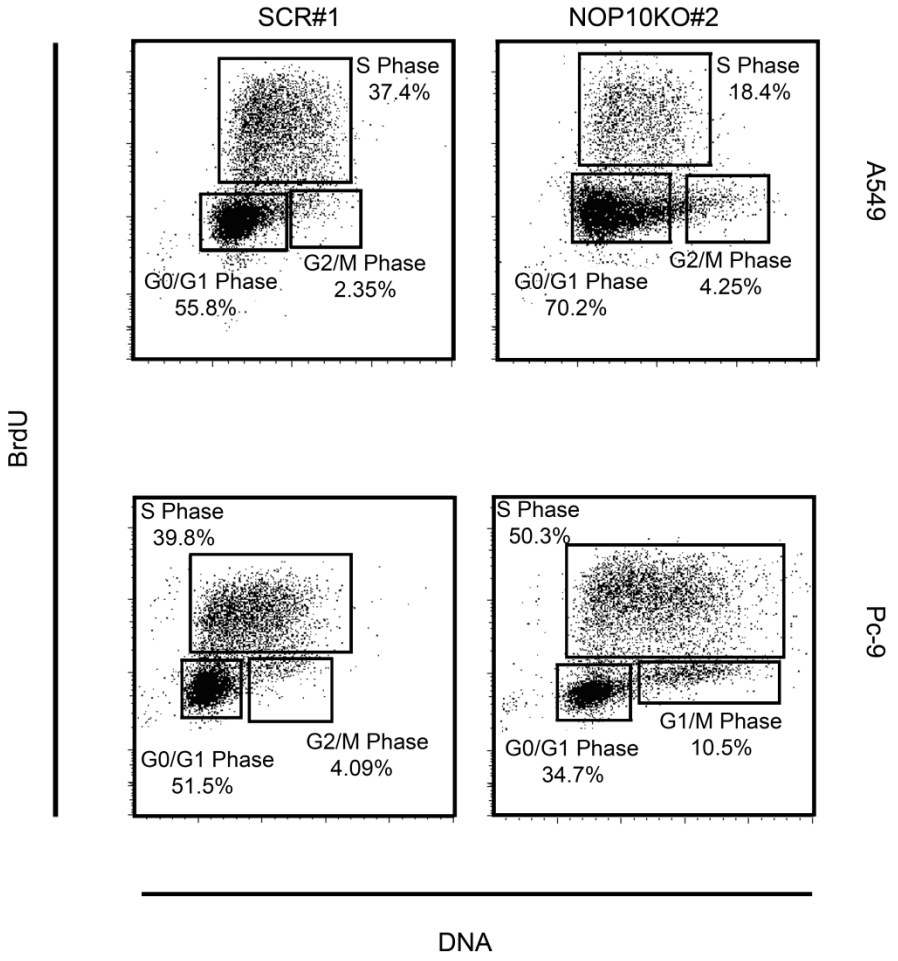

Figure 36: NOP10 KO has a different effect on cell cycle. (A) Representative BrdU incorporation into scramble and NOP10 KO A549 cells 2h after injection of BrdU. Percent of cells in G1, S, and G2 phases of the cell cycle are indicated. (B) Representative BrdU incorporation into scramble and NOP10 KO Pc-9 cells 2h after injection of BrdU. Percent of cells in G1, S, and G2 phases of the cell cycle are indicated.

Furthermore, we also confirmed the above results in another several cell lines. In H1975 and H358 cells, NOP10 KO could decrease the BrdU-incorporated cells. Similar to the phenotype in Pc-9 cells, the fraction of BrdU-incorporated cells increased significantly in NOP10 KO H661 cells (Fig. 37).

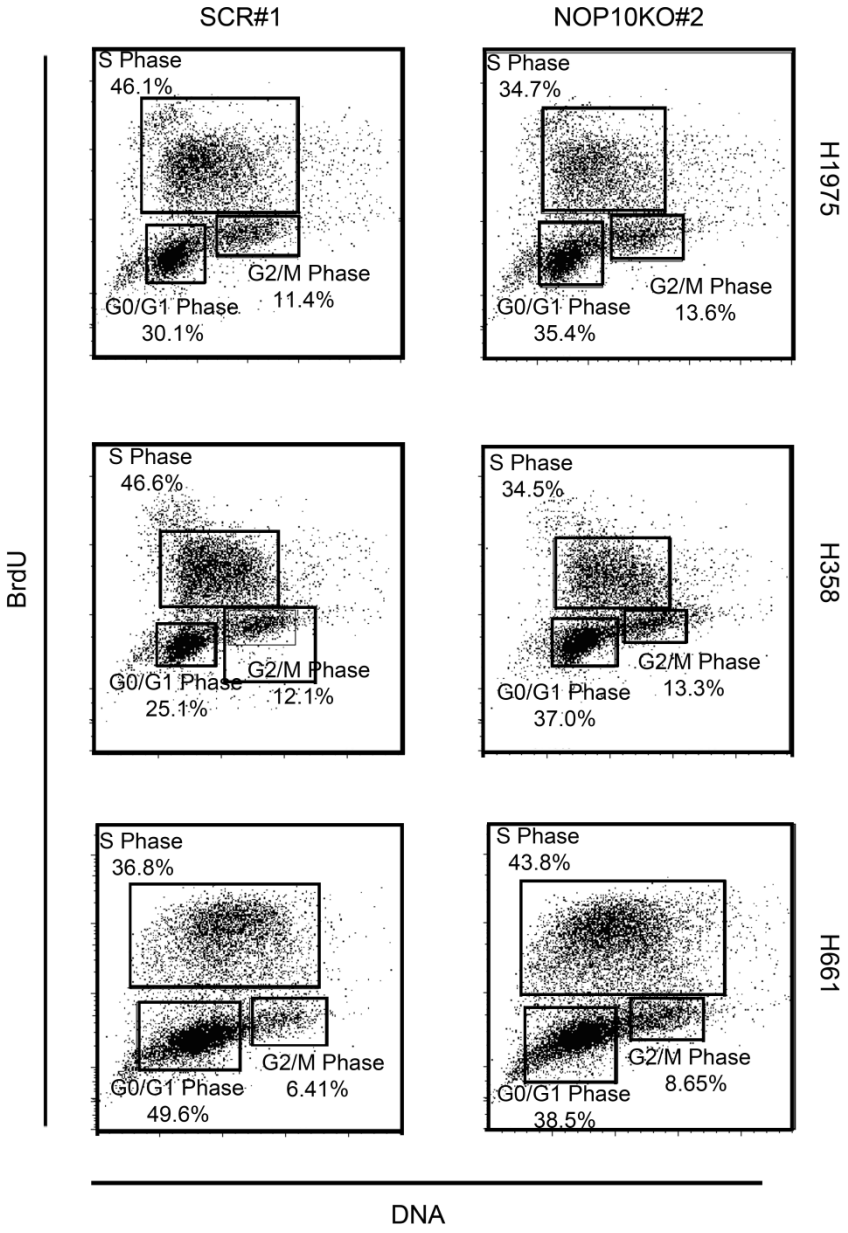

Figure 37: Representative BrdU incorporation assay in scramble and NOP10 KO H1975, H358, H661 cells after two hours of exposure to BrdU. The fractions of cells in G1, S, and G2 phases of the cell cycle are indicated.

3.10.2 NOP10 KO inhibits cells proliferation through different effects on the cell cycle in vitro

The previous results showed that NOP10 KO could inhibit proliferation and colony formation in lung cancer cells. But as shown in figures 36 and 37, NOP10 inhibition leads to different effects on the S phase of lung cancer cells. Thus, we wanted to know if NOP10 KO will affect the duration of the cell cycle. We utilized a BrdU chase approach to analyse time kinetics of DNA synthesis in lung cancer cells. Cells were pulsed with BrdU and then incubated without BrdU for 6 and 8 hours before analysing BrdU incorporation. This approach has been used for detection and quantification of BudU chase gaps, which are indicators of productive DNA synthesis. As shown in the results, NOP10 KO did not obviously change BudU chase gaps in A549 cells (Fig. 38).

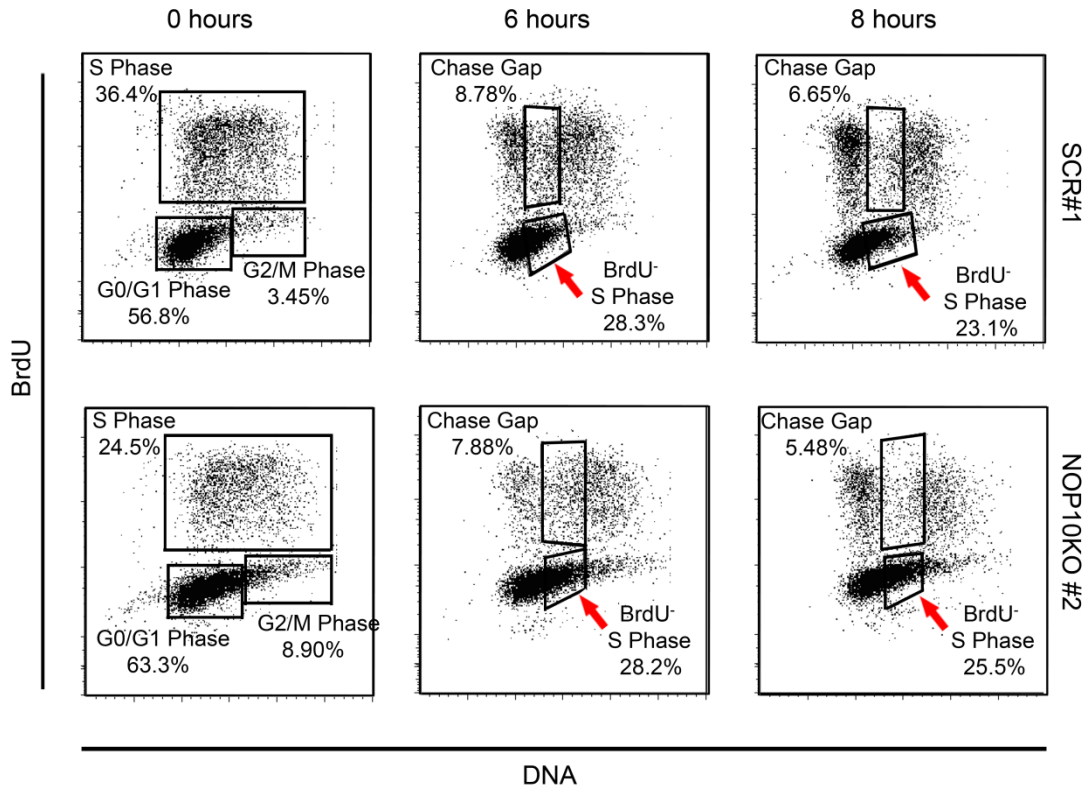

Figure 38: NOP10 KO does not affect on duration of S phase. Representative BrdU detection in scramble and NOP10 KO A549 cells after 0, 6 and 8 hours of BrdU chase.

Conversely, the BudU chase gaps assay showed us opposite results in Pc-9 cells. In the control group, $BrdU^+$ Pc-9 cells synthesized sufficient new DNA during the 6- and 8-hour chase points to generate typical BrdU chase gaps, but after NOP10 KO $BrdU^+$ Pc-9 cells did not display chase gaps, indicating its arrested DNA synthesis (Fig. 39). These results help to explain why proliferation and colony formation are inhibited but S phase cells increased after NOP10 KO in Pc-9 cells.

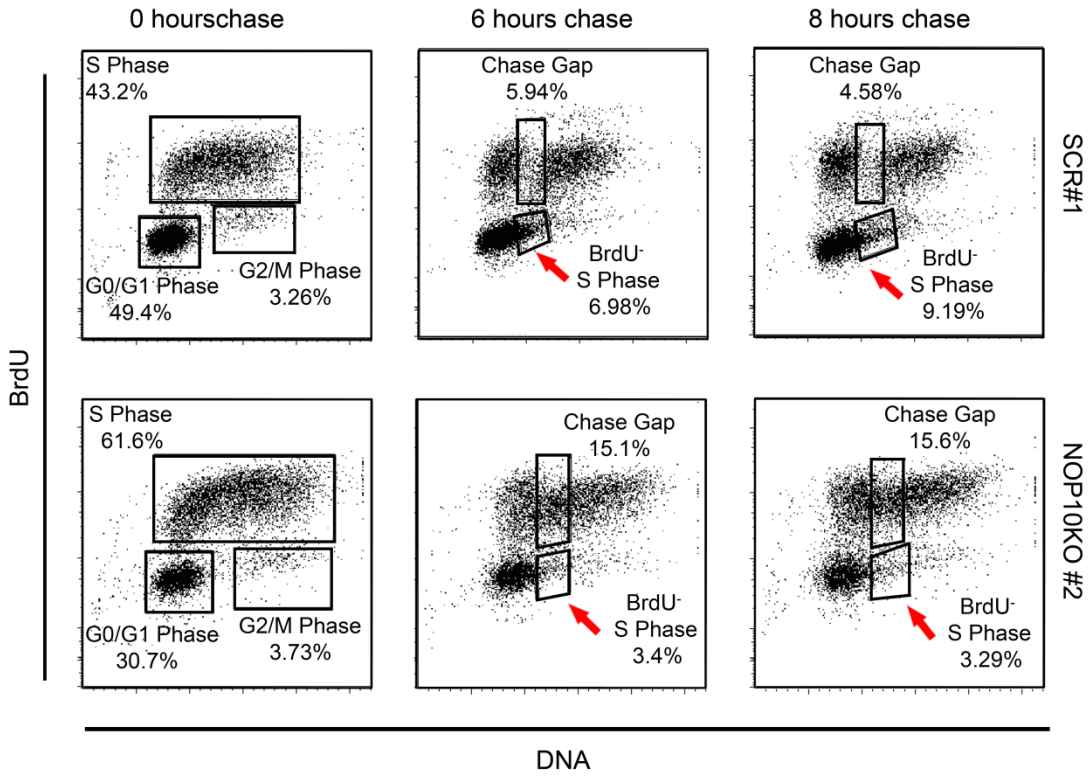

Figure 39: NOP10 KO arrests Pc-9 cells in S phase. Representative BrdU detection in scramble and NOP10 KO Pc-9 cells after 0, 6 and 8 hours of BrdU chase.

We next tried to investigate the different mechanisms between A549 and Pc-9 cells. As we show in figures 38 and figure 39, NOP10 KO lead to arrested DNA synthesis in Pc-9 cells but inhibited S phase cells in A549 cells. We hypothesized that there are two different mechanisms during NOP10 regulation of A549 cells and Pc-9 cells. It has been reported that arrested DNA synthesis was related with DNA damage response. In addition, histone H2A.X phosphorylated on Ser139 (pH2A.X) is the DNA damage response (DDR) marker. Thus, pH2A.X staining was performed in

A549 cells and Pc-9 cells after NOP10 KO. The results indicated that NOP10 KO leads to DNA damage response in Pc-9 cells compared with scrambled control, but NOP10 KO has no obvious effect on DNA damage response in A549 cells (Fig. 40).

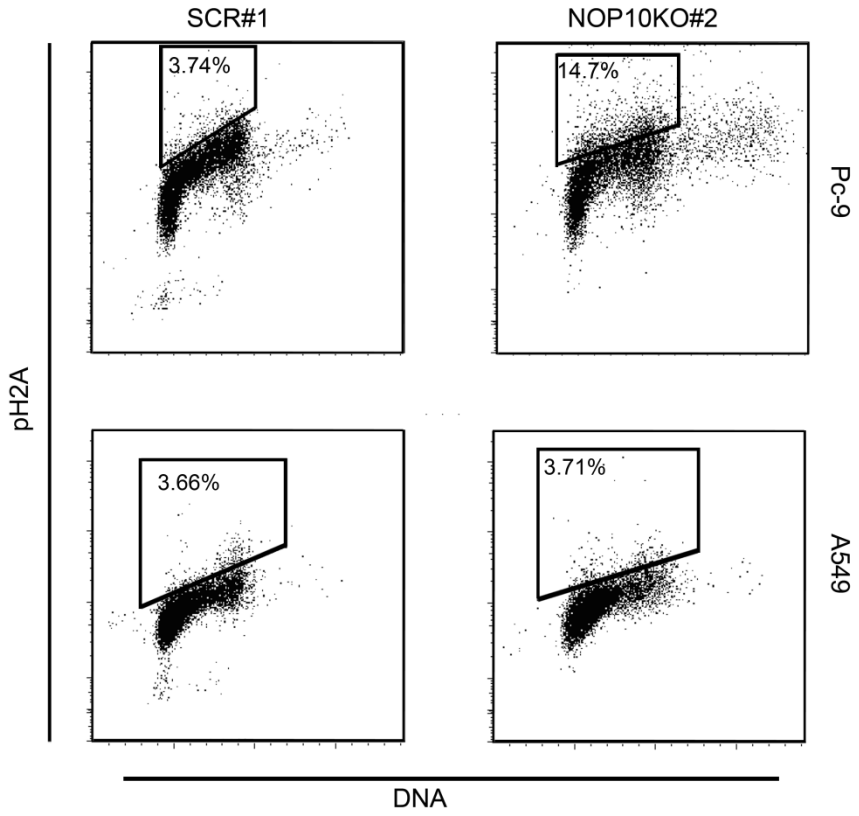

Figure 40: NOP10 KO induces DNA damage in Pc-9 cells but has no effect on A549 cells. Detection of H2A.X phosphorylated on Ser139 (pH2A.X) in scramble and NOP10 KO cells by flow cytometry. Percentages of pH2A.X-positive (pH2A.X+) cells are indicated.

Cellular senescence has been reported as an irreversible cell cycle arrest mechanism (van Deursen, 2014). It is generally believed that cellular senescence reflects some of the changes that occur during the aging of organisms. In most studies, cellular senescence was characterized by appearance of senescence-associated β-galactosidase (SA-β-gal). We also tested the expression of β-galactosidase (SA-β-gal) in NOP10 KO lung cancer cells. Conversely, we did not find upregulation of SA-β-gal in NOP10 KO Pc-9 cells that have arrested DNA synthesis (Fig. 41). However, SA-β-gal overexpression was found in NOP10 KO A549 cells (Fig. 41).

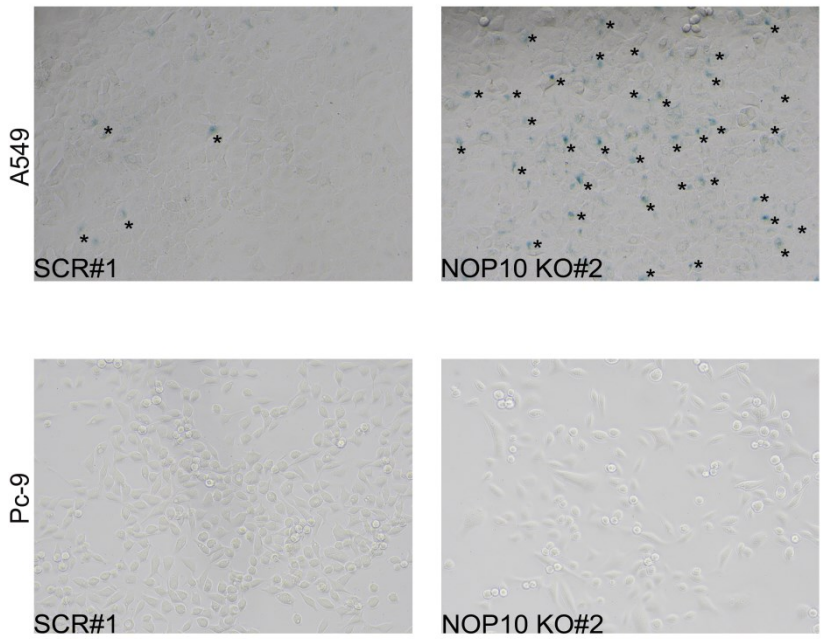

Figure 41: NOP10 KO induces senescence in A549 cells but not in Pc-9 cells. Senescence-associated beta-galactosidase (SA-betagal) staining in scramble and NOP10 KO cells is shown.

It has been reported that changes in rDNA transcription and ribosome biogenesis can contribute to tumorigenesis (Barna et al., 2008; Kondrashov et al., 2005; Ruggero and Pandolfi, 2003). Also, snoRNAs are essential for the processing of precursor ribosomal RNAs (Lafontaine, 2015). In our previous paper we have shown that reduced snoRNA expression and rRNA methylation in AES-depleted AE9a cells could impair ribosome biogenesis and/or protein synthesis (Zhou et al., 2017). Thus, we next measured the protein translation rates with O-propargylpuromycin (OP-Puro) incorporation assay in NOP10 KO lung cancer cells. We found that NOP10 KO Pc-9 cells incorporated much more OP-Puro than scramble control (Fig. 42B), but NOP10 KO inhibits OP-Puro incorporation compared with scramble control in A549 cells (Fig. 42A). These results are consistent with the results of the cell cycle assay.

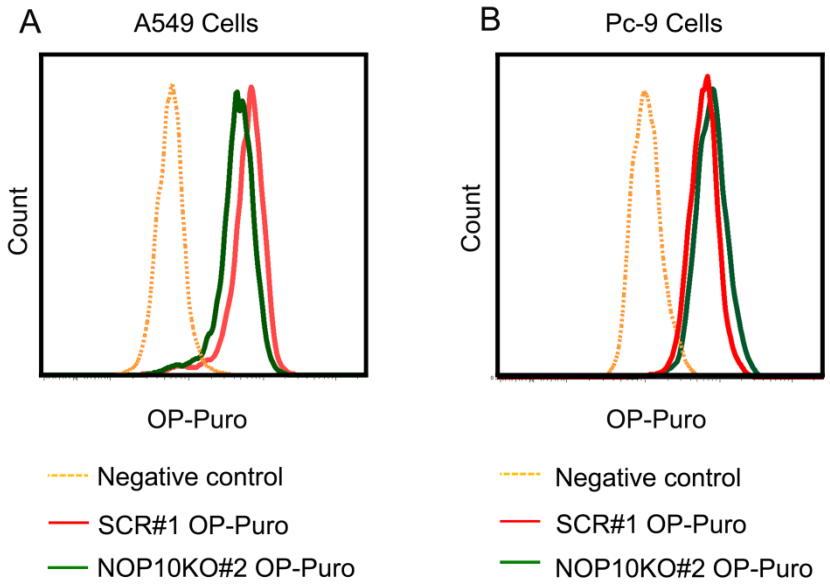

Figure 42: NOP10 KO regulates protein synthesis in lung cancer cells. (A) OP-Puro incorporation of control (SCR) and NOP10 KO A549 cells. One of n = 3 independent experiments is shown. (B) OP-Puro incorporation of control (SCR) and NOP10 KO Pc-9 cells. One of n = 3 independent experiments is shown.

Furthermore, single cell divisions were monitored with cell proliferation fluorescent dye. In our study, NOP10 KO had no obvious effect on A549 cells divisions (Fig. 43A). However, NOP10 KO inhibited Pc-9 cells divisions (Fig. 43B). These results were consistent with the results of the OP-Puro incorporation assay.

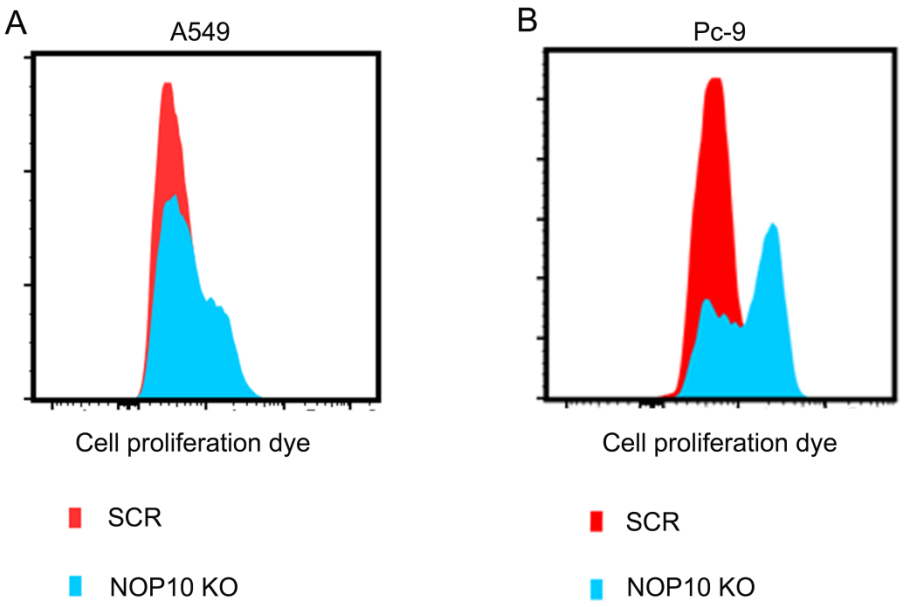

Figure 43: NOP10 KO affects cells divisions in lung cancer cells. (A) Cell proliferation dye analysis of control (SCR) and NOP10 KO A549 cells. One of n = 3 independent experiments is shown. (B) Cell proliferation dye analysis of control (SCR) and NOP10 KO Pc-9 cells. One of n = 3 independent experiments is shown.

3.10.3 NOP10 KO affects cell cycle related protein expression in vitro

In the next step, we wanted to know why we observed two opposite mechanisms in two lung cancer cell lines. It has been reported that the snoRNA pathway could regulate cancer through a P53-dependent way (Chen et al., 2015; Mei et al., 2012). First, we compared the difference between A549 cell lines and Pc-9 cells lines. P53 expression information of lung cancer cells was showed in Supplemental Table 2. We found that A549 cells are a P53 wild-type cell line, but Pc-9 cells are a P53 mutation cell line. Thus, we try to investigate the expression of cell cycle-related protein and DNA damage-related protein with western blot. As shown in the results, P21 and P27 proteins were upregulated in NOP10 KO A549 cells compared with scramble control cells. But pH2A.X was not found in either scramble control or NOP10 KO A549 cells. Conversely, NOP10 KO out could not affect the expression of P21 and P27 proteins in Pc-9 cells but NOP10 KO upregulated the expression of DNA damage response-related protein pH2A.X (Fig. 44). The results strongly support the different effects of NOP10 KO on A549 cells and Pc-9 cells.

Table 2: P53 hotspot mutation lung cancer cell panel

Cell line	WT or Mut						Reference
A549	WT						*Jia LQ, et al. 1997*
H1975	WT						*Forbes S, et al. 2006*
H1650	WT						*Phelps RM, et al. 1996*
Cell line	**WT or Mut**						**Reference**
H358	Mut (deletion or rearrangement)						no
Cell line	**WT or Mut**	**WT**	**Mut**	**AA**	**Mut**	**composition**	**Reference**
Pc-9	Mut (single mutation)	CGG	CAG	Arg	Gln	248	*Kashii T, et al. 1994*
H661	Mut (single mutation)	AGT	ATT	Ser	Ile	215	*Mitsudomi T, et al. 1992*

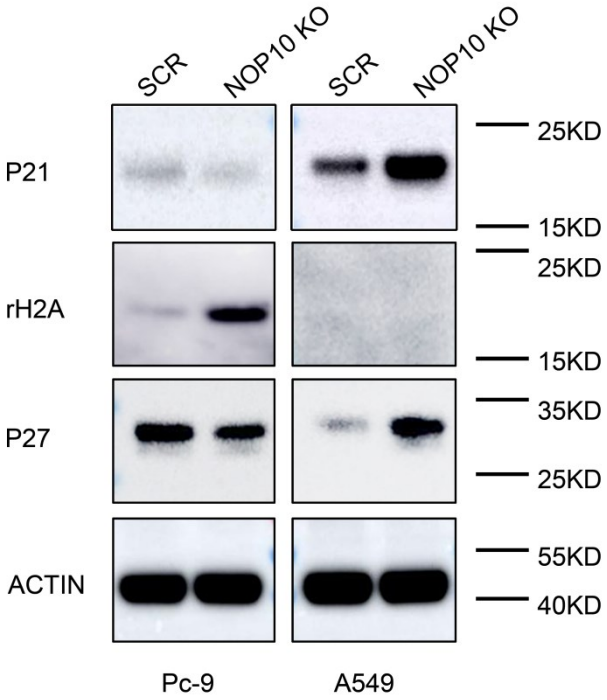

Figure 44: NOP10 KO affects cell cycle-related protein expression in vitro. Western blot detection of cell cycle-related protein expression in scramble and NOP10 KO cells in different lung cancer cell lines.

All these data suggest that NOP10 could regulate NSCLC development through H/ACA box snoRNA with a different mechanism. Also, NOP10 regulates the cell cycle in a different mechanism that depends on P53 function.

4. Discussion

4.1 NOP10 in non-small cell lung cancer

H/ACA box snoRNPs mainly include four conserved snoRNPs, which contain DKC1, NOP10, NHP2, and Gar1. Previous studies have reported that all of these four conserved proteins are important for snoRNPs' structure and function (Filipowicz and Pogacic, 2002; Kiss, 2002). H/ACA box snoRNPs are mainly responsible for RNA pseudouridylation in mRNA, rRNA, spliceosomal snRNAs and various other types of ncRNAs. In our study, we found that NOP10 KO could inhibit almost all ribosomal RNA pseudouridylation. It has been reported that pseudouridylation plays a critical role in cell physiology (Agarwal et al., 2010; Fong et al., 2014). These reports are consistent with our results. DKC1 KO significantly inhibited cell growth and colony formation in lung cancer cells. Also, inhibition of NOP10 protein decreased cell growth and colony formation in lung cancer cells. Interestingly, we found that DKC1 and NOP10 were highly expressed in NSCLC tumour samples.

DKC1 is the catalytic component of the snoRNP complex. DKC1 has been linked to a human disease called dyskeratosis congenita (Bessler et al., 2010; Ruggero et al., 2003). It has been reported that DKC1 has two separate functions. One function is to pseudouridylate ribosomal RNA molecules as H/ACA box ribonucleoproteins. The other function is to stabilize the telomerase RNA component. But as one of the conserved H/ACA box snoRNPs, there are few reports about NOP10 function. Through Kaplan Meier plotter data online we found that in NSCLC patients, NOP10 mRNA expression intimately correlated with prognosis, other than DKC1, NHP2 and Gar1. Consistently, our immunohistochemistry results also indicated that NOP10 protein expression correlated with overall survival in NSCLC patients. Furthermore, NOP10 protein was highly expressed in NSCLC tumour samples. And NOP10 KO inhibits lung cancer cells migration significantly. These data provide strong evidence that NOP10 acts as an important role in NSCLC development.

SnoRNA biogenesis is a multistep process and snoRNPs are required for snoRNA biogenesis (Lafontaine, 2015). During snoRNA maturation, core proteins of snoRNPs are recruited to snoRNA sequences to protect the newly produced snoRNA from degradation. Consistent with previous reports, NOP10 KO decreases expression

of most H/ACA box snoRNAs, but does not affect the expression of other snoRNAs. Previous studies have reported that snoRNA could affect tumour development in many types of carcinoma (Kiss, 2002; Mannoor et al., 2014; Stepanov et al., 2015; Thorenoor and Slaby, 2015; Zhou et al., 2017). Furthermore, snoRNA has been considered as a potential oncogene and molecular marker in the development and progression of lung cancer.

NSCLC is the leading cause of cancer death all over the world. Identification of effective therapeutic targets for NSCLC may reduce mortality. Each of H/ACA box snoRNPs is necessary for its traditional function to perform pseudouridylation modification of target RNA guiding by snoRNA. As one of the H/ACA box snoRNPs, NOP10 protein makes more sense in the prognosis of lung cancer patients than other ribonucleoproteins. In our study, NOP10 upregulation was frequently found in NSCLC tissues but rarely present in paired normal tissues, which indicates a potential diagnostic biomarker for lung cancer. Furthermore, our results have identified the oncogenic role of the NOP10 molecule in lung cancer development. The critical role of the NOP10 molecule indicates that it could be a potential target for therapeutic treatment in NSCLC.

4.2 SnoRNA regulates development of lung cancer cells

Traditionally, the canonical function of snoRNA has been considered as housekeeping genes to guide pseudouridylation modification of target RNA. Recent reports showed that snoRNAs play roles in controlling cell fate and oncogenesis (Dong et al., 2009; Dong et al., 2008; Gee et al., 2011; Martens-Uzunova et al., 2012). Both H/ACA box snoRNA and C/D box snoRNA may function in regulating cancer biology. SNORA65, comprised of 137 nucleotides and located between exons 4 and 5 of RPL12 gene, is poorly understood until now. What we know about SNORA65 is that it could induce rRNA maturation by guiding the pseudouridylation of residues U4373 and U4427 of the 28S rRNA. In our study we found that SNORA65 KO inhibited lung cancer cell proliferation and colony formation. These findings are consistent with our genome-scale CRISPR/Cas9 screening, in which SNORA65 KO showed negative proliferation. Notably, according to the TCGA data, SNORA65 was highly expressed in lung cancer tumour samples. These data are also consistent with

our results in the matched tumour and normal lung cancer tissue, in which SNORA65 always had higher expression in tumour samples than in normal samples.

In addition, the canonical function of H/ACA box snoRNA is to guide pseudouridylation of target RNA. Pseudouridylation, as the most common and evolutionarily conserved modification of rRNA, is necessary for normal functioning of the ribosome and for the correct packing of rRNA, stabilization of its structure and for correct interaction of rRNA with other participants of translation (Karijolich and Yu, 2010). SNORA7A is comprised of 139 nucleotides and is located between exons 1 and 2 of the RPL32 gene. SNORA7B is comprised of 139 nucleotides and is located between exons 1 and 2 of RPL32P3 gene. These have common target site on residues U1569 and U1779 of 28S rRNA. Interestingly, we found that the ribosomal RNA 28S 1779 site has a higher pseudouridylation level in tumour samples than in matched normal samples, and this site is the target site of SNORA7A and SNORA7B. According to the TCGA data, SNORA7A/7B was highly expressed in lung cancer tumour samples. We also found that SNORA7A/7B KO could inhibit lung cancer cell proliferation and colony formation. SNORA7A or SNORA7B KO appeared to result in a negative proliferation phenotype in our genome-scale CRISPR/Cas9 screening. These data provide strong evidence that SNORA7A and SNORA7B could regulate lung cancer development. Some studies have reported that host genes of some snoRNAs also take part in the molecular pathology of cancer (Thorenoor and Slaby, 2015). But in our study, the expression of RPL32, which is host gene of SNORA7A, appears to not change after SNORA7A KO. These results indicate that SNORA7A, other than its host gene, has a function in lung cancer development.

So far, there are no studies on the contributions of SNORA65, SNORA7A and SNORA7B to the genesis and progression of cancer. In this study, we have identified potential oncogenic roles of SNORA65, SNORA7A and SNORA7B through enhanced cellular proliferation and colony formation in lung cancer development. Furthermore, the expression of these three snoRNAs in lung cancer tissue potentially can be used as a diagnostic biomarker. These data highlight the critical role that snoRNAs play in lung cancer biology. SNORA65, SNORA7A and SNORA7B could be used as potential therapeutic targets in NSCLC patients.

4.3 NOP10 regulates cell cycle progression

In this study we found that NOP10 KO did inhibit the cell cycle in lung cancer cells and inhibited colony formation and proliferation of lung cancer cells. A previous study reported that SNORD76 overexpression could arrest cancer cells in the S phase of the cell cycle (Chen et al., 2015). The cell cycle consists of four distinct phase: G1 phase, S phase, G2 phase and M phase. Interestingly, we found that there are two distinct mechanisms that inhibit cell cycle progression in these lung cancer cells. In A549 cells, NOP10 KO resulted in accumulation of cells in the G0/G1 phase but decreased the cells in the S phase. These results are consistent with previous reports that snoRNA pathway deficiency will induce significant G0/G1 cell cycle arrest. However, in Pc-9 cells, NOP10 KO led to the accumulation of cells in the S phase, but blocked exit from the S phase because there was no significant increase in the G2/M phase. Notably, both cell cycle mechanisms led to the same result: cell proliferation and colony formation are inhibited after NOP10 KO. Accordingly, chase gap pulse assay showed us that NOP10 KO did not affect the duration of the cell cycle in A549 cells, but in Pc-9 cells NOP10 KO significantly elongated the duration of the cell cycle. Pc-9 cells with NOP10 KO could not accomplish one cell cycle and most of the cells were arrested in the S phase. The different cell cycle phenotypes in two different cell lines were all induced by NOP10 inhibition.

Protein synthesis requires protein components of the translation machinery and also ribosomal RNAs (rRNAs). Recently more studies have shown the importance of the nucleolus as the ribosome factory in cancer development (Bastide and David, 2018). However, the involvement of the snoRNA and snoRNPs, which are essential for proper modification of rRNA and its maturation, remains unclear. The critical role of protein synthesis is to support cancer cell growth. It has been reported that leukaemia cells with globally decreased C/D box snoRNAs showed decreased protein synthesis with concomitant smaller cell size (Zhou et al., 2017). Similar findings were observed for globally decreasing H/ACA box snoRNA after NOP10 KO in A549 cells. In contrast, increasing protein synthesis with bigger cell size has been found after NOP10 KO in Pc-9 cells. Interestingly, these findings could help to explain the two different cell cycle results.

A previous study reported that SNORD76 overexpression will induce accumulation of cells in the S phase (Chen et al., 2015). Conversely, some studies have reported that snoRNA pathway deficiency will lead to significant G0/G1 cell cycle arrest (Mei et al., 2012). In our study we found a different cell cycle phenotype after NOP10 KO: G0/G1 cell cycle arrest in A549 cells and S phase cell cycle arrest in Pc-9 cells. However, the effects are the same: growth of lung cancer cells will be inhibited after NOP10 KO. These data represent a previously unrecognized role of snoRNPs in human cancer ad these mechanism may provide new prospective approaches to lung cancer therapy.

4.4 NOP10 KO inhibits lung cell proliferation via P53-dependent and -independent way mechnisms

The Tp53 gene is frequently mutated in NSCLC (Takahashi et al., 1989); however, the effect of P53 gene mutations on patients remains unclear. It has been reported that under stress conditions such as snoRNA pathway deficiency, some ribosomal proteins will move to the cytoplasm and help to stabilize the P53 molecule (Thorenoor and Slaby, 2015). P21 was also markedly induced during the snoRNA pathway deficiency and led to significant G0/G1 cell cycle arrest. We obtained similar results in A549 cells, which present the wild type P53 gene. We found that NOP10 KO led to higher expression of P21 and P27, which are related with cell cycle regulation. And NOP10 deficient induced accumulation of cells in G0/G1 phase resulted in lower proliferation of cells. These data are in line with the overexpression of NOP10 in lung cancer cells and indicate an important role of deregulated NOP10 in human lung cancer, showing a critical role of P53 in coordinating the snoRNA pathway with cell proliferation. This is also consistent with previous reports that activation of P53 will induce growth arrest, differentiation or apoptosis of cells (Brameier et al., 2011; Williams and Farzaneh, 2012b). These data suggest that NOP10 KO could induce P53 response and lead to inhibition of tumour growth in certain lung cancer cell line.

In contrast, we found an opposite phenomenon in Pc-9 cells, which presented a mutated P53 gene. The results showed us that NOP10 KO did not affect the expression of P21 and P27, consistent with the P53 mutation in this cell line.

Furthermore, NOP10 downregulation induced accumulation of cells in the S phase and resulted in lower proliferation of cells at the same extent with A549 cells. Interestingly, NOP10 KO induced higher expression of a DNA damage response related to molecule phosphorylation of histone H2X (Rh2X) in P53 mutated Pc-9 cells but had no effect in P53 wild type A549 cells. These data suggest that NOP10 KO could induce DNA damage and inhibit tumour growth in a P53 mutated cell line without P53 response. DNA can be damaged in a variety of ways.

Previous studies have reported that SNORA42 could increase apoptosis of NSCLC in a P53-dependent manner (Mei et al., 2012). But in P53 null or P53 mutated cell lines, SNORA42 did not induce cell apoptosis. SNORD76 overexpression has been reported to induce accumulation of cells in the S phase and prevent tumour growth (Chen et al., 2015). In other kinds of cancer snoRNAs also have important functions. In our study, we first found that NOP10 regulate cell growth in both P53 wild type and p53 mutated cell lines with two different mechanisms. NOP10 KO significantly affects the expression of entire H/ACA box snoRNAs.

4.5 SnoRNA pathway maybe one key point for NSCLC therapy

It has been reported that ribosome maturation and function defects can cause transformation of normal cells to tumour cells (Goudarzi and Lindstrom, 2016). SnoRNAs take part in alternative splicing and posttranscriptional modification of mRNA (Kishore and Stamm, 2006; Nakamoto et al., 2017; Vitali et al., 2005). C-myc directly binds to promoters of snoRNAs' host gene, leading to increased transcription of snoRNA. It is reasonable for us to assume that changes in snoRNA may lead to various diseases. In our study we found that snoRNPs are necessary during lung cancer development, including snoRNAs and snoRNA proteins.

Previous studies have reported that C/D box snoRNA and H/ACA box snoRNA exhibit altered expression patterns in different tissues, and these snoRNAs appear to have tissue-specific functions. For example, SNORD115 and SNORD116 could be processed into smaller RNAs and prevent formation of particular pre-mRNA splicing variants, specifically in brain tissue (Kishore et al., 2010). Furthermore, in cancer diseases, the oncogenic process could induce altered of snoRNA expression and its

host gene (Stepanov et al., 2015). C/D box snoRNA and H/ACA box snoRNA expression profiles were found to vary in different types and subtypes of cancer, which could be used to characterize and classify cancer types (Gong et al., 2017). SNORA42, which is overexpressed in NSCLC, was identified as a lung cancer oncogene (Mei et al., 2012). Our studies found that SNORA65, SNORA7A and SNORA7B were highly expressed in NSCLC cells. This suggests that SNORA65, SNORA7A and SNORA7B could be used as biomarkers to reflect tumour progression. In addition, inhibition each of these three snoRNAs correlated with tumour cell colony formation, indicating that these snoRNAs have a considerable impact on oncogenesis and should be treated as oncogenes.

For the snoRNA-related proteins, it has been reported that expression of fibrillarin correlates with c-myc in cancer cells (Koh et al., 2011). High-level expression of fibrillarin has been found in breast, prostate and many other cancer cells (Stepanov et al., 2015) and fibrillarin overexpression could lead to a significantly compromised P53-dependent response in cancer cells. The most important point in our study is that NOP10 KO could inhibit lung cancer cell proliferation in a P53-dependent and -independent way.

SNORA42 has been considered a potential therapeutic target because it could increase apoptosis of NSCLC in a P53-dependent manner (Mei et al., 2012). But as leading cause of cancer death, P53-dependent apoptosis is not enough for lung cancer therapy. As reported in a previous study, SNORA42 has no effect on P53 mutation or P53 null lung cancer cells. Thus our findings are important for the next strategies in lung cancer therapy.

Taken together, NOP10 could be used as a diagnostic and prognostic marker during lung cancer development. NOP10 has effects on almost all H/ACA box snoRNAs, and this pathway might constitute a potential therapeutic target in NSCLC patients.

Reference

Agarwal, S., Loh, Y.H., McLoughlin, E.M., Huang, J., Park, I.H., Miller, J.D., Huo, H., Okuka, M., Dos Reis, R.M., Loewer, S.*, et al.* (2010). Telomere elongation in induced pluripotent stem cells from dyskeratosis congenita patients. Nature *464*, 292-296.

Appaiah, H.N., Goswami, C.P., Mina, L.A., Badve, S., Sledge, G.W., Jr., Liu, Y., and Nakshatri, H. (2011). Persistent upregulation of U6:SNORD44 small RNA ratio in the serum of breast cancer patients. Breast cancer research : BCR *13*, R86.

Atzorn, V., Fragapane, P., and Kiss, T. (2004). U17/snR30 is a ubiquitous snoRNA with two conserved sequence motifs essential for 18S rRNA production. Molecular and cellular biology *24*, 1769-1778.

Barna, M., Pusic, A., Zollo, O., Costa, M., Kondrashov, N., Rego, E., Rao, P.H., and Ruggero, D. (2008). Suppression of Myc oncogenic activity by ribosomal protein haploinsufficiency. Nature *456*, 971-975.

Bastide, A., and David, A. (2018). The ribosome, (slow) beating heart of cancer (stem) cell. Oncogenesis *7*, 34.

Beltrame, M., and Tollervey, D. (1995). Base pairing between U3 and the pre-ribosomal RNA is required for 18S rRNA synthesis. The EMBO journal *14*, 4350-4356.

Bessler, M., Wilson, D.B., and Mason, P.J. (2010). Dyskeratosis congenita. FEBS letters *584*, 3831-3838.

Boland, C.R. (2017). Erratum to: Non-coding RNA: It's Not Junk. Digestive diseases and sciences *62*, 3260.

Boon, K., Caron, H.N., van Asperen, R., Valentijn, L., Hermus, M.C., van Sluis, P., Roobeek, I., Weis, I., Voute, P.A., Schwab, M.*, et al.* (2001). N-myc enhances the expression of a large set of genes functioning in ribosome biogenesis and protein synthesis. The EMBO journal *20*, 1383-1393.

Borowicz, S., Van Scoyk, M., Avasarala, S., Karuppusamy Rathinam, M.K., Tauler, J., Bikkavilli, R.K., and Winn, R.A. (2014). The soft agar colony formation assay. Journal of visualized experiments : JoVE, e51998.

Brameier, M., Herwig, A., Reinhardt, R., Walter, L., and Gruber, J. (2011). Human box C/D snoRNAs with miRNA like functions: expanding the range of regulatory RNAs. Nucleic acids research *39*, 675-686.

Branlant, C., Krol, A., Machatt, M.A., Pouyet, J., Ebel, J.P., Edwards, K., and Kossel, H. (1981). Primary and secondary structures of Escherichia coli MRE 600 23S ribosomal RNA. Comparison with models of secondary structure for maize chloroplast 23S rRNA and for large portions of mouse and human 16S mitochondrial rRNAs. Nucleic acids research *9*, 4303-4324.

Brown, J.W., Echeverria, M., and Qu, L.H. (2003). Plant snoRNAs: functional evolution and new modes of gene expression. Trends in plant science *8*, 42-49.

Campbell, K.J., and White, R.J. (2014). MYC regulation of cell growth through control of transcription by RNA polymerases I and III. Cold Spring Harbor perspectives in medicine *4*.

Carlile, T.M., Rojas-Duran, M.F., Zinshteyn, B., Shin, H., Bartoli, K.M., and Gilbert, W.V. (2014). Pseudouridine profiling reveals regulated mRNA pseudouridylation in yeast and human cells. Nature *515*, 143-146.

Chamberlain, S.J. (2013). RNAs of the human chromosome 15q11-q13 imprinted region. Wiley interdisciplinary reviews RNA *4*, 155-166.

Chen, L., Han, L., Wei, J., Zhang, K., Shi, Z., Duan, R., Li, S., Zhou, X., Pu, P., Zhang, J.*, et al.* (2015). SNORD76, a box C/D snoRNA, acts as a tumor suppressor in glioblastoma. Scientific reports *5*, 8588.

Dacic, S., Shuai, Y., Yousem, S., Ohori, P., and Nikiforova, M. (2010). Clinicopathological predictors of EGFR/KRAS mutational status in primary lung adenocarcinomas. Modern pathology : an official journal of the United States and Canadian Academy of Pathology, Inc *23*, 159-168.

Darzacq, X., Kittur, N., Roy, S., Shav-Tal, Y., Singer, R.H., and Meier, U.T. (2006). Stepwise RNP assembly at the site of H/ACA RNA transcription in human cells. The Journal of cell biology *173*, 207-218.

Dieci, G., Preti, M., and Montanini, B. (2009). Eukaryotic snoRNAs: a paradigm for gene expression flexibility. Genomics *94*, 83-88.

Ding, F., Li, H.H., Zhang, S., Solomon, N.M., Camper, S.A., Cohen, P., and Francke, U. (2008). SnoRNA Snord116 (Pwcr1/MBII-85) deletion causes growth deficiency and hyperphagia in mice. PloS one *3*, e1709.

Dong, X.-Y., Guo, P., Boyd, J., Sun, X., Li, Q., Zhou, W., and Dong, J.-T. (2009). Implication of snoRNA U50 in human breast cancer. Journal of Genetics and Genomics *36*, 447-454.

Dong, X.Y., Rodriguez, C., Guo, P., Sun, X., Talbot, J.T., Zhou, W., Petros, J., Li, Q., Vessella, R.L., Kibel, A.S.*, et al.* (2008). SnoRNA U50 is a candidate tumor-suppressor gene at 6q14.3 with a mutation associated with clinically significant prostate cancer. Human molecular genetics *17*, 1031-1042.

Fernandez, I.S., Ng, C.L., Kelley, A.C., Wu, G., Yu, Y.T., and Ramakrishnan, V. (2013). Unusual base pairing during the decoding of a stop codon by the ribosome. Nature *500*, 107-110.

Filipowicz, W., and Pogacic, V. (2002). Biogenesis of small nucleolar ribonucleoproteins. Current opinion in cell biology *14*, 319-327.

Fong, Y.W., Ho, J.J., Inouye, C., and Tjian, R. (2014). The dyskerin ribonucleoprotein complex as an OCT4/SOX2 coactivator in embryonic stem cells. eLife *3*.

Ganot, P., Bortolin, M.L., and Kiss, T. (1997). Site-specific pseudouridine formation in preribosomal RNA is guided by small nucleolar RNAs. Cell *89*, 799-809.

Garneau, J.E., Dupuis, M.E., Villion, M., Romero, D.A., Barrangou, R., Boyaval, P., Fremaux, C., Horvath, P., Magadan, A.H., and Moineau, S. (2010). The CRISPR/Cas bacterial immune system cleaves bacteriophage and plasmid DNA. Nature *468*, 67-71.

Gasiunas, G., Barrangou, R., Horvath, P., and Siksnys, V. (2012). Cas9-crRNA ribonucleoprotein complex mediates specific DNA cleavage for adaptive immunity in bacteria. Proceedings of the National Academy of Sciences of the United States of America *109*, E2579-2586.

Gee, H.E., Buffa, F.M., Camps, C., Ramachandran, A., Leek, R., Taylor, M., Patil, M., Sheldon, H., Betts, G., Homer, J.*, et al.* (2011). The small-nucleolar RNAs commonly used for microRNA normalisation correlate with tumour pathology and prognosis. Br J Cancer *104*, 1168-1177.

Gong, J., Li, Y., Liu, C.J., Xiang, Y., Li, C., Ye, Y., Zhang, Z., Hawke, D.H., Park, P.K., Diao, L.*, et al.* (2017). A Pan-cancer Analysis of the Expression and Clinical Relevance of Small Nucleolar RNAs in Human Cancer. Cell reports *21*, 1968-1981.

Goudarzi, K.M., and Lindstrom, M.S. (2016). Role of ribosomal protein mutations in tumor development (Review). International journal of oncology *48*, 1313-1324.

Grosjean, H., Sprinzl, M., and Steinberg, S. (1995). Posttranscriptionally modified nucleosides in transfer RNA: their locations and frequencies. Biochimie *77*, 139-141.

Gyorffy, B., Surowiak, P., Budczies, J., and Lanczky, A. (2013). Online survival analysis software to assess the prognostic value of biomarkers using transcriptomic data in non-small-cell lung cancer. PloS one *8*, e82241.

Hirose, T., Ideue, T., Nagai, M., Hagiwara, M., Shu, M.D., and Steitz, J.A. (2006). A spliceosomal intron binding protein, IBP160, links position-dependent assembly of intron-encoded box C/D snoRNP to pre-mRNA splicing. Molecular cell *23*, 673-684.

Hoareau-Aveilla, C., Bonoli, M., Caizergues-Ferrer, M., and Henry, Y. (2006). hNaf1 is required for accumulation of human box H/ACA snoRNPs, scaRNPs, and telomerase. Rna *12*, 832-840.

Hopper, A.K., and Phizicky, E.M. (2003). tRNA transfers to the limelight. Genes & development *17*, 162-180.

Jack, K., Bellodi, C., Landry, D.M., Niederer, R.O., Meskauskas, A., Musalgaonkar, S., Kopmar, N., Krasnykh, O., Dean, A.M., Thompson, S.R.*, et al.* (2011). rRNA pseudouridylation defects affect ribosomal ligand binding and translational fidelity from yeast to human cells. Molecular cell *44*, 660-666.

Jemal, A., Siegel, R., Ward, E., Hao, Y., Xu, J., Murray, T., and Thun, M.J. (2008). Cancer statistics, 2008. CA: a cancer journal for clinicians *58*, 71-96.

Jinek, M., Chylinski, K., Fonfara, I., Hauer, M., Doudna, J.A., and Charpentier, E. (2012). A programmable dual-RNA-guided DNA endonuclease in adaptive bacterial immunity. Science *337*, 816-821.

Justus, C.R., Leffler, N., Ruiz-Echevarria, M., and Yang, L.V. (2014). In vitro cell migration and invasion assays. Journal of visualized experiments : JoVE.

Karapetyan, A.R., Buiting, C., Kuiper, R.A., and Coolen, M.W. (2013). Regulatory Roles for Long ncRNA and mRNA. Cancers *5*, 462-490.

Karijolich, J., Kantartzis, A., and Yu, Y.T. (2010). RNA modifications: a mechanism that modulates gene expression. Methods in molecular biology *629*, 1-19.

Karijolich, J., and Yu, Y.T. (2010). Spliceosomal snRNA modifications and their function. RNA biology *7*, 192-204.

Karijolich, J., and Yu, Y.T. (2011). Converting nonsense codons into sense codons by targeted pseudouridylation. Nature *474*, 395-398.

King, T.H., Liu, B., McCully, R.R., and Fournier, M.J. (2003). Ribosome structure and activity are altered in cells lacking snoRNPs that form pseudouridines in the peptidyl transferase center. Molecular cell *11*, 425-435.

Kishore, S., Khanna, A., Zhang, Z., Hui, J., Balwierz, P.J., Stefan, M., Beach, C., Nicholls, R.D., Zavolan, M., and Stamm, S. (2010). The snoRNA MBII-52 (SNORD 115) is processed into smaller RNAs and regulates alternative splicing. Human molecular genetics *19*, 1153-1164.

Kishore, S., and Stamm, S. (2006). The snoRNA HBII-52 regulates alternative splicing of the serotonin receptor 2C. Science *311*, 230-232.

Kiss-Laszlo, Z., Henry, Y., Bachellerie, J.P., Caizergues-Ferrer, M., and Kiss, T. (1996). Site-specific ribose methylation of preribosomal RNA: a novel function for small nucleolar RNAs. Cell *85*, 1077-1088.

Kiss, A.M., Jady, B.E., Bertrand, E., and Kiss, T. (2004). Human box H/ACA pseudouridylation guide RNA machinery. Molecular and cellular biology *24*, 5797-5807.

Kiss, T. (2002). Small nucleolar RNAs: an abundant group of noncoding RNAs with diverse cellular functions. Cell *109*, 145-148.

Kiss, T., Fayet-Lebaron, E., and Jady, B.E. (2010). Box H/ACA small ribonucleoproteins. Molecular cell *37*, 597-606.

Kiss, T., Fayet, E., Jady, B.E., Richard, P., and Weber, M. (2006). Biogenesis and intranuclear trafficking of human box C/D and H/ACA RNPs. Cold Spring Harbor symposia on quantitative biology *71*, 407-417.

Koh, C.M., Gurel, B., Sutcliffe, S., Aryee, M.J., Schultz, D., Iwata, T., Uemura, M., Zeller, K.I., Anele, U., Zheng, Q.*, et al.* (2011). Alterations in nucleolar structure and gene expression programs in prostatic neoplasia are driven by the MYC oncogene. The American journal of pathology *178*, 1824-1834.

Kondrashov, A.V., Kiefmann, M., Ebnet, K., Khanam, T., Muddashetty, R.S., and Brosius, J. (2005). Inhibitory effect of naked neural BC1 RNA or BC200 RNA on eukaryotic in vitro translation systems is reversed by poly(A)-binding protein (PABP). Journal of molecular biology *353*, 88-103.

Kufel, J., Allmang, C., Chanfreau, G., Petfalski, E., Lafontaine, D.L., and Tollervey, D. (2000). Precursors to the U3 small nucleolar RNA lack small nucleolar RNP proteins but are stabilized by La binding. Molecular and cellular biology *20*, 5415-5424.

Lafontaine, D.L. (2015). Noncoding RNAs in eukaryotic ribosome biogenesis and function. Nature structural & molecular biology *22*, 11-19.

Langer, C.J. (2012). Individualized therapy for patients with non-small cell lung cancer: emerging trends and challenges. Critical reviews in oncology/hematology *83*, 130-144.

Liao, J., Yu, L., Mei, Y., Guarnera, M., Shen, J., Li, R., Liu, Z., and Jiang, F. (2010). Small nucleolar RNA signatures as biomarkers for non-small-cell lung cancer. Molecular cancer *9*, 198.

Liuksiala, T., Teittinen, K.J., Granberg, K., Heinaniemi, M., Annala, M., Maki, M., Nykter, M., and Lohi, O. (2014). Overexpression of SNORD114-3 marks acute promyelocytic leukemia. Leukemia *28*, 233-236.

Maden, B.E. (1990). The numerous modified nucleotides in eukaryotic ribosomal RNA. Progress in nucleic acid research and molecular biology *39*, 241-303.

Mannoor, K., Shen, J., Liao, J., Liu, Z., and Jiang, F. (2014). Small nucleolar RNA signatures of lung tumor-initiating cells. Molecular cancer *13*, 104.

Martens-Uzunova, E.S., Jalava, S.E., Dits, N.F., van Leenders, G.J., Moller, S., Trapman, J., Bangma, C.H., Litman, T., Visakorpi, T., and Jenster, G. (2012). Diagnostic and prognostic signatures from the small non-coding RNA transcriptome in prostate cancer. Oncogene *31*, 978-991.

Martin, R., Hackert, P., Ruprecht, M., Simm, S., Bruning, L., Mirus, O., Sloan, K.E., Kudla, G., Schleiff, E., and Bohnsack, M.T. (2014). A pre-ribosomal RNA interaction network involving snoRNAs and the Rok1 helicase. Rna *20*, 1173-1182.

Massenet, S., Bertrand, E., and Verheggen, C. (2017). Assembly and trafficking of box C/D and H/ACA snoRNPs. RNA biology *14*, 680-692.

Matera, A.G., Terns, R.M., and Terns, M.P. (2007). Non-coding RNAs: lessons from the small nuclear and small nucleolar RNAs. Nature reviews Molecular cell biology *8*, 209-220.

Mei, Y.P., Liao, J.P., Shen, J., Yu, L., Liu, B.L., Liu, L., Li, R.Y., Ji, L., Dorsey, S.G., Jiang, Z.R.*, et al.* (2012). Small nucleolar RNA 42 acts as an oncogene in lung tumorigenesis. Oncogene *31*, 2794-2804.

Meier, U.T. (2005). The many facets of H/ACA ribonucleoproteins. Chromosoma *114*, 1-14.

Menssen, A., and Hermeking, H. (2002). Characterization of the c-MYC-regulated transcriptome by SAGE: identification and analysis of c-MYC target genes. Proceedings of the National Academy of Sciences of the United States of America *99*, 6274-6279.

Mishima, E., Jinno, D., Akiyama, Y., Itoh, K., Nankumo, S., Shima, H., Kikuchi, K., Takeuchi, Y., Elkordy, A., Suzuki, T.*, et al.* (2015). Immuno-Northern Blotting: Detection of RNA Modifications by Using Antibodies against Modified Nucleosides. PloS one *10*, e0143756.

Morrissey, J.P., and Tollervey, D. (1993). Yeast snR30 is a small nucleolar RNA required for 18S rRNA synthesis. Molecular and cellular biology *13*, 2469-2477.

Mourtada-Maarabouni, M., Hedge, V.L., Kirkham, L., Farzaneh, F., and Williams, G.T. (2008). Growth arrest in human T-cells is controlled by the non-coding RNA growth-arrest-specific transcript 5 (GAS5). Journal of cell science *121*, 939-946.

Mourtada-Maarabouni, M., Pickard, M.R., Hedge, V.L., Farzaneh, F., and Williams, G.T. (2009). GAS5, a non-protein-coding RNA, controls apoptosis and is downregulated in breast cancer. Oncogene *28*, 195-208.

Nakamoto, M.A., Lovejoy, A.F., Cygan, A.M., and Boothroyd, J.C. (2017). mRNA pseudouridylation affects RNA metabolism in the parasite Toxoplasma gondii. Rna *23*, 1834-1849.

Narlikar, G.J., Fan, H.Y., and Kingston, R.E. (2002). Cooperation between complexes that regulate chromatin structure and transcription. Cell *108*, 475-487.

Ni, J., Tien, A.L., and Fournier, M.J. (1997). Small nucleolar RNAs direct site-specific synthesis of pseudouridine in ribosomal RNA. Cell *89*, 565-573.

Nicoloso, M., Qu, L.H., Michot, B., and Bachellerie, J.P. (1996). Intron-encoded, antisense small nucleolar RNAs: the characterization of nine novel species points to their direct role as guides for the 2'-O-ribose methylation of rRNAs. Journal of molecular biology *260*, 178-195.

Ofengand, J. (2002). Ribosomal RNA pseudouridines and pseudouridine synthases. FEBS letters *514*, 17-25.

Okugawa, Y., Toiyama, Y., Toden, S., Mitoma, H., Nagasaka, T., Tanaka, K., Inoue, Y., Kusunoki, M., Boland, C.R., and Goel, A. (2017). Clinical significance of SNORA42 as an oncogene and a prognostic biomarker in colorectal cancer. Gut *66*, 107-117.

Ran, F.A., Hsu, P.D., Wright, J., Agarwala, V., Scott, D.A., and Zhang, F. (2013). Genome engineering using the CRISPR-Cas9 system. Nature protocols *8*, 2281-2308.

Richard, P., Kiss, A.M., Darzacq, X., and Kiss, T. (2006). Cotranscriptional recognition of human intronic box H/ACA snoRNAs occurs in a splicing-independent manner. Molecular and cellular biology *26*, 2540-2549.

Richard, P., and Kiss, T. (2006). Integrating snoRNP assembly with mRNA biogenesis. EMBO reports *7*, 590-592.

Ruggero, D., Grisendi, S., Piazza, F., Rego, E., Mari, F., Rao, P.H., Cordon-Cardo, C., and Pandolfi, P.P. (2003). Dyskeratosis congenita and cancer in mice deficient in ribosomal RNA modification. Science *299*, 259-262.

Ruggero, D., and Pandolfi, P.P. (2003). Does the ribosome translate cancer? Nat Rev Cancer *3*, 179-192.

Sahoo, T., del Gaudio, D., German, J.R., Shinawi, M., Peters, S.U., Person, R.E., Garnica, A., Cheung, S.W., and Beaudet, A.L. (2008). Prader-Willi phenotype caused by paternal deficiency for the HBII-85 C/D box small nucleolar RNA cluster. Nature genetics *40*, 719-721.

Samarsky, D.A., Fournier, M.J., Singer, R.H., and Bertrand, E. (1998). The snoRNA box C/D motif directs nucleolar targeting and also couples snoRNA synthesis and localization. The EMBO journal *17*, 3747-3757.

Seshadri, T., Uzman, J.A., Oshima, J., and Campisi, J. (1993). Identification of a transcript that is down-regulated in senescent human fibroblasts. Cloning, sequence analysis, and regulation of the human L7 ribosomal protein gene. The Journal of biological chemistry *268*, 18474-18480.

Shalem, O., Sanjana, N.E., Hartenian, E., Shi, X., Scott, D.A., Mikkelson, T., Heckl, D., Ebert, B.L., Root, D.E., Doench, J.G.*, et al.* (2014). Genome-scale CRISPR-Cas9 knockout screening in human cells. Science *343*, 84-87.

Siprashvili, Z., Webster, D.E., Johnston, D., Shenoy, R.M., Ungewickell, A.J., Bhaduri, A., Flockhart, R., Zarnegar, B.J., Che, Y., Meschi, F.*, et al.* (2016). The noncoding RNAs SNORD50A and SNORD50B bind K-Ras and are recurrently deleted in human cancer. Nature genetics *48*, 53-58.

Smith, C.M., and Steitz, J.A. (1997). Sno storm in the nucleolus: new roles for myriad small RNPs. Cell *89*, 669-672.

Smith, C.M., and Steitz, J.A. (1998). Classification of gas5 as a multi-small-nucleolar-RNA (snoRNA) host gene and a member of the 5'-terminal oligopyrimidine gene family reveals common features of snoRNA host genes. Molecular and cellular biology *18*, 6897-6909.

Steffen, B., Knop, M., Bergholz, U., Vakhrusheva, O., Rode, M., Kohler, G., Henrichs, M.P., Bulk, E., Hehn, S., Stehling, M.*, et al.* (2011). AML1/ETO induces self-renewal in hematopoietic progenitor cells via the Groucho-related amino-terminal AES protein. Blood *117*, 4328-4337.

Steller, H. (1995). Mechanisms and genes of cellular suicide. Science *267*, 1445-1449.

Stepanov, G.A., Filippova, J.A., Komissarov, A.B., Kuligina, E.V., Richter, V.A., and Semenov, D.V. (2015). Regulatory role of small nucleolar RNAs in human diseases. BioMed research international *2015*, 206849.

Su, H., Xu, T., Ganapathy, S., Shadfan, M., Long, M., Huang, T.H., Thompson, I., and Yuan, Z.M. (2014). Elevated snoRNA biogenesis is essential in breast cancer. Oncogene *33*, 1348-1358.

Takahashi, T., Nau, M.M., Chiba, I., Birrer, M.J., Rosenberg, R.K., Vinocour, M., Levitt, M., Pass, H., Gazdar, A.F., and Minna, J.D. (1989). p53: a frequent target for genetic abnormalities in lung cancer. Science *246*, 491-494.

Tanaka, R., Satoh, H., Moriyama, M., Satoh, K., Morishita, Y., Yoshida, S., Watanabe, T., Nakamura, Y., and Mori, S. (2000). Intronic U50 small-nucleolar-RNA (snoRNA) host gene of no protein-coding potential is mapped at the chromosome breakpoint t(3;6)(q27;q15) of human B-cell lymphoma. Genes to cells : devoted to molecular & cellular mechanisms *5*, 277-287.

Terns, M., and Terns, R. (2006). Noncoding RNAs of the H/ACA family. Cold Spring Harbor symposia on quantitative biology *71*, 395-405.

Thorenoor, N., and Slaby, O. (2015). Small nucleolar RNAs functioning and potential roles in cancer. Tumour biology : the journal of the International Society for Oncodevelopmental Biology and Medicine *36*, 41-53.

Tollervey, D., and Kiss, T. (1997). Function and synthesis of small nucleolar RNAs. Current opinion in cell biology *9*, 337-342.

Torre, L.A., Bray, F., Siegel, R.L., Ferlay, J., Lortet-Tieulent, J., and Jemal, A. (2015). Global cancer statistics, 2012. CA: a cancer journal for clinicians *65*, 87-108.

Tycowski, K.T., Shu, M.D., and Steitz, J.A. (1996a). A mammalian gene with introns instead of exons generating stable RNA products. Nature *379*, 464-466.

Tycowski, K.T., Smith, C.M., Shu, M.D., and Steitz, J.A. (1996b). A small nucleolar RNA requirement for site-specific ribose methylation of rRNA in Xenopus. Proceedings of the National Academy of Sciences of the United States of America *93*, 14480-14485.

Valleron, W., Laprevotte, E., Gautier, E.F., Quelen, C., Demur, C., Delabesse, E., Agirre, X., Prosper, F., Kiss, T., and Brousset, P. (2012). Specific small nucleolar RNA expression profiles in acute leukemia. Leukemia *26*, 2052-2060.

van Deursen, J.M. (2014). The role of senescent cells in ageing. Nature *509*, 439-446.

van Zijl, F., Krupitza, G., and Mikulits, W. (2011). Initial steps of metastasis: cell invasion and endothelial transmigration. Mutation research *728*, 23-34.

Vitali, P., Basyuk, E., Le Meur, E., Bertrand, E., Muscatelli, F., Cavaille, J., and Huttenhofer, A. (2005). ADAR2-mediated editing of RNA substrates in the nucleolus is inhibited by C/D small nucleolar RNAs. The Journal of cell biology *169*, 745-753.

Wang, L., Soria, J.C., Kemp, B.L., Liu, D.D., Mao, L., and Khuri, F.R. (2002). hTERT expression is a prognostic factor of survival in patients with stage I non-small cell lung cancer. Clinical cancer research : an official journal of the American Association for Cancer Research *8*, 2883-2889.

White, R.J. (2005). RNA polymerases I and III, growth control and cancer. Nature reviews Molecular cell biology *6*, 69-78.

Williams, G.T., and Farzaneh, F. (2012a). Are snoRNAs and snoRNA host genes new players in cancer? Nat Rev Cancer *12*, 84-88.

Williams, G.T., and Farzaneh, F. (2012b). Are snoRNAs and snoRNA host genes new players in cancer? Nat Rev Cancer *12*, 84-88.

Yan, M., Kanbe, E., Peterson, L.F., Boyapati, A., Miao, Y., Wang, Y., Chen, I.M., Chen, Z., Rowley, J.D., Willman, C.L*., et al.* (2006). A previously unidentified alternatively spliced isoform of t(8;21) transcript promotes leukemogenesis. Nature medicine *12*, 945-949.

Zemann, A., op de Bekke, A., Kiefmann, M., Brosius, J., and Schmitz, J. (2006). Evolution of small nucleolar RNAs in nematodes. Nucleic acids research *34*, 2676-2685.

Zhao, Y., Dunker, W., Yu, Y.T., and Karijolich, J. (2018). The Role of Noncoding RNA Pseudouridylation in Nuclear Gene Expression Events. Frontiers in bioengineering and biotechnology *6*, 8.

Zhou, F., Liu, Y., Rohde, C., Pauli, C., Gerloff, D., Kohn, M., Misiak, D., Baumer, N., Cui, C., Gollner, S.*, et al.* (2017). AML1-ETO requires enhanced C/D box snoRNA/RNP formation to induce self-renewal and leukaemia. Nature cell biology *19*, 844-855.

Abbreviations

NSCLC, non-small cells lung cancer

GeCKO, genome-scale CRISPR-Cas9 knockout

SnoRNAs, small nucleolar RNAs

SCLC, small-cell lung cancer

EGFR, epidermal growth factor receptor

BSA, Bovine serum albumin

c-Myc, Myelocytomatosis viral oncogene homolog

DMEM, Dulbecco's Modified Eagle medium

DMSO, Dimethyl sulfoxid

dNTP, deoxynucleotide triphosphate

EDTA, Ethylenediaminetetraacetatic acid

EGFP, Enhanced green-fluorescent protein

FACS, Fluorescent activated cell sorting

FCS, Fetal calf serum

GAS5, Growth arrest specific 5

OP-Puro, O-propargyl-Puromycin

PBS, Phosphate buffered saline

PCR, Polymerase-chain-reaction

rRNA, ribosomal RNA

RT, Room temperature

RT-PCR, Reverse transcription real time polymerase chain reaction

ScaRNAs, small Cajal body-specific RNAs

shRNA, short hairpin RNA

SnoRNP, small nucleolar ribonucleic protein complexes

tRNA, transfer RNA

Abbreviations

WT, Wild type

LncRNA, long non-coding RNA

DKC1, Dyskerin Pseudouridine Synthase 1

NHP2, non-histone chromosome protein 2

Gar1, protein glycine arginine rich 1

NHEJ, non-homologous end joining

Acknowledgements

I would like to thank my supervisor Prof. Dr. Carsten Müller-Tidow for providing me the opportunity to pursue a PhD degree in our lab and for his permanent scientific support to my project. I would also like to thanks a lot for Prof. Dr. Mike Schutkowski to be my first supervisor.

Besides, I thank a lot to Dr. Bayram Edemir and Annette Becker.M.A for science coordination in our lab. Many thanks to Dr. Fengbiao Zhou, Dr. Yi Liu and Dr. Christian Rohde for their support in the lab. Thanks a lot to Dr. Volker Eckstein and Stefanie Hoffman for sorting cells with flow cytometer. Thanks a lot to all other members of AG Müller-Tidow for their help.

Thanks a lot to my parents, my brother and sister in law for their unconditional support and love.

CURRICULUM VITAE

PERSONAL INFORMATION

Name: Chunhong Cui

Birthday: 02.02.1984

Gender: Female

Nationality: Chinese

E-mail Address: chunhong.cui01@gmail.com

UNIVERSITY EXPERIENCE

2013. 09-2018. 09 Halle University/PhD student/Biochemistry and Biotechnology

Supervisor: Prof. Dr. rer. nat. Mike. Schutkowski (Doctor Father)

Supervisor: Prof. Dr. med. Carsten Müller-Tidow

Project: The role of small nucleolar Ribonucleoprotein complexes in lung cancer.

2009. 09-2012. 07 Fudan University/Master/Biochemistry and molecular Biology

Suporvisor: Prof. Jianhai Jiang

Project: β1, 4-Galactosyltransferase V activates Notch1 signaling in glioma stem-like cells and promotes their transdifferentiation into endothelial cells.

2004. 09-2009. 07 JiNing Medical College/Bachelor/Clinical Medicine

I hereby declare under oath that this dissertation is entirely my own work and has been written without any external assistance. I used only the sources and resources as indicated, and have clearly marked as such all the quotations and content taken from the works to which I referred.

Chunhong Cui

December 2018, Halle